

**HELICITY AND PHYSICAL FIDELITY IN  
TURBULENCE MODELING**

by

**Leo Gregory Rebholz**

B.S. Mathematics, Duquesne University, 2000

M.S. Computational Mathematics, Duquesne University, 2002

M.A. Mathematics, University of Pittsburgh, 2003

Submitted to the Graduate Faculty of  
the Department of Mathematics in partial fulfillment  
of the requirements for the degree of

**Doctor of Philosophy**

University of Pittsburgh

2006

UNIVERSITY OF PITTSBURGH  
MATHEMATICS DEPARTMENT

This dissertation was presented

by

Leo Gregory Rebholz

It was defended on

December 15, 2006

and approved by

Prof. William J. Layton, University of Pittsburgh

Prof. Vince Ervin, Clemson University

Prof. Beatrice Riviere, University of Pittsburgh

Dr. Myron Sussman, University of Pittsburgh

Prof. Ivan Yotov, University of Pittsburgh

Dissertation Director: Prof. William J. Layton, University of Pittsburgh

# HELICITY AND PHYSICAL FIDELITY IN TURBULENCE MODELING

Leo Gregory Rebholz , PhD

University of Pittsburgh, 2006

This thesis is a study of physical fidelity in turbulence modeling. We first consider conservation laws in several popular turbulence models and find that of the Leray, Leray-deconvolution, Bardina and Stolz-Adams approximate deconvolution model (ADM), all but the Bardina model conserve a model energy. Only the ADM conserves a model helicity. Since the ADM conserves a model energy and helicity, we then investigate a joint helicity-energy spectrum in the ADM. We find that up to a filter-dependent length scale, the ADM cascades energy and helicity jointly in the same manner as the Navier-Stokes equations.

We also investigate helicity treatment in discretizations of turbulence models. For inviscid, periodic flow, we implement energy conserving discretizations of the ADM, Leray, and Leray-deconvolution models as well as the Navier-Stokes equations (NSE) and observe helicity treatments. We find that of none of the models conserve helicity (or model helicity) in the discretizations. Since the Leray-deconvolution model of turbulence is newly developed, our implementation is new and thus we analyze the trapezoidal Galerkin scheme that we implement and compare it to the usual Leray model.

Lastly, we develop an energy and helicity conserving trapezoidal Galerkin scheme for the Navier-Stokes equations. We prove conservation properties for the scheme, stability, and show the scheme does not lose asymptotic accuracy compared to the usual trapezoidal Galerkin scheme. We also present numerical experiments that compare the energy and helicity conserving scheme to more typical schemes.

## TABLE OF CONTENTS

<b>PREFACE</b> . . . . .	x
<b>1.0 INTRODUCTION</b> . . . . .	1
<b>2.0 CONSERVATION LAWS OF TURBULENCE MODELS</b> . . . . .	7
2.1 INTRODUCTION . . . . .	7
2.2 NOTATION AND PRELIMINARIES . . . . .	10
2.2.1 The Models Considered . . . . .	12
2.3 CONSERVATION LAWS . . . . .	14
2.3.1 Momentum and Mass . . . . .	14
2.3.2 Energy . . . . .	15
2.3.3 Helicity . . . . .	17
2.3.4 Enstrophy . . . . .	20
2.4 CONCLUSIONS . . . . .	23
<b>3.0 THE JOINT ENERGY-HELICITY CASCADE IN THE ADM</b> . . . . .	24
3.1 INTRODUCTION . . . . .	24
3.2 NOTATION AND PRELIMINARIES . . . . .	27
3.2.1 Nomenclature . . . . .	28
3.2.2 Norm Equivalence . . . . .	31
3.3 PROPERTIES OF APPROXIMATE DECONVOLUTION LES MODELS . . . . .	35
3.3.1 Spectral Representation of the Kinetic Energy . . . . .	36
3.3.2 Helical Mode Decomposition . . . . .	38
3.4 PHENOMENOLOGY OF THE ADM JOINT ENERGY AND HELICITY CASCADE . . . . .	40

3.5	MODEL'S HELICITY MICROSCALE AND CONSISTENCY OF THE CASCADE . . . . .	42
3.5.1	Model's Helicity Microscale . . . . .	43
3.5.2	Consistency of the ADM Joint Cascade . . . . .	45
3.6	CONCLUSIONS . . . . .	46
3.6.1	Other Filters . . . . .	47
<b>4.0</b>	<b>HELICITY CONSERVATION IN TRAPEZOIDAL GALERKIN DISCRETIZATIONS . . . . .</b>	<b>49</b>
<b>5.0</b>	<b>AN ENERGY AND HELICITY CONSERVING FINITE ELEMENT SCHEME FOR THE NAVIER-STOKES EQUATIONS . . . . .</b>	<b>53</b>
5.1	INTRODUCTION . . . . .	53
5.2	NOTATION AND PRELIMINARIES . . . . .	55
5.3	AN ENERGY AND HELICITY CONSERVING SCHEME FOR PERIODIC FLOWS . . . . .	57
5.3.1	Existence of Solutions for the Scheme . . . . .	60
5.4	ERROR ANALYSIS OF THE SCHEME . . . . .	64
5.5	NUMERICAL EXPERIMENTS . . . . .	70
5.5.1	Computational Cost . . . . .	71
5.5.2	Experiment 1: Helicity Conservation for $\nu = f = 0$ . . . . .	71
5.5.3	Experiment 2: Accuracy Comparison for a Known Solution . . . . .	72
5.6	CONCLUSIONS . . . . .	73
<b>6.0</b>	<b>A NUMERICAL STUDY OF A HIGHER-ORDER LERAY-DECONVOLUTION TURBULENCE MODEL . . . . .</b>	<b>75</b>
6.1	INTRODUCTION . . . . .	75
6.2	NOTATION AND PRELIMINARIES . . . . .	77
6.3	ANALYSIS OF THE SCHEME . . . . .	84
6.4	NUMERICAL EXPERIMENTS . . . . .	92
6.4.1	$3d$ Convergence Rate Verification . . . . .	92
6.4.2	$3d$ Error Comparisons at $Re=5000$ . . . . .	93
6.4.3	Underresolved flows in $2d$ . . . . .	94

6.5 CONCLUSIONS . . . . .	99
<b>7.0 CONCLUSIONS AND FUTURE WORK . . . . .</b>	<b>103</b>
7.1 Conclusions . . . . .	103
7.2 Future Work . . . . .	104
<b>BIBLIOGRAPHY . . . . .</b>	<b>106</b>

## LIST OF TABLES

1	$L^2$ and $H^1$ errors and rates at $Re = 1$ and $t=0.5$ . . . . .	93
---	--	----

## LIST OF FIGURES

1	Turbulence is chaotic, three dimensional and rotational! The picture shows flow in a box, where inside are streamtubes, and the sides of the box are colored with velocity magnitude (magnitude scale given on the right) overlaid with streamlines. . . . .	6
2	Approximate de-convolution operators, $N=0,1,2$ . . . . .	34
3	The helicity spectrum of Approximate Deconvolution Models . . . . .	48
4	Helicity vs Time for inviscid periodic flow with trapezoidal Galerkin and linearly extrapolated trapezoidal Galerkin schemes for the NSE . . . . .	51
5	Energy vs Time for inviscid periodic flow with trapezoidal Galerkin and linearly extrapolated trapezoidal Galerkin schemes for the NSE . . . . .	52
6	Helicity and ADM-Helicity vs Time for inviscid periodic flow for a trapezoidal Galerkin scheme for the ADM . . . . .	52
7	Helicity Conservation in different trapezoid schemes for the NSE with $\nu = f = 0$ and $u_0 = (\cos(2\pi z), \sin(2\pi z), \sin(2\pi x))$ . . . . .	72
8	Helicity error in the schemes . . . . .	73
9	$L^2$ error in the schemes . . . . .	74
10	$H^1$ error in the schemes . . . . .	74
11	$L^2$ Error vs. Time for CNLE and LDLE with $N=0,1,2,3$ . . . . .	94
12	$H^1$ Error vs. Time for CNLE and LDLE with $N=0,1,2,3$ . . . . .	95
13	NSE at $\nu = 1/600$ , 41,538 d.o.f. grid . . . . .	96
14	SMA at $\nu = 1/600$ , $\delta = 1.5$ and 5,845 d.o.f. grid . . . . .	97
15	Boundary conditions . . . . .	98

16	Grid with 1,537 d.o.f. . . . .	99
17	LerayDC0 at $\nu = 1/600$ , $\delta = 1.5$ and 5,845 d.o.f. grid . . . . .	100
18	LerayDC1 at $\nu = 1/600$ , $\delta = 1.5$ and 5,845 d.o.f. grid . . . . .	101
19	LerayDC2 at $\nu = 1/600$ , $\delta = 1.5$ and 5,845 d.o.f. grid . . . . .	101
20	LerayDC0, LerayDC1, LerayDC2, respectively at $T = 40$ , $\nu = 1/600$ , $\delta = 3.0$ and 1,537 d.o.f. grid . . . . .	102

## PREFACE

There are several people I need to thank for making the past four and a half years not only successful, but fun and exciting as well.

First I need to thank my wife Amy. She has endured a meager lifestyle, and put up with a spouse who has been constantly busy.

My advisor, Professor William Layton, has kept me on track and played a major role in making my time at Pitt a great success.

There are several others who have been a great help and/or resource during my time in graduate school. Professor Vince Ervin was a big help in getting the codes used in this thesis working. Dr. Mike Sussman has been a tremendous resource here at Pitt, as well as an excellent mentor to me at Bettis Laboratory. Collaborations with fellow graduate students Dr. Carolina Manica and Ms. Monika Neda have been both helpful and productive. Professors Beatrice Riviere and Ivan Yotov are both excellent teachers from whom I have learned a lot, and were both also nice enough to sit on my thesis committee.

Lastly, I need to thank my undergraduate and masters thesis advisor, Professor Abhay Gaur. His guidance has proved invaluable.

## 1.0 INTRODUCTION

This thesis is a study of physical fidelity in turbulence modeling. Simulating turbulent flow is essential to many important engineering applications, including aerodynamics, weather prediction, and heat exchangers. However, modern science does not yet have a good understanding of turbulent phenomena. There are many difficulties associated with turbulence which leads many to believe a complete understanding is not even in the foreseeable future. The main difficulties are that turbulence is diffusive, chaotic and irregular, three dimensional and rotational, highly dissipative, is a continuum phenomena, and that the vortex stretching mechanism generates very small scales. Since turbulence itself is not well understood, accurately simulating turbulence is not either.

The equations of motion for an incompressible, Newtonian fluid (e.g. water) are the Navier-Stokes equations. They are given below in nondimensional form, with  $u$  and  $p$  representing fluid velocity and pressure,  $\nu$  the kinematic viscosity (which is inversely proportional to the Reynolds number  $Re$ ), and external force  $f$ .

$$u_t + u \cdot \nabla u + \nabla p - \nu \Delta u = f \tag{1.1}$$

$$\nabla \cdot u = 0 \tag{1.2}$$

These equations are not a model for turbulent (or laminar) fluid flow; they are built directly from physical conservation laws. However, only for very basic flows can analytic solutions to (1.1)-(1.2) be found. Furthermore, a complete mathematical theory for these equations is lacking, and will be difficult to discover - it is hard enough that the most famous gap in the theory, existence and smoothness of NSE solutions in three dimensions, is a One Million Dollar Clay Prize Problem.

Without the availability of analytic solutions to the NSE, scientists have resorted to computer simulation. This has been partially successful; for slow moving, viscosity dominated flows on small domains, accurate solutions can be obtained using direct numerical simulations (DNS). However, for turbulent flows, DNS often fails. The main reason for this was discovered by Kolmogorov [31], and discussed in [37]: From the critical length scale determined by Kolmogorov, the smallest persistent eddy containing energy in a turbulent flow has length scale  $= O(Re^{-3/4})$ . Thus for an accurate simulation that *captures everything*, one must choose

$$\Delta x = \Delta y = \Delta z = O(Re^{-3/4}), \quad (1.3)$$

and therefore the number of meshpoints will be on the order of  $Re^{9/4}$ . This presents a problem, since  $Re$  can be very high for not very large domains (Reynolds number for flow around a car is on the order of  $10^6$ , and for flow around an airplane is on the order of  $10^7$  [33]). Hence it is simply not computationally feasible to use DNS for turbulent flows in many settings. Further, even when computational power is enough to use a DNS for these problems, there will be larger problems of interest (aircraft carriers, even geophysical flow which has  $Re$  on the order of  $10^{20}$ ).

In many cases, this need for such a large number of degrees of freedom leaves scientists to either compute on an underresolved mesh or solve a model of the NSE which requires less degrees of freedom. Large eddy simulation (LES) turbulence models, for example, are a class of turbulence models that require many less degrees of freedom than a DNS. This is because they solve for flow averages, and do not require the small scale detail they filter out.

There are many other models of turbulence besides LES models. The plethora of models in existence can create a problem for scientists who must choose a model for a simulation. Hence there has been a recent push to distinguish between models by examining their physical properties, and comparing these properties to the Navier-Stokes equations. For example, it has long been known that the NSE conserve energy ( $E = \int_{\Omega} u^2$ ) for inviscid flow, and from the K41 theory it is known that the NSE cascades energy through wave space up to a cut-off length scale where viscosity takes over [31]. For a turbulence model's solution to have physical relevance, the model should share these the same physical characteristics of the NSE. In 2005, a re-examination of the Leray LES model [39] by Cheskidov, Holm

and Titi studied the energy cascade of the model, and found that not only does the Leray model conserve energy, but up to a filter-dependent length scale cascades energy at the same rate as the NSE. In [37], Layton and Neda found a similar result for the Stolz-Adams approximate deconvolution model (ADM) of turbulence. Such results give physical relevance to the solutions of the Leray model and the ADM.

Energy is not the only physical quantity meaningful in fluid flow. It has recently been discovered that helicity, which is defined to be the scalar product of the velocity and vorticity integrated over the domain  $\Omega$ ,

$$H = \int_{\Omega} u \cdot (\nabla \times u) \tag{1.4}$$

is a physical quantity whose importance in understanding turbulent flow has *a status comparable to energy* [46]. The physical interpretation of helicity is the degree to which the vortex lines of a flow are tangled and intertwined. Like energy, helicity is also a conserved quantity of inviscid flow. Also like energy, the NSE has a helicity spectrum [15],[19]; the cascades of energy and helicity have been dubbed a *joint cascade* since both quantities travel through the inertial range of wave numbers at the same rate. Helicity also has a topological interpretation:  $H = 0$  if and only if the turbulent field is rotationally symmetric [46]. Thus the importance of helicity is evident, and hence it should not simply be ignored in turbulence modeling.

However, what is known about helicity has only recently been discovered. Helicity's inviscid invariance was discovered by Moreau in 1961 [47], its topological interpretation by Moffatt and Tsoniber in 1992 [46], and the joint helicity-energy cascade was only proposed by Ditlevson and Guiliani in 2001 [19] - and is still being studied; the size of the smallest length scale containing helicity was being debated in 2003 [15]. With such new and powerful results concerning helicity in fluid flow, an examination of the treatment of helicity in existing turbulence models should be performed. For a model to have physical fidelity, it should at least conserve helicity for inviscid flow, and to match the true physics a model's helicity spectrum should match that of the NSE.

Since helicity conservation is a first and necessary step in showing a helicity spectrum, we investigate helicity conservation in several popular turbulence models in Chapter 2. For inviscid flow, we show that of the ADM, Leray, Leray-deconvolution, and Bardina models,

only the ADM conserves a model helicity, and thus only for the ADM should an examination of a helicity spectrum be done. Chapter 2 also investigates the conservation of other integral invariants of these models: energy, and for two dimensional flow, enstrophy ( $Ens = \frac{1}{2} \int_{\Omega} |\nabla \times u|^2$  is a conserved rotational quantity in two dimensions only). We find that of the four models, only the Bardina model does not conserve a model energy. Furthermore, the ADM and Leray model both conserve a model enstrophy in two dimensions [52].

Since it was found that the ADM conserves a model helicity for inviscid flow, we investigate the helicity spectrum in the ADM in Chapter 3. Since we know that a model energy is cascaded up to a filter-dependent length scale in the ADM [37], we study the possibility of a joint cascade of model energy and helicity in the ADM. We find that, indeed, model energy and helicity are cascaded by the ADM through the inertial range at the same rate as in true fluid flow - up to a filter-dependent length scale. After this length scale, the spectrums decay at a faster rate than that of true fluid flow [36].

In turbulence simulations, the discretization, in addition to the model used, is also important for physical relevance of solutions. For example, the backward Euler Galerkin direct implementation of the NSE does not conserve energy, whereas the trapezoidal Galerkin (i.e. Crank-Nicholson) implementation does. For reasons such as this, care must be taken in choosing a discretization to give the solution as much physical relevance as possible.

To determine the impact of the helicity treatment in the continuous forms of the turbulence models from Chapter 2 on the treatment of helicity in their discretizations, we implement (model) energy conserving trapezoidal Galerkin schemes for the Leray, Leray-deconvolution, and ADM turbulence models. We developed code in MATLAB to test these three dimensional models. We find that none of these implementations conserve helicity for periodic, inviscid flow. However, we also implement similar schemes for the NSE, we find these do not conserve helicity either. Hence it is also the discretizations which can prevent helicity conservation. These results are given in Chapter 4. It is clear from these numerical experiments that it is the discrete form of the nonlinearity which is creating and dissipating helicity in the simulations. Hence for a scheme to conserve both energy and helicity, a usual trapezoidal Galerkin needs to be improved upon.

It is not surprising that these schemes do not conserve helicity. The first scheme to conserve both energy and helicity was discovered in 2004 by Liu and Wang [42], and is for axisymmetric flow. Conserving both of these quantities in a scheme is important for several reasons. First, true fluid flow conserves them; for a scheme to do so also provides physical relevance for its solutions. This also means that the nonlinearity is not creating or dissipating helicity. In the NSE, the nonlinearity is responsible only for moving helicity through wave space, not for creating or destroying it. Since the nonlinearity is not creating small errors by altering helicity, it is possible to achieve better accuracy in longer time intervals (versus schemes that do not conserve helicity). This is because there are no small errors (from helicity) that can eventually cause significant error in a helicity conserving scheme. Analogously in two dimensions, where the rotational quantity enstrophy is conserved, schemes such as the Arakawa scheme [6] that conserve both energy and enstrophy are widely believed to be more accurate in long time intervals than other schemes that conserve only energy.

The scheme of Liu and Wang (known as EHPS) is for axisymmetric flow only, and is derived from the vorticity-stream function formulation of the Navier-Stokes equations. In Chapter 5, we present an energy and helicity conserving finite element scheme for more general flows [50]. For periodic flows, we prove inviscid conservation, stability and convergence of the scheme. Some of the analysis is similar to that in [51]. We also present numerical examples comparing the scheme to more typical NSE finite element schemes.

In Chapter 6, we give a numerical analysis of a trapezoidal Galerkin implementation of the (new,[34]) Leray-deconvolution model. We also present numerical experiments to verify proven convergence rates and to compare the scheme to the classical Leray scheme, which is the  $0^{th}$  order Leray-deconvolution model.

We end this thesis with conclusions and a discussion of possible future work.

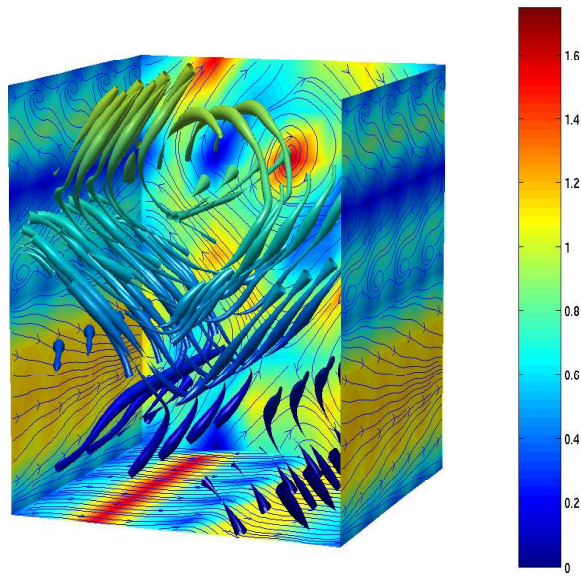


Figure 1: Turbulence is chaotic, three dimensional and rotational! The picture shows flow in a box, where inside are streamtubes, and the sides of the box are colored with velocity magnitude (magnitude scale given on the right) overlaid with streamlines.

## 2.0 CONSERVATION LAWS OF TURBULENCE MODELS

### 2.1 INTRODUCTION

A major difficulty in turbulence modeling is selecting a model from among the plethora of turbulence models in existence. It is rarely known à priori if a particular model will perform well for a given flow setting. However, there are other ways to compare turbulence models. For example, determining the physical relevance of a model's solution can give insight into a model's accuracy. It is well known that kinetic energy, ( $E = \int_{\Omega} |u|^2 dx$ ), is critical in the organization of a flow, and hence if a model is to accurately predict turbulent flow, it must also accurately predict the flow's kinetic energy. Enstrophy ( $Ens = \int_{\Omega} |\nabla \times u|^2 dx$ ) and helicity ( $H = \int_{\Omega} u \cdot (\nabla \times u) dx$ ) are rotational quantities which play critical roles in the organization of two and three dimensional fluid flow, respectively. An accurate turbulence model must also predict these quantities correctly. This chapter compares four popular turbulence models based on the analysis of their treatment of kinetic energy, enstrophy, and helicity.

Conservation of kinetic energy in turbulence models has been extensively studied for many years [22],[25],[20],[24]. Kinetic energy conservation in a model yields stability, is the key step in an existence theory, and is the first step in proving a model's energy cascades from large to small scales. The conservation of enstrophy for two dimensional turbulence has also been extensively studied [22][25], and models such as the classical Arakawa scheme [6] have been developed that preserve both energy and enstrophy for inviscid flow. Enstrophy is not conserved in three dimensions because of vortex stretching, a quantity which vanishes in two dimensions but not necessarily in three dimensions.

Many turbulence models, by their construction, cannot conserve energy, helicity, or en-

strophy. Large Eddy Simulation (LES) models of turbulence, for example, solve for approximate averages of flows. These models are often used where fine scale detail is not necessary. To illustrate their development, consider the NSE in an  $L$ -periodic box  $\Omega \subset \mathbf{R}^3$  or  $\mathbf{R}^2$ .

$$u_t + \nabla \cdot (uu) + \nabla p - \nu \Delta u = f, \quad \nabla \cdot u = 0, \quad (2.1)$$

$$u(0, x) = u_0(x), \quad \int_{\Omega} p \, dx = 0, \quad \text{and } u(x + Le_i) = u(x), \quad (2.2)$$

where  $e_i$  is any of the three standard basis vectors in  $\mathbf{R}^3$ .

Note that from these equations, in absence of dissipation ( $\nu = 0$ ) and external force ( $f = 0$ ), one can derive for every  $t \geq 0$ , the conservation of

- mass:  $\nabla \cdot u(x, t) = 0 \, \forall x \in \Omega$ ,
- momentum:  $\int_{\Omega} u(x, t) = \int_{\Omega} u_0(x)$ ,
- energy:  $E(t) = \frac{1}{2} \int_{\Omega} |u(x, t)|^2 = \frac{1}{2} \int_{\Omega} |u_0(x)|^2 = E(0)$ ,
- helicity:  $H(t) = \int_{\Omega} u(t) \cdot (\nabla \times u(t)) = \int_{\Omega} u_0 \cdot (\nabla \times u_0) = H(0)$ ,
- and enstrophy:  $Ens(t) = \frac{1}{2} \int_{\Omega} |\nabla \times u(t)|^2 = \frac{1}{2} \int_{\Omega} |\nabla u_0|^2 = Ens(0)$ .

See, for example, [22] or [25].

An LES model can be derived from the NSE as follows. Let  $\bar{\phi}$  denote a spacial average of  $\phi$  where the operator  $(\bar{\cdot})$  is a differential filter (defined precisely in Section 2). Then the spacially filtered NSE (SFNSE) are

$$\bar{u}_t + \nabla \cdot \bar{u}\bar{u} + \nabla \bar{p} - \nu \Delta \bar{u} = \bar{f}, \quad \nabla \cdot \bar{u} = 0, \quad (2.3)$$

$$\bar{u}(0, x) = \bar{u}_0(x), \quad \int_{\Omega} \bar{p} \, dx = 0, \quad \text{and } \bar{u}(x + Le_i) = \bar{u}(x) \quad (2.4)$$

A closure problem arises in the SFNSE; the  $\bar{u}\bar{u}$  term must be modeled, and each different way of modeling this term leads to a different LES model. Since  $\overline{u\bar{u}} \neq \bar{u}\bar{u}$ , not every LES model will conserve energy, helicity or enstrophy. However, LES models can conserve naturally

arising model quantities analogous to energy, helicity, or enstrophy. In the Navier-Stokes-alpha ( $NS\alpha$ ) model studied by Foias, Holm and Titi in [21], a model energy and a model helicity were found to be conserved for inviscid flow:

$$E_{NS\alpha} = \int_{\Omega} v \cdot \bar{v}, \quad H_{NS\alpha} = \int_{\Omega} v \cdot (\nabla \times v),$$

where  $v$  is the model's velocity solution and  $\bar{v}$  is a spacial average of the solution. In the  $N^{th}$  order Stolz-Adams approximate deconvolution model (ADM) studied in [20], a model energy  $E_{ADM}$ , defined in Section 2, was found to be conserved for inviscid flow under periodic boundary conditions.

The work of Foias, Holm, Titi, et al. [21],[17] motivated this work. The fact that model quantities can have cascades is shown in [17], where an energy cascade for the Leray model is discussed, and [21] shows model quantities other than energy can be conserved. Since a cascade theory must begin with inviscid conservation, showing the inviscid conservation of energy, helicity, and enstrophy in a turbulence model would be an essential first step toward finding the cascades of these quantities in a model. Furthermore, for a turbulence model, conservation of quantities analogous to the five conserved in the NSE is highly desirable; it can provide a diagnostic check for stability and accuracy of a model, and in practice, the presence of conserved quantities in a model allows solutions to be monitored for physical relevance (e.g. any model of the NSE or filtered NSE, without external forces, should never have energy grow above the energy level at the starting time). In addition, as LES models are often used for modeling large scale rotational flows, such as in geophysics or oceanic modeling, they should exhibit the conservation of rotational quantities as well as energy. Hence in this chapter we present a study of conservation laws in four popular LES models to determine if they also conserve quantities analogous to those conserved in the NSE. The models we study are: the ADM [3] [2], the Leray model [17], the Bardina scale-similarity model [8], and a new alteration of the Leray model proposed by A. Dunca and studied by Layton and Lewandowski [34] which we will refer to as the Leray deconvolution model. Formal definitions of these models will be given in Section 2.

The rest of this chapter is arranged as follows. Section 2 will give notation and preliminaries, Section 3 will present the conservation laws of the models, and Section 4 presents comparisons and conclusions.

## 2.2 NOTATION AND PRELIMINARIES

The domain  $\Omega$  used throughout this chapter will be a box:  $\Omega = (0, L)^d$ ,  $d = 2$  or  $3$ , with periodic boundary conditions. All results except for that of enstrophy will hold for either  $d = 2$  or  $d = 3$ , but conservation of enstrophy (as explained above) is restricted in these models, as well as in the NSE, to only two dimensions.

We shall assume that solutions are smooth enough to justify each manipulation used.

The usual  $L^2$  norm and inner product will be denoted by  $\|\cdot\|$  and  $(\cdot, \cdot)$ , respectively:

$$(v, w) = \int_{\Omega} v \cdot w, \quad \|v\| = (v, v)^{\frac{1}{2}}$$

**Definition 2.1.** (*The differential filter  $\overline{\cdot}$* ) Given  $\phi \in L^2(\Omega)$  and a filtering radius  $\delta$ , define the average of  $\phi$ ,  $\overline{\phi}$ , to be the unique  $L$ -periodic solution of

$$-\delta^2 \Delta \overline{\phi} + \overline{\phi} = \phi \tag{2.5}$$

This filtering operation will also be denoted by  $\overline{\phi} = A^{-1}\phi$  for ease of notation. Note  $A = (-\delta^2 \Delta + I)$  is self adjoint.

This is a popular filter used in analysis of LES models [21],[20],[10],[17], although its practicality is sometimes called into question. The use of this specific filter is essential for all results in this chapter with two exceptions: the Leray and Leray-deconvolution models conserve energy for inviscid flow regardless of the filter choice, provided filtered quantities remain in  $H^1$ . Specifying a filter is necessary when showing cascades for model quantities, and thus the results found here can be considered a first step in developing cascade theory for quantities which are exactly conserved in a model. However, for a general filter with an explicit inverse, the analysis used would take the same general form as that found in this chapter, although any specific results would be filter dependent.

**Definition 2.2.** (The approximate deconvolution operator  $D_N$ ) For a fixed finite  $N$ , define the  $N^{\text{th}}$  approximate deconvolution operator by

$$D_N\phi = \sum_{n=0}^N (I - A^{-1})^n \phi$$

Note that since  $A$  is self adjoint,  $D_N$  is also.  $D_N$  was shown to be an  $O(\delta^{2N+2})$  approximate inverse to the filter operator in [20].

**Corollary 2.1.**  $D_N$  is compact, positive, and is an asymptotic inverse to the filter  $A^{-1}$ : for very smooth  $\phi$  and as  $\delta \rightarrow 0$ ,

$$\phi = D_N \bar{\phi} + (-1)^{(N+1)} \delta^{2N+2} \Delta^{N+1} A^{-(N+1)} \phi$$

The proof of Corollary 2.1 is found in [20].

**Lemma 2.1.**  $\|\cdot\|_N$  defined by  $\|v\|_N = (v, D_N v)$  is a norm on  $\Omega$  equivalent to the  $L^2(\Omega)$  norm, and  $(\cdot, \cdot)_N$  defined by  $(v, w)_N = (v, D_N w)$  is an inner product on  $\Omega$ .

*Proof.* See [10], Lemma 8.2 for proof that  $\|\cdot\|_{D_N}$  is a norm. This fact coupled with the linearity of  $G_N$  immediately implies  $(\cdot, \cdot)_{G_N}$  is an inner product.  $\square$

The next lemma gives four useful vector identities which are used throughout this chapter.

**Lemma 2.2.** For sufficiently smooth  $u$ ,

$$u \cdot \nabla u = \frac{1}{2} \nabla u^2 - u \times (\nabla \times u) \quad (2.6)$$

For sufficiently smooth, periodic  $u, v$ ,

$$(u, \nabla \times v) = (\nabla \times u, v) \quad (2.7)$$

For sufficiently smooth, periodic  $u, v$  with  $v$  divergence free,

$$(u, \Delta v) = -(\nabla \times u, \nabla \times v) \quad (2.8)$$

For sufficiently smooth, periodic, two dimensional divergence free  $u$ ,

$$(u \cdot \nabla u, \Delta u) = 0 \quad (2.9)$$

For proofs, see, for example, [22],[25].

Note that  $u^2$  is a commonly used notation for  $u \cdot u$ .

### 2.2.1 The Models Considered

We have now provided enough preliminaries to define the four LES models considered as well as the respective models' energies, helicities and enstrophies. As discussed in the introduction, inviscid conservation of a quantity is essential for the quantity to be cascaded accurately through the inertial range. This is the motivation for our definitions of *model* quantities similar to the usual energy, helicity, and enstrophy.

In the ADM, due to the complexity of the model, finding conservation of the usual quantities is difficult, and may not even be possible. However, the model quantities we define are conserved, and thus an analysis of their cascades may be possible. What gives these quantities physical relevance is the fact that, with assumptions on solution smoothness, the quantities are all “close” to the usual ones – and thus the usual quantities are at least close to being conserved.

Similarly in the Leray model, we give two different definitions of enstrophy. The first is the usual one, but this quantity was found only to be asymptotically conserved. The second definition, with smoothness assumptions, is similar to the usual one, but yields an exactly conserved quantity.

Note that we present the models without the “corrections” typically used with them (i.e. relaxation term with the ADM, mixed models, etc.) which add necessary dissipation. This is done because our interest here is for conservation in the inertial range.

**Definition 2.3.** *The Stolz-Adams ADM:*

*The ADM is given by*

$$v_t + \overline{D_N v \cdot \nabla D_N v} + \nabla q - \nu \Delta v = 0, \quad \nabla \cdot v = 0. \quad (2.10)$$

**Definition 2.4.** *The Leray/Leray- $\alpha$  model:*

*The Leray model is given by*

$$v_t + \bar{v} \cdot \nabla v + \nabla q - \nu \Delta v = 0, \quad \nabla \cdot v = 0. \quad (2.11)$$

The name Leray-alpha corresponds to the Leray model with the use of the filter (2.5). Our analysis is restricted to this so-called Leray-alpha model, although the Leray model itself has been used with a number of different filters.

**Definition 2.5.** *The Bardina scale similarity model*

*The Bardina scale similarity model is given by*

$$v_t + v \cdot \nabla v + \nabla q - \nu \Delta v + \nabla \cdot (\overline{v\overline{v}} - \overline{v}\overline{v}) = 0, \quad \nabla \cdot v = 0. \quad (2.12)$$

**Definition 2.6.** *(Leray-deconvolution Model)*

*The Leray devonvolution model is defined to be*

$$v_t + D_N \overline{v} \cdot \nabla v + \nabla q - \nu \Delta v = 0, \quad \nabla \cdot v = 0. \quad (2.13)$$

The model energies, helicities, and enstrophies defined in a usual form are

$$\begin{aligned} E_{Leray}, E_{LD}, E_{Bard} &:= \frac{1}{2} \|v\|^2, \\ H_{Leray}, H_{LD}, H_{Bard} &:= (v, \nabla \times v), \\ EnS_{Leray}, EnS_{LD}, EnS_{Bard} &:= \frac{1}{2} \|\nabla \times v\|^2, \end{aligned}$$

where  $v$  is a solution to a respective model. As stated above, the model energy, helicity and enstrophy for the ADM take a slightly different form, as does a definition for a filtered enstrophy for the Leray model. These quantities are important because it is these which are exactly conserved, and hence it is these quantities for which cascades can be considered. We define them as

$$\begin{aligned} E_{ADM} &= \|v\|_N^2 + \delta^2 \|\nabla v\|_N, \\ H_{ADM} &= (v, \nabla \times v)_N + \frac{\delta^2}{2} (\nabla \times v, (\nabla \times)^2 v)_N, \\ EnS_{ADM} &= \frac{1}{2} \|\nabla \times v\|_N^2 + \frac{\delta^2}{2} \|\Delta v\|_N, \\ \overline{v} EnS_{Leray} &= \frac{1}{2} \|\nabla \times \overline{v}\|^2 + \frac{\delta^2}{2} \|\Delta \overline{v}\|^2, \end{aligned}$$

## 2.3 CONSERVATION LAWS

We develop conservation laws for the models considered together for momentum, mass, energy, helicity and enstrophy. The conservation laws are presented for inviscid flow (i.e.  $\nu = 0$  or the Euler equations) and without external force ( $f = 0$ ). However, we leave  $\nu$  arbitrarily non-negative until the final step of each proof, as the case when dissipation is present is also of interest because it gives a clue about the decay of these quantities in the presence of dissipation.

Also note that throughout the analysis in this Chapter, we extensively use the fact that under periodic boundary conditions, differential operators commute.

### 2.3.1 Momentum and Mass

Solutions to each of the models conserve momentum and mass. The conservation of a model mass comes directly from  $\nabla \cdot v = 0$ . Conservation of momentum follows for each model because each term in all the models, except for the time derivative term, is a spatial derivative (the nonlinear terms all can be expressed as spatial derivatives because of the commutation of differential operators under periodic boundary conditions coupled with the constraint that  $v$  be divergence free). Hence, integrating the first equation of each model over  $\Omega$  vanishes all terms except the time derivative. Hence if  $v$  is a solution to any of the models, we have the relation

$$\frac{d}{dt} \int_{\Omega} v = 0$$

for that model. Thus integrating this equation from 0 to  $T$  yields

$$\int_{\Omega} v(T, x) = \int_{\Omega} v(0, x),$$

which establishes conservation of model momentum.

### 2.3.2 Energy

The ADM, Leray and Leray deconvolution models *exactly* conserve a model energy, whereas the Bardina model conserves a model energy only approximately (asymptotically as  $\delta \rightarrow 0$ ). For smooth flows and as  $\delta \rightarrow 0$ , the energy estimate for the Bardina model of three dimensional flow is  $O(\delta^2)$ , and for two dimensional flow is  $O(\delta^4)$ . However, for flows with chaotic behavior or when large  $\delta$  is required, a blow up to infinity of  $E_{Bardina}$  cannot be ruled out.

**Theorem 2.1.** *The following energy conservation laws hold,  $\forall T > 0$ , when  $\nu = f = 0$ .*

$$E_{ADM}(T) = E_{ADM}(0)$$

$$E_{Leray}(T) = E_{Leray}(0)$$

$$E_{LD}(T) = E_{LD}(0)$$

*The Bardina model satisfies*

$$\begin{aligned} E_{Bardina}^{3d}(T) &= E_{Bardina}^{3d}(0) - \int_0^T \{2\delta^2(\bar{v} \cdot \nabla \bar{v}, \Delta \bar{v}) - \delta^4((\Delta \bar{v}) \cdot \nabla \bar{v}, \Delta \bar{v})\} dt \\ E_{Bardina}^{2d}(T) &= E_{Bardina}^{2d}(0) + \delta^4 \int_0^T \{((\Delta \bar{v}) \cdot \nabla \bar{v}, \Delta \bar{v})\} dt \end{aligned}$$

*Proof.* For the ADM, multiplying (2.10) by its solution  $AD_N v$  and integrating over  $\Omega$ , we obtain

$$(v_t, AD_N v) + \overline{(D_N v \cdot \nabla D_N v, AD_N v)} + (\nabla q, AD_N v) - \nu(\Delta v, AD_N v) = 0. \quad (2.14)$$

As the operator  $A$  is self adjoint, the nonlinear term in (2.14) vanishes.

$$\overline{(D_N v \cdot \nabla D_N v, AD_N v)} = (D_N v \cdot \nabla D_N v, D_N v) = 0$$

The pressure term also vanishes, which can be seen by applying Green's Theorem, and using commutativity of the differential operators under periodic boundary conditions.

$$(\nabla q, AD_N v) = -(q, \nabla \cdot AD_N v) = (q, AD_N(\nabla \cdot v)) = 0$$

The time derivative and dissipation terms do not vanish, and so we rewrite (9) and simplify by decomposing  $A$ .

$$-\delta^2(v_t, \Delta D_N v) + (v_t, D_N v) + \delta^2 \nu(\Delta v, \Delta D_N v) - \nu(\Delta v, D_N v) = 0$$

Green's Theorem and the fact that  $\Delta$  and  $D_N v$  commute under periodic boundary conditions allows this to be written as

$$\frac{1}{2} \frac{d}{dt} \|v\|_N^2 + \frac{\delta^2}{2} \frac{d}{dt} \|\nabla v\|_N^2 = -\nu \|\nabla v\|_N^2 - \delta^2 \nu \|\Delta v\|_N^2. \quad (2.15)$$

Setting  $\nu = 0$  and integrating over time in (10) gives the stated result.

For Leray and Leray deconvolution energy, the stated laws follow immediately by simply multiplying each model by its respective solution, integrating over the domain, setting  $\nu = 0$ , and integrating over time. Note that we do not use any properties of the filter for these results.

For Bardina, we begin by multiplying (2.12) by  $v$ , where  $v$  solves (2.12), and integrate over the domain. As with the other models, the pressure term vanishes, leaving

$$\frac{1}{2} \frac{d}{dt} \|v\|^2 + \nu \|\nabla \times v\|^2 + (\overline{v \cdot \nabla v}, v) + (\bar{v} \cdot \nabla \bar{v}, v) = 0.$$

Repeatedly applying the identity  $v = A\bar{v}$  and the fact that under periodic boundary conditions the filter commutes with differential operators, followed by simplifying allows this to be written as

$$\frac{d}{dt} E_{Bard} + \nu \|\nabla \times v\|^2 + 2\delta^2 (\bar{v} \cdot \nabla \bar{v}, \Delta \bar{v}) - \delta^4 ((\Delta \bar{v}) \cdot \nabla \bar{v}, \Delta \bar{v}) = 0$$

Setting  $\nu = 0$  and integrating over time now gives the 3d result. In 2d, note that by Lemma 2.2,  $(\bar{v} \cdot \nabla \bar{v}, \Delta \bar{v}) = 0$ . Making this substitution gives the 2d result.  $\square$

### 2.3.3 Helicity

We now present the helicity conservation of the models. Only the ADM was found to exactly conserve a model helicity. The other three models were found to only approximately (asymptotically as  $\delta \rightarrow 0$ ) conserve a model helicity. For each of these other three models, a blow up of helicity cannot be ruled out in this analysis.

**Theorem 2.2.** *For  $\nu = f = 0$ , the ADM conserves a model helicity:  $\forall T > 0$ .*

$$H_{ADM}(T) = H_{ADM}(0)$$

The remaining models satisfy,  $\forall T > 0$ ,

$$\begin{aligned} H_{Leray}(T) &= H_{Leray}(0) + 2\delta^2 \int_0^T ((\bar{v} \cdot \nabla v, \nabla \Delta \bar{v}) + (\bar{v} \cdot \nabla(\Delta \bar{v}), \nabla \times \bar{v})) dt \\ H_{Bardina}(T) &= H_{Bardina}(0) - 2\delta^2 \int_0^T ((v + \bar{v}) \cdot \nabla(\nabla \times \bar{v}), \nabla \times \Delta \bar{v}) dt \\ H_{LD}(T) &= H_{LD}(0) + (-2)^N \delta^{2N+2} \int_0^T (\Delta^{N+1} A^{-(N+1)} v \cdot \nabla v, \nabla \times v) dt \end{aligned}$$

*Proof.* The proof for ADM helicity is similar to that of ADM energy. Multiply (2.10) by  $(\nabla \times AD_N v)$ , where  $v$  solves (2.10), and integrate over  $\Omega$ .

$$\begin{aligned} (v_t, \nabla \times AD_N v) + \overline{(D_N v \cdot \nabla D_N v, \nabla \times AD_N v)} + \\ (\nabla q, \nabla \times AD_N v) - \nu(\Delta v, \nabla \times AD_N v) = 0 \end{aligned} \quad (2.16)$$

As in the energy proof, the nonlinear term vanishes. To show this, we use the commutativity of differential operators under periodic boundary conditions, the fact that  $A$  is self adjoint, and apply Lemma 2.2.

$$\begin{aligned} &\overline{(D_N v \cdot \nabla D_N v, \nabla \times AD_N v)} \\ &= (D_N v \cdot \nabla D_N v, \nabla \times D_N v) \\ &= \left(\frac{1}{2} \nabla((D_N v)^2), \nabla \times D_N v\right) - (D_N v \times (\nabla \times D_N v), \nabla \times D_N v) \\ &= \frac{1}{2} (\nabla \times \nabla((D_N v)^2), D_N v) - 0 \\ &= 0 \end{aligned}$$

The pressure term also vanishes.

$$(\nabla q, \nabla \times AD_N v) = (\nabla \times (\nabla q), AD_N v) = 0$$

The time derivative term is simplified using commutativity of the differential operators after decomposing  $A$  and applying Lemma 2.2.

$$\begin{aligned} (v_t, \nabla \times (-\delta^2 \Delta + I)D_N v) &= -\delta^2 (v_t, \nabla \times \Delta(D_N v)) + (v_t, \nabla \times D_N v) \\ &= \delta^2 ((\nabla \times v)_t, \nabla \times D_N (\nabla \times v)) + (v_t, \nabla \times D_N v) \\ &= \frac{\delta^2}{2} \frac{d}{dt} (\nabla \times v, \nabla \times)^2 v)_N + \frac{1}{2} \frac{d}{dt} (v, \nabla \times v)_N \end{aligned}$$

The dissipation term simplifies by decomposing  $A$  and applying Lemma 2.2.

$$\begin{aligned} -\nu(\Delta v, \nabla \times AD_N v) &= \delta^2 \nu(\Delta v, \nabla \times (\Delta G_n v)) - \nu(\Delta v, \nabla \times D_N v) \\ &= \delta^2 \nu ((\nabla \times)^2 v, (\nabla \times)^3 v)_N + \nu (\nabla v, (\nabla \times)^2 v)_N \end{aligned} \quad (2.17)$$

Recombining all the terms and setting  $\nu = 0$  gives

$$\frac{\delta^2}{2} \frac{d}{dt} (\nabla \times v, \nabla \times)^2 v)_N + \frac{1}{2} \frac{d}{dt} (v, \nabla \times v)_N = 0 \quad (2.18)$$

Integrating over time give the stated conservation law.

For the Leray helicity relation, we multiply (2.11) by the curl of its solution,  $(\nabla \times v)$ , and integrate over the domain. After simplifying, this yields

$$\frac{1}{2} \frac{d}{dt} (v, \nabla \times v) = -\nu(\nabla \times v, (\nabla \times)^2 v) - (\bar{v} \cdot \nabla v, \nabla \times v) \quad (2.19)$$

Expand the nonlinear term by using the identity  $v = A\bar{v}$  and simplifying.

$$\begin{aligned} (\bar{v} \cdot \nabla v, \nabla \times v) &= (\bar{v} \cdot \nabla v, \nabla \times A\bar{v}) \\ &= -\delta^2 (\bar{v} \cdot \nabla v, \nabla \times \Delta \bar{v}) + (\bar{v} \cdot \nabla v, \nabla \times \bar{v}) \\ &= -\delta^2 (\bar{v} \cdot \nabla v, \nabla \times \Delta \bar{v}) - \delta^2 (\bar{v} \cdot \nabla (\Delta \bar{v}), \nabla \times \bar{v}) \end{aligned}$$

Recombining terms and setting  $\nu = 0$  gives

$$\frac{1}{2} \frac{d}{dt} = \delta^2 (\bar{v} \cdot \nabla v, \nabla \times \Delta \bar{v}) + \delta^2 (\bar{v} \cdot \nabla (\Delta \bar{v}), \nabla \times \bar{v}) \quad (2.20)$$

Integrating over time will now give the stated Leray helicity conservation.

For Bardina, multiply (2.12) by  $(\nabla \times v)$ , where  $v$  solves (2.12), and integrate over the domain. Then using Lemma 2.2 to decompose the nonlinearity and simplifying gives

$$\begin{aligned} \frac{1}{2} \frac{d}{dt} (v, \nabla \times v) + \nu (\nabla \times v, \nabla \times \nabla \times v) \\ - \overline{(v \times (\nabla \times v), \nabla \times v)} + (\bar{v} \times (\nabla \times \bar{v}), \nabla \times v) = 0. \end{aligned} \quad (2.21)$$

Using the identity  $v = A\bar{v}$  and properties of the cross product, (2.21) becomes

$$\begin{aligned} \frac{1}{2} \frac{d}{dt} (v, \nabla \times v) + \nu (\nabla \times v, \nabla \times \nabla \times v) \\ + \delta^2 (v \times (\nabla \times \Delta \bar{v}), \nabla \times \bar{v}) - \delta^2 (\bar{v} \times (\nabla \times \bar{v}), \nabla \times \Delta \bar{v}) = 0. \end{aligned} \quad (2.22)$$

Thus combining the two trilinear terms and setting  $\nu = 0$  gives

$$\frac{d}{dt} H_{Bard} = -2\delta^2 ((v + \bar{v}) \times (\nabla \times \Delta \bar{v}), \nabla \times \bar{v}).$$

Integrating over time now gives the Bardina helicity result.

For the Leray deconvolution model, the analysis is exactly the same as the Leray model except for the nonlinear term, after multiplying (2.13) by the curl of its solution. The nonlinear term can be written as

$$(D_N \bar{v} \cdot \nabla v, \nabla \times v) = ((v - (-1)^{N+1} \delta^{2N+2} \Delta^{N+1} A^{-(N+1)} v) \cdot \nabla v, \nabla \times v). \quad (2.23)$$

Thus we have the stated result, since  $(v \cdot \nabla v, \nabla \times v) = 0$ . □

### 2.3.4 Enstrophy

The ADM exactly conserves a 2d model enstrophy. Although the Leray model does not exactly conserve a “usual” model enstrophy, a quantity similar to enstrophy is exactly conserved. As in the helicity case, the other models have approximate laws which may not be useful without restrictive assumptions on the size of higher derivatives and the size of  $\delta$ .

**Theorem 2.3.** *The ADM conserves enstrophy in 2d, and the Leray model conserves a quantity similar to enstrophy:  $\forall T > 0$  and for  $\nu = f = 0$ ,*

$$\begin{aligned} Ens_{ADM}(T) &= Ens_{ADM}(0) \\ \bar{v}Ens_{Leray}(T) &= \bar{v}Ens_{Leray}(0) \end{aligned}$$

The remaining models, in 2d, satisfy

$$\begin{aligned} Ens_{Bard}(T) &= Ens_{Bard}(0) + \delta^2 \int_0^T ((\bar{v} \cdot \bar{v}, \Delta^2 \bar{v}) - (\Delta \bar{v} \cdot \nabla \bar{v}, \Delta \bar{v})) dt \\ Ens_{LD}(T) &= Ens_{LD}(0) + (-1)^N \delta^{2N+2} \int_0^T (\Delta^{N+1} A^{-(N+1)} v \cdot \nabla v, \Delta v) dt \\ Ens_{Leray}(T) &= Ens_{Leray}(0) - \int_0^T (\delta^2 (\bar{v} \cdot \nabla \bar{v}, \Delta^2 \bar{v}) - \delta^4 (\bar{v} \cdot \nabla (\Delta \bar{v}), \Delta^2 \bar{v})) dt \end{aligned}$$

*Proof.* To prove the (2d) ADM enstrophy relation, we multiply (2.10) by  $\Delta A D_N v$  where  $v$  solves (2.10) and integrate over  $\Omega$ .

$$\begin{aligned} (v_t, \Delta A D_N v) + (\overline{D_N v \cdot \nabla D_N v}, \Delta A D_N v) + (\nabla q, \Delta A D_N v) \\ - \nu (\Delta v, \Delta A D_N v) = 0 \end{aligned} \quad (2.24)$$

The nonlinear term is handled differently than in any of the previous proofs, and it is this term which makes the stated enstrophy relation hold only in two dimensions (it does not necessarily vanish in 3d). We use that  $A$  is self adjoint,  $A$  and  $\Delta$  commute, and that  $D_N v$  is two dimensional.

$$\begin{aligned} (\overline{D_N v \cdot \nabla D_N v}, \Delta A D_N v) &= (D_N v \cdot \nabla D_N v, \Delta D_N v) \\ &= 0 \end{aligned}$$

The pressure vanishes.

$$(\nabla q, \Delta AD_N v) = -(\nabla \times \nabla q, \nabla \times AD_N v) = 0$$

For the time derivative, decompose  $A$ , apply Lemma 2.2, and simplify.

$$\begin{aligned} (v_t, \Delta AD_N v) &= -\delta^2 (v_t, \Delta \Delta D_N v) + (v_t, \Delta D_N v) \\ &= -\delta^2 ((\Delta v)_t, \Delta v) - ((\nabla \times v)_t, \nabla \times v) \\ &= -\frac{\delta^2}{2} \frac{d}{dt} \|\Delta v\|_N^2 - \frac{1}{2} \frac{d}{dt} \|\nabla \times v\|_N^2 \end{aligned}$$

The dissipation term also requires decomposition of  $A$  and Lemma 2.2.

$$\begin{aligned} -\nu(\Delta v, \Delta AD_N v) &= -\delta^2 \nu (\nabla \times \Delta v, \nabla \times \Delta D_N v) + \nu (\nabla \times \Delta D_N v, \nabla \times D_N v) \\ &= -\delta^2 \nu \|\nabla \times \Delta v\|_N^2 - \nu \|\Delta D_N v\|_N \end{aligned} \quad (2.25)$$

Recombining the terms and setting  $\nu = 0$  gives

$$\frac{1}{2} \frac{d}{dt} \|\nabla \times v\|_N^2 + \frac{\delta^2}{2} \frac{d}{dt} \|\Delta v\|_N^2 = 0. \quad (2.26)$$

Integrating over time now gives the stated ADM 2d enstrophy conservation law.

For the Leray  $\bar{v}Ens_{Leray}$  enstrophy result, multiply (2.11) by  $\Delta \bar{v}$ , where  $v$  solves (2.11), integrate over the domain, and write  $v = A\bar{v}$  in the time derivative and viscosity terms.

$$((A\bar{v})_t, \Delta \bar{v}) + (\bar{v} \cdot \nabla(A\bar{v}), \Delta \bar{v}) + (q, \Delta \bar{v}) - \nu(\Delta(A\bar{v}), \Delta \bar{v}) = 0$$

Next decompose each  $A$ , and simplify. The pressure term vanishes by applying Lemma 2.2.

$$\begin{aligned} (\bar{v}_t, \Delta \bar{v}) - \delta^2 (\Delta \bar{v}_t, \Delta \bar{v}) - \delta^2 (\bar{v} \cdot \nabla(\Delta \bar{v}), \Delta \bar{v}) + (\bar{v} \cdot \nabla \bar{v}, \Delta \bar{v}) \\ - \nu \delta^2 \|\nabla \times (\Delta \bar{v})\|^2 - \nu \|\Delta \bar{v}\|^2 = 0 \end{aligned}$$

Since both trilinear terms vanish, this expression can be simplified and rewritten as

$$\frac{1}{2} \frac{d}{dt} \|\nabla \times \bar{v}\|^2 + \delta^2 \|\Delta \bar{v}\|^2 = -\nu \|\Delta \bar{v}\|^2 - \delta^2 \|\nabla \times \Delta \bar{v}\|^2$$

Setting  $\nu = 0$  and integrating over time gives the result.

For the Leray-deconvolution enstrophy, multiply (2.13) by  $\Delta v$ , where  $v$  solves (2.13), integrate over the domain, and simplify. This gives

$$\frac{1}{2} \frac{d}{dt} \|\nabla v\|^2 = -\nu \|\Delta v\|^2 + (D_N \bar{v} \cdot \nabla v, \Delta v) \quad (2.27)$$

For the nonlinear term, we reduce by expanding the  $D_N \bar{v}$  term.

$$(D_N \bar{v} \cdot \nabla v, \Delta v) = (v - (-1)^{N+1} \delta^{2N+2} \Delta^{N+1} A^{-(N+1)} v \cdot \nabla v, \Delta v) \quad (2.28)$$

Applying Lemma 2.2, setting  $\nu = 0$  and integrating over time will then give the desired result.

For the Bardina model, multiply (2.12) by  $\Delta v$ , where  $v$  solves (2.12), and integrate over the domain. Since the pressure term and first nonlinear term vanish, we have

$$\frac{1}{2} \frac{d}{dt} \|\nabla \times v\|^2 + \nu \|\Delta v\|^2 = (\overline{v \cdot \nabla v}, \Delta v) - (\bar{v} \cdot \nabla \bar{v}, \Delta v). \quad (2.29)$$

In the first trilinear term, we substitute  $\Delta v = \Delta A \bar{v} = A \Delta \bar{v}$ , and use the fact that  $A$  is self adjoint. This gives

$$\frac{1}{2} \frac{d}{dt} \|\nabla \times v\|^2 + \nu \|\Delta v\|^2 = (v \cdot \nabla v, \Delta \bar{v}) - (\bar{v} \cdot \nabla \bar{v}, \Delta v) \quad (2.30)$$

Repeatedly using the identity  $v = A \bar{v}$  and using Lemma 2.2 reduces (2.30) to

$$\frac{d}{dt} En_{S_{Bard}} = \delta^2 ((\Delta \bar{v} \cdot \nabla \bar{v}, \Delta \bar{v}) - (\bar{v} \cdot \nabla \bar{v}, \Delta^2 \bar{v})) - \nu \|\Delta v\|^2 \quad (2.31)$$

Setting  $\nu = 0$  and integrating over time now yields the stated Bardina enstrophy result.

For the usual Leray enstrophy, multiply (2.11) by  $\Delta v$ , where  $v$  solves (2.11), and integrate over the domain. Since the pressure term drops, we have

$$\frac{d}{dt} En_{S_{Leray}} + \nu \|\Delta v\|^2 = (\bar{v} \cdot \nabla v, \Delta v). \quad (2.32)$$

Use of Lemma 2.2 and repeated substitutions of  $v = A \bar{v}$  gives

$$\frac{d}{dt} En_{S_{Leray}} = -\delta^2 (\bar{v} \cdot \bar{v}, \Delta^2 \bar{v}) + \delta^4 (\bar{v} \cdot \nabla (\Delta \bar{v}), \Delta^2 \bar{v}) - \nu \|\Delta v\|^2. \quad (2.33)$$

Setting  $\nu = 0$  and integrating over time gives the result for the usual Leray enstrophy.  $\square$

## 2.4 CONCLUSIONS

This chapter studied conservation laws in the Bardina, ADM, Leray and Leray deconvolution models in an effort to establish which of these models had conservation laws analogous to those of the Navier Stokes equations. Only the ADM was found to exactly conserve a model helicity, and only the ADM and Leray models exactly conserved a model enstrophy. The Bardina model was the only model found to not conserve a model energy. The Leray and Leray-deconvolution results for the conservation of energy are not limited to the filter used throughout this chapter, and hold for any smoothing filter.

Since inviscid conservation is a first and necessary step for a quantity to cascade through the inertial range, our results show that new cascade theories may be possible for the ADM model quantities, and for an enstrophy-like quantity in the Leray model. The next chapter is an examination of the joint helicity-energy cascade in the ADM.

### 3.0 THE JOINT ENERGY-HELICITY CASCADE IN THE ADM

#### 3.1 INTRODUCTION

We consider in this chapter aspects of flow statistics and the physical fidelity related to the coherent rotational structures and integral invariants (helicity and helicity statistics) predicted by a family of parameter free large eddy simulation models of turbulence. Broadly speaking, if  $\delta$  is the (user-selected) filter length scale and *overbar* denotes the associated local, spacial averaging, the true averages,  $\bar{u}$ ,  $\bar{p}$ , of an incompressible viscous fluid satisfy the well known Space Filtered Navier-Stokes equations given by

$$\bar{u}_t + \nabla \cdot (\overline{u u}) - \nu \Delta \bar{u} + \nabla \bar{p} = \bar{f} \quad \text{and} \quad \nabla \cdot \bar{u} = 0. \quad (3.1)$$

The closure problem (which occurs since  $\overline{u u} \neq \bar{u} \bar{u}$ ) leads to the deconvolution problem:

$$\text{given } \bar{u}, \text{ find } u \text{ (approximately)}. \quad (3.2)$$

Calling this approximate deconvolution of  $\bar{u}$ ,  $D(\bar{u})$ :

$$\text{approximation to } u = D(\bar{u}),$$

an approximate solution to the closure problem is then  $\overline{u u} \approx \overline{D(\bar{u}) D(\bar{u})}$ . The LES model induced is to find  $(v, q)$  (sought to approximate  $(\bar{u}, \bar{p})$ ) satisfying

$$v_t + \nabla \cdot (\overline{D(v) D(v)}) - \nu \Delta v + \nabla q = \bar{f} \quad \text{and} \quad \nabla \cdot v = 0 \quad (3.3)$$

with initial condition  $v(x, 0) = v_0(x)$ . Here we take  $\Omega = (0, L)^3$  and impose periodic boundary conditions on all variables (with the usual normalization condition of the periodic case  $\int_{\Omega} \phi = 0$ ,  $\phi = v, v_0, f$  and  $q$ )

The deconvolution problem (3.2) is typically ill-posed and any method for approximate solution of an ill-posed problem can be tested as a Large Eddy Simulation (LES) model in (3.3). We study herein the family ( $N = 0, 1, 2, \dots$ ) of Approximate Deconvolution Models (ADM), introduced in LES by Stolz and Adams [2], [3], based on the van Cittert algorithm, see Bertero and Boccacci [11]. This deconvolution operator,  $D_N$ , which we define in (2.2) satisfies the consistency condition (for  $N = 0, 1, 2, \dots$ ):

$$u = D_N(\bar{u}) + O(\delta^{2N+2}) \quad \text{for smooth } u,$$

and thus  $\overline{u u} = \overline{D_N(\bar{u}) D_N(\bar{u})} + O(\delta^{2N+2})$ . This model has remarkable mathematical properties and its accuracy has been established in the tests of Stolz and Adams [2], [3] and the theoretical studies in the work of Dunca and Epshteyn [20] and [35].

In this chapter, we study the joint energy-helicity cascade for homogeneous, isotropic turbulence generated by the Stolz-Adams approximate deconvolution models (ADM). Our goal is to give a comparison of the energy and helicity statistics of ADM's to the true flow statistics and a comparison of their respective energy and helicity cascades.

Both energy,

$$E(t) := \frac{1}{2L^3} \int_{\Omega} |u(\mathbf{x}, t)|^2 d\mathbf{x}, \quad (3.4)$$

and helicity,

$$H(t) := \frac{1}{L^3} \int_{\Omega} u(\mathbf{x}, t) \cdot (\nabla \times u(\mathbf{x}, t)) d\mathbf{x}, \quad (3.5)$$

are conserved by the Euler equations and dissipated (primarily at the small scales) by viscosity. It is widely believed that both cascades, André and Lesieur [5], and the details of their respective cascades are intertwined. Recent studies of Bourne and Orszag in [12] have suggested that for homogeneous, isotropic turbulence averaged fluid velocities exhibit a joint energy and helicity cascade through the inertial range of wave numbers given by

$$E(k) = C_E \epsilon^{2/3} k^{-5/3}, \quad H(k) = C_H \gamma \epsilon^{-1/3} k^{-5/3}, \quad (3.6)$$

where  $k$  is wave number,  $\epsilon$  the mean energy dissipation, and  $\gamma$  the mean helicity dissipation, see also Q. Chen, S. Chen and Eyink [15], Q. Chen, S. Chen, Eyink and Holm [16], Ditlevsen

and Giuliani [19]. The cascades are referred to as “joint” because they travel with the same speed through wave space (i.e. the exponents of  $k$  are equal). The energy cascade given in (3.6) is the famous Kolmogorov cascade, and the work of Q. Chen, S. Chen and Eyink [15] showed that the helicity cascade in (3.6) is consistent for wave numbers up to the standard Kolmogorov wave number,  $k_E = \nu^{-3/4} \epsilon^{1/4}$ , where  $\nu$  is the fluid viscosity. Herein, we explore the existence and details of a comparable joint cascade in the ADM (3.3), to examine if this qualitative feature of the NSE is matched in the ADM.

Exact conservation of helicity for a turbulence model, a first and necessary step for correct helicity cascade statistics, was studied in [52] for the ADM, Leray, Leray-deconvolution, and the Bardina LES models. This work shows that all these models exactly conserve a model mass and model momentum. However, of these only the ADM exactly conserves helicity in the absence of viscosity and external forces, implying that the existence of a helicity cascade is possible.

Other authors have compared LES model energy cascades to energy cascades of the NSE. This was pioneered by Muschinsky [48] for the Smagorinsky model. In [17] by Cheskidov, Holm, Olson and Titi the energy cascade of the Leray- $\alpha$  model was explored, as was the energy cascade of the ADM (3.3) in [37] and associated regularization in [38]. The work in [37] found that, with some key assumptions, the energy cascade in the ADM is identical to that of the NSE up to the cutoff length scale of  $\delta$ , and begins to truncate scales like  $k^{-11/3}$  for length scales  $< \delta$ , until viscosity takes over at a length scale larger than  $\eta_{Kolmogorov}$ . The effects of time relaxation on scale truncation was explored using similar tools in [38]. There are many other applications of  $K41$  phenomenology to understanding LES models, Sagaut [53].

The study of helicity in fluid flow and turbulence has only recently begun. It was not until 1961 that helicity’s inviscid invariance was discovered by Moreau [47], and two decades later Moffatt gave the topological interpretation of helicity [45]: helicity is nonzero if and only if the flow is not reflectionally symmetric. This topological interpretation leads to the commonly accepted interpretation of helicity: it is the degree to which the vortex lines are knotted and intertwined. Another interesting and important feature of helicity is that it is a *rotationally* meaningful quantity that can be checked for accuracy in a simulation. Moffat

and Tsouber gave a good summary of the early results on helicity in [46].

In this study, we show that solutions of the ADM possess a joint energy/helicity cascade that is asymptotically (in the filter width  $\delta$ ) equivalent to that of the NSE. In [37], it is shown that there exists a piecewise cascade for energy in the ADM; that is, up to wave number  $\frac{1}{\delta}$ , i.e., over the resolved scales, the ADM cascades energy in the same manner as in the NSE ( $k^{-5/3}$ ). However, after this wave number and up to the model's microscale, the ADM cascades energy at a faster rate ( $k^{-11/3}$ ). Interestingly, the results for helicity in the ADM are analogous; helicity is cascaded at the correct rate of  $k^{-5/3}$  for wave numbers less than  $\frac{1}{\delta}$ , and for higher wave numbers up to the model's microscale, helicity is cascaded at a rate of  $k^{-11/3}$ . This  $k^{-11/3}$  rate of enhanced decay is filter dependent, Section 3.6.1. We deduce the microscale helicity in the ADM and we also show that the helicity cascade is consistent (in the sense introduced by Q. Chen, S. Chen and Eyink [15]) up to the model's energy microscale.

Section 2 gives notation and preliminaries and shows how the deconvolution operator renormalizes the energy. Section 3 gives properties of the ADM, Section 4 derives the joint cascade of energy and helicity in the ADM, Section 5 shows how the ADM truncates scales for helicity, and Section 6 presents conclusions.

### 3.2 NOTATION AND PRELIMINARIES

The  $L^2(\Omega)$  norm is denoted (as usual) by  $\|\phi\| = (\int_{\Omega} |\phi(x)|^2 dx)^{1/2}$  and the deconvolution weighted  $L^2$ -norm is denoted by  $\|\phi\|_N := (\phi, D_N \phi)^{1/2}$ , where  $D_N$  is defined precisely in Section 3.2.2. Every other norm will be explicitly indicated. The space  $L^2_0(\Omega)$  contains functions in  $L^2(\Omega)$  with zero mean.

Given two real quantities  $A, B$  (such as energy and helicity) we shall write

$$A \simeq B$$

if there are positive constants  $C_1, C_2$  depending only on  $N$  (which is fixed) with

$$C_1(N)A \leq B \leq C_2(N)A.$$

For example, in Section 3.2.2 we show that

$$\|\phi\| \leq \|\phi\|_N \leq \sqrt{N+1}\|\phi\|, \quad \forall \phi \in L^2(\Omega),$$

which is written as  $\|\phi\| \simeq \|\phi\|_N$ .

### 3.2.1 Nomenclature

The nomenclature used is standard and defined where first used herein. We briefly give a summary of it next.

$u, p$  : The true velocity and pressure, solutions of the underlying Navier-Stokes equations.

$v, q$  : The continuum velocity and pressure predicted by the LES model.

$\delta$  : The averaging radius of the filter used in the LES model.

$\hat{v}$  : The Fourier transform of the function  $v$  for the Cauchy problem and the Fourier coefficient of  $v$  for the periodic problem.

$\mathbf{k}, k$  : The dual variable or wave number vector and wave number, respectively;

$$k = |\mathbf{k}| = (\mathbf{k}_1^2 + \mathbf{k}_2^2 + \mathbf{k}_3^2)^{\frac{1}{2}}.$$

$\|v\|$  : The  $L^2$  norm of the indicated function,  $\|v\| = (\int_{\Omega} |v(\cdot, t)|^2 d\mathbf{x})^{1/2}$ .

$\|v\|_N$  : The deconvolution norm of the indicated function,  $\|v\|_N = (v(\cdot, t), D_N v(\cdot, t))^{1/2}$ .

$E(v)(t)$  : The true, total kinetic energy of the indicated velocity field at time  $t$ :

$$E(v)(t) := \frac{1}{2L^3} \|v(\cdot, t)\|^2.$$

$H(v)(t)$  : The true, total helicity of the indicated velocity field at time  $t$ :

$$H(v)(t) := \frac{1}{L^3} \int_{\Omega} v(\cdot, t) \cdot (\nabla \times v(\cdot, t)) d\mathbf{x}.$$

$E_{model}(v)(t)$ : The kinetic energy of the LES model at time  $t$ , given by:

$$E_{model}(v)(t) := \frac{1}{2L^3} \{ \|v(\cdot, t)\|_N^2 + \delta^2 \|v(\cdot, t)\|_N^2 \}.$$

$H_{model}(v)(t)$ : The helicity of the LES model at time  $t$ , given by:

$$H_{model}(v)(t) := \frac{1}{L^3} \{ v(\cdot, t), \nabla \times v(\cdot, t) \}_N + \delta^2 \{ \nabla \times v(\cdot, t), (\nabla \times)^2 v(\cdot, t) \}_N \}.$$

$E(v)(k)$ : The distribution of the kinetic energy of the time average of the indicated flow field by wave number.

$H(v)(k)$ : The distribution of the helicity of the time average of the indicated flow field by wave number.

$E_{model}(v)(k)$  : The distribution by wave number of the LES model's kinetic energy of time or ensemble averages of the indicated flow field.

$H_{model}(v)(k)$  : The distribution by wave number of the LES model's helicity of time or ensemble averages of the indicated flow field.

$\langle \cdot \rangle$ : Time averaging of the indicated function,

$$\langle v \rangle = \limsup_{T \rightarrow \infty} \frac{1}{T} \int_0^T v(t) dt.$$

$\varepsilon(v)(t)$  : The (non-averaged) energy dissipation rate,

$$\varepsilon(v)(t) := \frac{\nu}{L^3} \|\nabla v(\cdot, t)\|^2.$$

$\gamma(v)(t)$  : The (non-averaged) helicity dissipation rate,

$$\gamma(v)(t) := \frac{2\nu}{L^3} (\nabla \times v(\cdot, t), (\nabla \times)^2 v(\cdot, t)).$$

$\varepsilon$  : The mean (time-averaged) energy dissipation rate of the true, Navier-Stokes velocity.

$$\varepsilon := \langle \varepsilon(v)(t) \rangle .$$

$\gamma$  : The mean (time-averaged) energy dissipation rate of the true, Navier-Stokes velocity.

$$\gamma := \langle \gamma(v)(t) \rangle .$$

$\varepsilon_{model}(v)(t)$  : The (non-averaged) LES model's energy dissipation rate, given by:

$$\varepsilon_{model}(v)(t) := \frac{\nu}{L^3} (\|\nabla v(\cdot, t)\|_N^2 + \delta^2 \|\Delta v(\cdot, t)\|_N^2).$$

$\gamma_{model}(v)(t)$  : The (non-averaged) LES model's helicity dissipation rate, given by:

$$\gamma_{model}(v)(t) := \frac{2\nu}{L^3} ((\nabla \times v(\cdot, t), (\nabla \times)^2 v(\cdot, t))_N + \delta^2 ((\nabla \times)^2 v(\cdot, t), (\nabla \times)^3 v(\cdot, t))_N).$$

$\varepsilon_{model}$  : The mean (time-averaged) energy dissipation rate of the LES model.

$$\varepsilon_{model} := \langle \varepsilon_{model}(v)(t) \rangle .$$

$\gamma_{model}$  : The mean (time-averaged) helicity dissipation rate of the LES model.

$$\gamma_{model} := \langle \gamma_{model}(v)(t) \rangle .$$

$P(v)(t)$  : Power input

$$P(v)(t) := \frac{1}{L^3} (f(\cdot, t), v(\cdot, t)).$$

$P_{model}(v)(t)$  : Power input of the LES model

$$P_{model}(v)(t) := \frac{1}{L^3} (f(\cdot, t), v(\cdot, t))_N.$$

$Re$  : The Reynolds number.

$\rho, \mu, \nu$  : Respectively, the fluids density, viscosity and kinematic viscosity.

$U, L$  : The large scales characteristic velocity and length scale used to define the Reynolds number.

$A$  : The differential operator that defines the differential filter,  $Av := (-\delta^2\Delta + I)v$ .

$G$  : The filter  $G = A^{-1}$ .

$D_N$  : The approximate deconvolution operator.

$\bar{v}$  : Overbar denotes the average of the indicated function,  $\bar{v} = Gv$ .

$\eta_{Kolmogorov}$  : The length scale of the smallest persistent eddies; the Kolmogorov microscale.

$k_E$  : The wave number of the smallest persistent eddies.

$\eta_H$  : The length scale of the smallest persistent helical structures; analogous to the Kolmogorov microscale for helicity.

$k_H$  : The wave number of the smallest persistent helical structures.

$\eta_{model}^E$  : The model's energy microscale being the length scale of the model's smallest persistent eddies.

$k_{E_{model}}$  : The model's energy wave number being the wave number of the model's smallest persistent eddies.

$\eta_{model}^H$  : The model's helicity microscale being the length scale of the model's smallest persistent helical structures.

$k_{H_{model}}$  : The model's helicity wave number being the wave number of the model's smallest persistent helical structures.

$w_{small}$  : The velocity scale of the smallest persistent eddies in the model's solution.

$[\cdot]$  : The units or dimensions.

$Re_{small}, Re_{large}$  : A Reynolds number based on the scales of the smallest/largest persistent eddies.

**Remark 3.1.** *For notational compactness, we frequently omit explicit reference to the indicated velocity field. We may write, for instance,  $E(t)$  instead of  $E(v)(t)$ ,  $H(t)$  instead of  $H(v)(t)$ , and so on.*

### 3.2.2 Norm Equivalence

We focus on the case where averaging is performed by differential filters, Germano [23]. Specifically, given  $\phi$ ,  $\bar{\phi}$  is the unique  $L$ -periodic solution of

$$-\delta^2 \Delta \bar{\phi} + \bar{\phi} = \phi, \quad \text{in } \Omega, \quad (3.7)$$

where  $\delta$  is the selected filter length scale. Differential filters are used, for example, in Q. Chen, S. Chen, Eyink [15], Q. Chen, S. Chen, Eyink and Holm [16], Cheskidov, Holm, Olson, and Titi [17], Dunca and Epshteyn [20], [37], [43], and [52].

Let the averaging operator be denoted by  $G$  (so  $\bar{\phi} = G\phi := (-\delta^2 \Delta + I)^{-1}\phi$ ). The basic problem in approximate deconvolution is thus: given  $\bar{\phi} = G\phi$  find useful approximations of  $\phi$ . In other words,

$$G\phi = \bar{\phi}, \text{ solve for } \phi.$$

For most averaging operators,  $G$  is symmetric, positive semi-definite and not stably invertible. Thus, the deconvolution problem is generically ill-posed.

The approximate deconvolution algorithm we consider was studied by van Cittert in 1931. For each  $N = 0, 1, \dots$ , it computes an approximate solution  $\phi_N$  to the above deconvolution equation by  $N$  steps of a fixed point iteration, Bertero and Boccacci [11]. Rewrite the above deconvolution equation as the fixed point problem:

$$\text{given } \bar{\phi} \text{ solve } \phi = \phi + (\bar{\phi} - G\phi) \text{ for } \phi.$$

The deconvolution approximation is then computed as follows.

**Algorithm 3.1 (van Cittert approximate deconvolution algorithm).**  $\phi_0 = \bar{\phi}$ , where

*for*  $n=1,2,\dots,N-1$ , *perform*

$$\phi_{n+1} = \phi_n + (\bar{\phi} - G\phi_n)$$

$$\phi_N = D_N \bar{\phi}$$

By eliminating the intermediate steps, the  $N^{\text{th}}$  deconvolution operator  $D_N$  is

$$D_N \phi := \sum_{n=0}^N (I - G)^n \phi. \quad (3.8)$$

For example, the approximate deconvolution operators corresponding to  $N = 0, 1, 2$  are  $D_0 \bar{\phi} = \bar{\phi}$ , and  $D_1 \bar{\phi} = 2\bar{\phi} - \bar{\bar{\phi}}$ , and  $D_2 \bar{\phi} = 3\bar{\phi} - 3\bar{\bar{\phi}} + \bar{\bar{\bar{\phi}}}$ .

**Lemma 3.1 (Stability of approximate deconvolution).** *Let averaging be defined by the differential filter (3.7). Then  $D_N$  is a self-adjoint, positive semi-definite operator on  $L^2(\Omega)$  with norm*

$$\|D_N\| := \sup_{\phi \in L^2(\Omega)} \frac{\|D_N \phi\|}{\|\phi\|} = N + 1.$$

*Proof.* We summarize the proof from [10] for completeness. Note that  $G := (-\delta^2 \Delta + I)^{-1}$  is a self-adjoint positive definite operator with eigenvalues between zero and one, accumulating at zero. Since  $D_N := \sum_{n=0}^N (I - G)^n$ , is a function of  $G$ , it is also self-adjoint. By the spectral mapping theorem

$$\lambda(D_N) = \sum_{n=0}^N \lambda(I - G)^n = \sum_{n=0}^N (1 - \lambda(G))^n.$$

Thus,  $\lambda(D_N) \geq 0$  and  $D_N$  is also positive semi-definite. Since  $D_N$  is self-adjoint, the operator norm  $\|D_N\|$  is also easily bounded by the spectral mapping theorem by

$$\|D_N\| = \sum_{n=0}^N \lambda_{\max}(I - G)^n = \sum_{n=0}^N (1 - \lambda_{\min}(G))^n = N + 1. \quad (3.9)$$

□

**Definition 3.1.** *The deconvolution weighted norm and inner product are*

$$\|\phi\|_N = \sqrt{(\phi, D_N \phi)} \quad \text{and} \quad (\phi, \psi)_N := (\phi, D_N \psi).$$

for  $\phi, \psi \in L^2(\Omega)$ .

**Lemma 3.2.** *We have*

$$\|\phi\|^2 \leq \|\phi\|_N^2 \leq (N + 1)\|\phi\|^2, \quad \forall \phi \in L^2(\Omega). \quad (3.10)$$

*Proof.* As in (3.9),  $1 \leq \lambda(D_N) \leq N + 1$  since

$$\lambda(D_N) = \sum_{n=0}^N \lambda(I - G)^n = \sum_{n=0}^N (1 - \lambda(G))^n, \text{ and}$$

$$0 < \lambda(G) \leq 1.$$

Since  $D_N$  is a self-adjoint operator, this proves the above equivalence of norms.  $\square$

It is insightful to consider the Cauchy problem or the periodic problem and visualize the approximate deconvolution operators  $D_N$  in wave number space (re-scaled by  $k \leftarrow \delta k$ ). This shows how the  $N$  norm reweights the usual  $L^2(\Omega)$  norm. The transfer function or symbol of the first three are

$$\widehat{D}_0 = 1,$$

$$\widehat{D}_1 = 2 - \frac{1}{k^2 + 1} = \frac{2k^2 + 1}{k^2 + 1}, \text{ and}$$

$$\widehat{D}_2 = 1 + \frac{k^2}{k^2 + 1} + \left(\frac{k^2}{k^2 + 1}\right)^2.$$

Their transfer functions are plotted in Figure 2 below.

Note that the plot of  $\widehat{D}_N(k)$  is consistent with (3.10): the transfer functions are bounded below by 1, positive and uniformly bounded by  $N + 1$ . Figure 2 also reveals that the weighted norm is very close to the usual norm on the largest spacial scales but then overweights (by at most  $N + 1$ ) smaller scales.

The large scales are associated with the smooth components and with the wave numbers near zero (i.e.,  $|\mathbf{k}|$  small). Thus, the fact that  $D_N$  is a very accurate solution of the deconvolution problem for the large scales is reflected in the above graph in that the transfer functions  $\widehat{D}_N(k)$  have high order contact with  $\frac{1}{1+k^2}$  near  $k = 0$ .

**Lemma 3.3 (Error in approximate de-convolution).** *For any  $\phi \in L^2(\Omega)$ ,*

$$\begin{aligned} \phi - D_N \bar{\phi} &= (I - A^{-1})^{N+1} \phi \\ &= (-1)^{N+1} \delta^{2N+2} \Delta^{N+1} A^{-(N+1)} \phi, \end{aligned}$$

*i.e., for smooth  $\phi$ ,  $\phi = D_N \bar{\phi} + O(\delta^{2N+2})$ .*

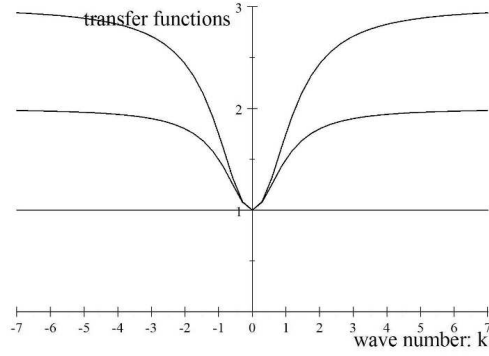


Figure 2: Approximate de-convolution operators,  $N=0,1,2$ .

*Proof.* See Dunca and Epshteyn [20]. □

**Proposition 3.1.** *For  $\phi$  smooth and  $N$  fixed,*

$$\|\phi\|_N^2 = \|\phi\|^2 + O(\delta^2).$$

*Proof.* Using  $\phi - \bar{\phi} = O(\delta^2)$  and  $\phi - D_N \bar{\phi} = O(\delta^{2N+2})$ :

$$(\phi, D_N \phi) = (\phi, \phi) + (\phi, D_N \bar{\phi} - \phi) + (\phi, D_N(\phi - \bar{\phi})) = \|\phi\|^2 + O(\delta^{2N+2}) + O(\delta^2).$$

□

### 3.3 PROPERTIES OF APPROXIMATE DECONVOLUTION LES MODELS

The following proposition recalls from Dunca and Epstheyn [20] and [52], respectively, the energy and helicity balances of the ADM (3.3).

**Proposition 3.2 (Model energy and helicity balance).** *Consider the ADM (3.3). The unique strong solution  $v$  of (3.3) satisfies*

$$\begin{aligned} \frac{1}{2}[\|v(t)\|_N^2 + \delta^2\|\nabla v(t)\|_N^2] + \int_0^t \nu\|\nabla v(t')\|_N^2 + \nu\delta^2\|\Delta v(t')\|_N^2 dt' = \\ = \frac{1}{2}[\|v_0\|_N^2 + \delta^2\|\nabla v_0\|_N^2] + \int_0^t (f(t'), v(t'))_N dt'. \end{aligned} \quad (3.11)$$

$$\begin{aligned} (v(t), \nabla \times v(t))_N + \delta^2(\nabla \times v(t), (\nabla \times)^2 v(t))_N \\ + 2\nu \int_0^t (\nabla \times v(t'), (\nabla \times)^2 v(t'))_N + \delta^2((\nabla \times)^2 v(t'), (\nabla \times)^3 v(t'))_N dt' \\ = (v_0, \nabla \times v_0)_N + \delta^2(\nabla \times v_0, (\nabla \times)^2 v_0)_N + \int_0^t (f(t'), v(t'))_N dt' \end{aligned} \quad (3.12)$$

*Proof.* Both (3.11) and (3.12) can easily be proven by multiplying (3.3) by  $AD_N w$  (or  $A(\nabla \times D_N w)$  for helicity), and integrating by parts. □

**Remark 3.2.** *From this proposition, we can clearly identify the analogs in the ADM (3.3) of the physical quantities of kinetic energy, energy dissipation rate, helicity, helicity dissipation rate, and power input, given next.*

**Definition 3.2.**

$$E_{model}(t) := \frac{1}{2L^3}(\|v(t)\|_N^2 + \delta^2\|\nabla v(t)\|_N^2) \quad (3.13)$$

$$\varepsilon_{model}(t) := \frac{\nu}{L^3}(\|\nabla v(t)\|_N^2 + \delta^2\|\Delta v(t)\|_N^2) \quad (3.14)$$

$$H_{model}(t) := \frac{1}{L^3} (v(t), \nabla \times v(t))_N + \delta^2(\nabla \times v(t), (\nabla \times)^2 v(t))_N \quad (3.15)$$

$$\gamma_{model}(t) := \frac{2\nu}{L^3}((\nabla \times v(t), (\nabla \times)^2 v(t))_N + \delta^2((\nabla \times)^2 v(t), (\nabla \times)^3 v(t))_N) \quad (3.16)$$

$$P_{model}(t) := \frac{1}{L^3}(f(t), v(t))_N \quad (3.17)$$

**Proposition 3.3.** *For smooth  $v$ ,*

$$\begin{aligned} E_{model}(w)(t) &= E(w)(t) + O(\delta^2), & \varepsilon_{model}(t) &= \varepsilon(t) + O(\delta^2), \\ H_{model}(w)(t) &= H(w)(t) + O(\delta^2), & \gamma_{model}(t) &= \gamma(t) + O(\delta^2) \\ P_{model}(w)(t) &= P(w)(t) + O(\delta^2). \end{aligned}$$

*Proof.* This follows directly from the Definition 3.2, Proposition 3.1 and Lemma 3.3.  $\square$

**Remark 3.3.** *The energy dissipation in the model*

$$\varepsilon_{model}(t) := \frac{\nu}{L^3} \|\nabla v(t)\|_N^2 + \frac{\nu}{L^3} \delta^2 \|\Delta v(t)\|_N^2 \quad (3.18)$$

is enhanced by the extra term (which is equivalent to  $\nu\delta^2\|\Delta v(t)\|^2$ ). This term acts as an irreversible energy drain localized at large local fluctuations. The kinetic energy of the model has an extra term:  $\delta^2\|\nabla w(t)\|_N^2$  which is uniformly equivalent to  $\delta^2\|\nabla w(t)\|^2$ .

$$E_{model}(t) := \frac{1}{2L^3} [\|v(t)\|_N^2 + \delta^2 \|\nabla v(t)\|_N^2] \quad (3.19)$$

### 3.3.1 Spectral Representation of the Kinetic Energy

In order to represent the true kinetic energy and the model's kinetic energy spectrally, we expand the velocity field  $v(\mathbf{x}, t)$  in Fourier series as follows:

$$v(\mathbf{x}, t) = \sum_k \sum_{|\mathbf{k}|=k} \hat{v}(\mathbf{k}, t) e^{i\mathbf{k}\cdot\mathbf{x}}, \quad (3.20)$$

where  $\mathbf{k} \in \mathbb{Z}^3$  is the wave number and

$$\hat{v}(\mathbf{k}, t) = \frac{1}{L^3} \int_{\Omega} v(\mathbf{x}, t) e^{-i\mathbf{k}\cdot\mathbf{x}} d\mathbf{x}$$

are the Fourier coefficients.

Using Parseval's equality

$$\frac{1}{2L^3} \|v(t)\|^2 = \sum_k \sum_{|\mathbf{k}|=k} \frac{1}{2} |\hat{v}(\mathbf{k}, t)|^2.$$

The above formula is equivalent to writing

$$E(t) = \frac{2\pi}{L} \sum_k E(k, t),$$

where

$$E(k, t) := \frac{L}{2\pi} \sum_{|\mathbf{k}|=k} \frac{1}{2} |\hat{v}(\mathbf{k}, t)|^2.$$

Then, the time averaged kinetic energy is

$$E = \langle E(t) \rangle, \quad \text{or} \quad E = \frac{2\pi}{L} \sum_k E(k),$$

where  $E(k) = \langle E(k, t) \rangle$ .

The model's kinetic energy (3.13) and energy dissipation rate (3.14) can also be decomposed in Fourier modes.

**Proposition 3.4.** *In Fourier space, (3.13) corresponds to*

$$E_{model}(t) = \sum_k \hat{D}_N(k) (1 + \delta^2 k^2) E(k, t), \quad (3.21)$$

or equivalently,

$$E_{model}(t) = \frac{2\pi}{L} \sum_k E_{model}(k, t), \quad (3.22)$$

where

$$E_{model}(k, t) := \hat{D}_N(k) (1 + \delta^2 k^2) E(k, t). \quad (3.23)$$

*Proof.* Using Parseval's equality again, we get

$$\frac{1}{2L^3} \|v(t)\|_N = \sum_k \sum_{|\mathbf{k}|=k} \frac{1}{2} \hat{D}_N(k) |\hat{v}(\mathbf{k}, t)|^2 \quad (3.24)$$

and

$$\frac{1}{2L^3} \|\nabla v(t)\|_N = \sum_k \sum_{|\mathbf{k}|=k} \frac{1}{2} k^2 \hat{D}_N(k) |\hat{v}(\mathbf{k}, t)|^2. \quad (3.25)$$

Adding (3.24) and (3.25) proves the claim. □

**Lemma 3.4.** *In wave number space, we can rewrite (3.14), the model's energy dissipation:*

$$\varepsilon_{model}(t) = \nu \frac{2\pi}{L} \sum_k \hat{D}_N(k) k^2 (1 + \delta^2 k^2) E(k, t). \quad (3.26)$$

Using (3.23), equation (3.26) can be further simplified to

$$\varepsilon_{model}(t) = \nu \frac{2\pi}{L} \sum_k k^2 E_{model}(k, t). \quad (3.27)$$

*Proof.* Beginning with (3.14), the proof of (3.26) follows similarly to that for Proposition 3.4.  $\square$

Next, we turn our attention to the spectral representation of helicity.

### 3.3.2 Helical Mode Decomposition

**Definition 3.3.** *The helical modes  $\mathbf{h}_\pm$  are orthonormal eigenvectors of the curl operator, i.e.  $i\mathbf{k} \times \mathbf{h}_\pm = \pm k \mathbf{h}_\pm$ .*

Since  $v$  is incompressible,  $\mathbf{k} \cdot \hat{v}(\mathbf{k}, t) = 0$  and we can write  $\hat{v}(\mathbf{k}, t) = a_+(\mathbf{k}, t) \mathbf{h}_+ + a_-(\mathbf{k}, t) \mathbf{h}_-$ . For the spectral decomposition of helicity, we follow Q. Chen, S. Chen and Eyink [15] and Waleffe [56] and expand  $\hat{v}(\mathbf{k}, t)$  in a basis of helical modes. Therefore, velocity and vorticity can be expanded as

$$v(\mathbf{x}, t) = \sum_k \sum_{|\mathbf{k}|=k} \sum_{s=\pm} a_s(\mathbf{k}, t) \mathbf{h}_s(\mathbf{k}) e^{i\mathbf{k} \cdot \mathbf{x}}, \quad (3.28)$$

$$\nabla \times v(\mathbf{x}, t) = \sum_k \sum_{|\mathbf{k}|=k} \sum_{s=\pm} s k a_s(\mathbf{k}, t) \mathbf{h}_s(\mathbf{k}) e^{i\mathbf{k} \cdot \mathbf{x}} \quad (3.29)$$

Similarly,

$$(\nabla \times)^n v(\mathbf{x}, t) = \sum_k \sum_{|\mathbf{k}|=k} \sum_{s=\pm} s^n k^n a_s(\mathbf{k}, t) \mathbf{h}_s(\mathbf{k}) e^{i\mathbf{k} \cdot \mathbf{x}}. \quad (3.30)$$

Recall first the definition of helicity, equation (3.5), for the model's velocity  $v$ . Expanding  $v$  in helical modes, we get

$$H(t) = \frac{2\pi}{L} \sum_k H(k, t),$$

where

$$H(k, t) := s k \frac{L}{2\pi} \sum_{|\mathbf{k}|=k} \sum_{s=\pm} |a_s(\mathbf{k}, t)|^2.$$

**Proposition 3.5.** *The model's helicity spectrum,  $H_{model}(k, t)$  is related to the true helicity spectrum,  $H(k, t)$ , as*

$$H_{model}(k, t) = \hat{D}_N(k)(1 + \delta^2 k^2)H(k, t). \quad (3.31)$$

*Proof.* Using (3.28)-(3.30), we have

$$\frac{1}{L^3}(v(t), \nabla \times v(t))_N = \sum_k \sum_{|\mathbf{k}|=k} \sum_{s=\pm} s \hat{D}_N(k) k |a(\mathbf{k}, t)|^2$$

and

$$\frac{1}{L^3}(\nabla \times v(t), (\nabla \times)^2 v(t))_N = \sum_k \sum_{|\mathbf{k}|=k} \sum_{s=\pm} s \hat{D}_N(k) k^3 |a(\mathbf{k}, t)|^2$$

so that

$$H_{model}(t) = \frac{2\pi}{L} \sum_k H_{model}(k, t) = \frac{2\pi}{L} \sum_k \hat{D}_N(k)(1 + \delta^2 k^2)H(k). \quad (3.32)$$

□

**Lemma 3.5.** *In wave number space, we can rewrite (3.16), the model's helicity dissipation:*

$$\gamma_{model}(t) = \nu \sum_k \sum_{|\mathbf{k}|=k} \sum_{s=\pm} \hat{D}_N(k) s k^3 (1 + \delta^2 k^2) |a_s(\mathbf{k}, t)|^2. \quad (3.33)$$

Using (3.32), equation (3.33) can be further simplified to

$$\gamma_{model}(t) = \nu \frac{2\pi}{L} \sum_k k^2 H_{model}(k, t). \quad (3.34)$$

*Proof.* Use (3.28)-(3.30) to write (3.16) in helical modes. □

### 3.4 PHENOMENOLOGY OF THE ADM JOINT ENERGY AND HELICITY CASCADE

Since helicity plays a key role in organizing three dimensional flows, it is important to understand the extent to which statistics of helicity predicted by an LES model are correct. We answer that question in this section by extending the similarity theory of approximate deconvolution models (begun in [37]) to elucidate the details of the model's helicity cascade and its connection to the model's energy. Inspired by the earlier work on helicity cascades in the Navier-Stokes equations done by Brissaud, Frisch, Leorat, Lesieur and Mazure [14], Ditlevsen and Giuliani [19, 18], Q. Chen, S. Chen and Eyink [15], we investigate the existence and details of the joint cascade of energy and helicity for the family of ADM's adapting a dynamic argument of Kraichnan, [32].

Let  $\Pi_{model}(k)$  and  $\Sigma_{model}(k)$  denote the total energy and helicity transfer from all wave numbers  $< k$  to all wave numbers  $> k$ .

**Definition 3.4.** *We say that the model exhibits a joint cascade of energy and helicity if in some inertial range,  $\Pi_{model}(k)$  and  $\Sigma_{model}(k)$  are independent of the wave number, i.e.,  $\Pi_{model}(k) = \varepsilon_{model}$  and  $\Sigma_{model}(k) = \gamma_{model}$ .*

Following Kraichnan's formulation of Kolmogorov's ideas of localness of interaction in  $k$  space, we assume the following.

**Remark 3.1.**  *$\Pi_{model}(k)$  ( $\Sigma_{model}(k)$ ) is proportional to the ratio of the total energy  $\sim kE_{model}(k)$  (total helicity  $\sim kH_{model}(k)$ ) available in wave numbers of order  $k$  and to some effective rate of shear  $\sigma(k)$  which acts to distort flow structures of scale  $1/k$ .*

The distortion time  $\tau(k)$  of flow structures of scale  $1/k$  due to the shearing action  $\sigma(k)$  of all wave numbers  $\leq k$  is given by:

$$\tau(k) \sim \frac{1}{\sigma(k)} \quad \text{with} \quad \sigma(k)^2 \sim \int_0^k p^2 E_{model}(p) dp. \quad (3.35)$$

The conjecture of joint linear cascades of energy and helicity is based on the idea (supported in numerical experiments of Bourne and Orszag [12]) that since energy and helicity

are both dissipated by the same mechanism (of viscosity), they relax over comparable time scales.

**Remark 3.2.**  $\tau(k)$  and  $\sigma(k)$  are the same for energy and helicity of the model.

We therefore write

$$\Pi_{model}(k) \sim kE_{model}(k)/\tau(k) \quad \text{and} \quad \Sigma_{model}(k) \sim kH_{model}(k)/\tau(k). \quad (3.36)$$

In the definition of mean-square shear (3.35) the major contribution is from  $p \sim k$ , in accord with Kolmogorov's localness assumption. This gives

$$\tau(k) \sim k^{-3/2}E_{model}^{-1/2}(k). \quad (3.37)$$

Putting (3.36) and (3.37) together with the fact that  $\Sigma_{model}(k) = \gamma_{model}$ , it follows that the ADM model helicity spectrum is given by:

$$H_{model}(k) \sim \gamma_{model}k^{-5/2}E_{model}^{-1/2}(k)$$

i.e.,

$$H_{model}(k) \sim \gamma_{model}\varepsilon_{model}^{-1/3}k^{-5/3}. \quad (3.38)$$

Using relation (3.31), we write

$$H(k) \sim \frac{\gamma_{model}\varepsilon_{model}^{-1/3}k^{-5/3}}{1 + \delta^2k^2},$$

which shows that the true helicity spectrum is cut by this family of models as

$$H(k) \sim \gamma_{model}\varepsilon_{model}^{-1/3}k^{-5/3}, \text{ for } k \leq \frac{1}{\delta}, \quad (3.39)$$

$$H(k) \sim \gamma_{model}\varepsilon_{model}^{-1/3}\delta^{-2}k^{-11/3}, \text{ for } k \geq \frac{1}{\delta}. \quad (3.40)$$

The above result is depicted in Figure 3.

The energy spectrum  $E_{model}(k)$  follows analogously [37]:

$$E_{model}(k) \sim \varepsilon_{model}^{2/3}k^{-5/3}. \quad (3.41)$$

Further,

$$E(k) \sim \varepsilon_{model}^{2/3} k^{-5/3}, \text{ for } k \leq \frac{1}{\delta}, \quad (3.42)$$

$$E(k) \sim \varepsilon_{model}^{2/3} \delta^{-2} k^{-11/3}, \text{ for } k \geq \frac{1}{\delta}. \quad (3.43)$$

Thus, down to the cutoff length scale (or up to the cutoff wave number) the ADM predicts the correct energy and helicity cascades.

### 3.5 MODEL'S HELICITY MICROSCALE AND CONSISTENCY OF THE CASCADE

On a small enough scale, viscosity grinds down all the flow's organized structures (including helicity) and ends all cascades (including the helicity cascade). The length scale,  $\eta_H$ , at which helical structures do not persist and begin to decay exponentially fast is called the helicity microscale (in analogy with the Kolmogorov microscale for kinetic energy). The correct estimate of the helicity microscale for the NSE is unclear: two estimates with strong arguments in favor of each appear in the literature. The microscale has been estimated for isotropic turbulence by Ditlevsen and Giuliani in [19] to be different (larger) from the Kolmogorov scale  $\eta_{Kolmogorov}$ :  $\eta_H \sim \nu^{-3/7} \gamma^{3/7} \varepsilon^{-2/7}$  based on the decomposition of helicity flux in  $\pm$  helical modes. On the other hand, Q. Chen, S. Chen and Eyink in [15] show that the net helicity flux is constant up to  $\eta_{Kolmogorov}$  ( $= k_E^{-1}$ ), so there is no shorter inertial range for helicity cascade.

In this section, we find that the same occurs when one computes the model's helicity microscale. Based on the equilibrium of the helicity flux, we derive a model's helicity microscale,  $\eta_{model}^H$ , whereas we show that the model's helicity cascade derived in Section 3.4 is consistent up to  $k_{E_{model}} (= (\eta_{model}^E)^{-1})$ , in the sense introduced by Q. Chen, S. Chen and Eyink in [15]. These two results do not contradict each other.

### 3.5.1 Model's Helicity Microscale

Using ideas in [37] from the derivation of the energy microscale,  $\eta_{model}^E$ , we estimate the ADM's helicity microscale to be:

$$\begin{aligned}\eta_{model}^H &\sim Re^{-3/11} \delta^{6/11} L^{5/11}, & \text{if } \delta < \eta_{model}^H \\ \eta_{model}^H &\sim Re^{-3/5} L, & \text{if } \delta > \eta_{model}^H\end{aligned}$$

Let the reference velocity and length scale for the large scales be  $U, L$ , and  $w_{small}, \eta_{model}^H$ , for the small scales. From [37] the analog of the small scales and large scales Reynolds number of the model. Recall that these are given by

$$Re_{large} \sim \left. \frac{|\text{nonlinearity}|}{|\text{viscous terms}|} \right|_{\text{large scales}}, \quad Re_{small} \sim \left. \frac{|\text{nonlinearity}|}{|\text{viscous terms}|} \right|_{\text{small scales}}.$$

**Definition 3.5.** *The effective Reynolds numbers at large and small scales (analogous to the usual NSE  $Re = \frac{UL}{\nu}$ ) in the model are given by*

$$Re_{model-Large} = \frac{UL}{\nu(1 + (\frac{\delta}{L})^2)} \quad \text{and} \quad Re_{model-Small} = \frac{w_{small}\eta_{model}^H}{\nu(1 + (\frac{\delta}{\eta_{model}^H})^2)} \quad (3.44)$$

The ADM's energy and helicity cascade are halted by viscosity grinding down eddies exponentially fast. This occurs when  $Re_{model-Small} \sim O(1)$ , that is, when

$$\frac{w_{small}\eta_{model}^H}{\nu(1 + (\frac{\delta}{\eta_{model}^H})^2)} \sim 1. \quad (3.45)$$

Equation (3.45) determines  $w_{small}$

$$w_{small} \sim \frac{\nu(1 + (\frac{\delta}{\eta_{model}^H})^2)}{\eta_{model}^H}. \quad (3.46)$$

The next important equation to determine the helicity microscale comes from statistical equilibrium of the helicity flux: the helicity input at the large scales must match helicity dissipation at the microscale. The rate of helicity input to the largest scales is the total helicity over the associated time scales

$$\frac{H_{model}}{(\frac{L}{U})} = \frac{\frac{U^2}{L}(1 + (\frac{\delta}{L})^2)}{(\frac{L}{U})} = \frac{U^3}{L^2} \left( 1 + \left( \frac{\delta}{L} \right)^2 \right). \quad (3.47)$$

Helicity dissipation at the model's microscale scales as

$$\gamma_{small} \sim \nu \left( \frac{w_{small}^2}{(\eta_{model}^H)^3} \left( 1 + \left( \frac{\delta}{\eta_{model}^H} \right)^2 \right) \right).$$

This must match the helicity input. There are three cases with the third being the only important one:  $\delta = O(\eta_{Kolmogorov})$ ,  $\delta = O(L)$  and the typical case of  $\delta$  in the inertial range:  $\eta_{Kolmogorov} \ll \delta \ll L$ . If  $\delta \sim O(\eta_{Kolmogorov})$ , then the simulation reduces to a direct numerical simulation of the NSE. If  $\delta \sim O(L)$ , then we do not have LES, but VLES (Very Large Eddy Simulation). In the case of VLES, results follow similarly to those below, but are omitted here.

In the case  $\delta = O(\eta_{Kolmogorov})$ , we have

$$\left( 1 + \left( \frac{\delta}{L} \right)^2 \right) \sim 1 \text{ and } \left( 1 + \left( \frac{\delta}{\eta_{model}^H} \right)^2 \right) \sim 1.$$

Thus, at statistical equilibrium,

$$\frac{U^3}{L^2} \sim \nu \frac{w_{small}^2}{(\eta_{model}^H)^3}.$$

Since  $w_{small}$  simplifies to  $\nu/\eta_{model}^H$ , we get

$$\eta_{model}^H \sim Re^{-3/5} L.$$

In the most important case,

$$\eta_{model}^H \ll \delta \ll L$$

we have

$$\left( 1 + \left( \frac{\delta}{L} \right)^2 \right) \sim 1 \text{ and } \left( 1 + \left( \frac{\delta}{\eta_{model}^H} \right)^2 \right) \sim \left( \frac{\delta}{\eta_{model}^H} \right)^2.$$

Matching helicity microscale dissipation to large scale input thus simplifies in this case to

$$\frac{U^3}{L^2} \sim \nu \frac{w_{small}^2 \delta^2}{(\eta_{model}^H)^3 (\eta_{model}^H)^2}. \quad (3.48)$$

Further, when  $\eta_{Kolmogorov} \ll \delta \ll L$ , the small scale velocity in (3.46) reduces to

$$w_{small} \sim \frac{\nu \delta^2}{(\eta_{model}^H)^3}. \quad (3.49)$$

Substituting (3.49) into (3.48) gives

$$\frac{U^3}{L^2} \sim \frac{\nu^3 \delta^6}{(\eta_{model}^H)^{11}}. \quad (3.50)$$

Solving (3.50) for  $\eta_{model}^H$ , and using  $Re = LU/\nu$  gives the model's helicity microscale,

$$\eta_{model}^H \sim Re^{-3/11} \delta^{6/11} L^{5/11}. \quad (3.51)$$

The ADM helicity microscale is slightly larger than the ADM energy microscale (found in [37]):  $\eta_{model}^E \sim Re^{-3/10} L^{4/10} \delta^{6/10}$ . Hence, capturing wave numbers up to the highest energetic wave number will also capture all wave numbers containing significant helicity.

### 3.5.2 Consistency of the ADM Joint Cascade

The model's energy and helicity dissipation rates are given by equations (3.27) and (3.34) above, which are equivalent to

$$\varepsilon_{model}(t) = \nu \int_0^\infty k^2 E_{model}(k, t) dk. \quad (3.52)$$

and

$$\gamma_{model}(t) = \nu \int_0^\infty k^2 H_{model}(k, t) dk. \quad (3.53)$$

**Lemma 3.6.** *The wave number of the energy microscale of the ADM model (3.3) is given by*

$$k_{E_{model}} \sim \nu^{-3/4} \epsilon_{model}^{1/4}.$$

*Proof.* Based on (3.52), the mean (time-averaged) energy dissipation equals to

$$\langle \varepsilon_{model}(t) \rangle = \nu \int_0^{k_{E_{model}}} k^2 E_{model}(k) dk,$$

where the upper limit of the integral is  $k_{E_{model}}$ , the wave number of the smallest persistent scales in the model's solution. Using also (3.41) we derive the estimate for  $k_{E_{model}}$  in the usual way as  $k_E$  was derived for NSE.

$$\langle \varepsilon_{model}(t) \rangle \sim \nu k_{E_{model}}^3 E_{model}(k_{E_{model}}) \sim \nu k_{E_{model}}^3 (\epsilon_{model}^{2/3} k_{E_{model}}^{-5/3}) \sim \epsilon_{model}.$$

Solving for  $k_{E_{model}}$  gives the result. □

Since we have  $\langle \gamma_{model}(t) \rangle = \gamma_{model}$  and the RHS can be calculated by spectral integration through the inertial range, checking this equality is a way to test if the estimate derived for the end of the inertial range is correct (or consistent).

**Lemma 3.7.** *Provided the largest wave number containing helicity is no larger than  $k_{E_{model}}$ :*

$$\langle \gamma_{model}(t) \rangle = \gamma_{model}.$$

*Proof.* Substituting the helicity cascade result (3.38) and evaluating the integral (3.53) up to  $k_{E_{model}}$  gives

$$\begin{aligned} \langle \gamma_{model}(t) \rangle &\sim \nu \gamma_{model} \epsilon_{model}^{-1/3} (k_{E_{model}}^{4/3}) \\ &\sim \nu \gamma_{model} \epsilon_{model}^{-1/3} \nu^{-1} \epsilon_{model}^{1/3} \\ &\sim \gamma_{model} \end{aligned}$$

□

**Remark 3.1.** *We want to stress out that  $\langle \gamma_{model}(t) \rangle = \gamma_{model}$  only if we integrate up to  $k_{E_{model}}$ , i.e. only if the end of the inertial range for helicity is the same as the end of the inertial range of energy.*

### 3.6 CONCLUSIONS

A joint energy and helicity cascade has been shown to exist for homogeneous, isotropic turbulence generated by approximate deconvolution models. The energy and helicity both cascade at the correct  $O(k^{-5/3})$  rate for inertial range wave numbers up to the cutoff wave number of  $O(\frac{1}{\delta})$ , and at  $O(k^{-11/3})$  afterward until the model's energy and helicity microscale. This establishes consistency of the model's helicity and energy cascades with the true cascades of the true, underlying turbulent flow.

Furthermore, a microscale for helicity dissipation has been identified for flows predicted by ADMs. As expected, it is larger than the Kolmogorov scale (i.e. the ADM truncates scales) and the microscale for energy dissipation in the ADM (i.e. capturing all scales containing energy will also capture all scales containing helicity).

### 3.6.1 Other Filters

With the differential filter (3.7), scales begin to be truncated by the model at the lengthscale  $l = O(\delta)$  by an enhanced decay of the energy and helicity cascade of  $k^{-11/3}$ . Examining the derivation, the exponent  $-11/3$  ( $= -5/3 + (-2)$ ) occurs because the filter decays as  $k^{-2}$ . With a fourth order differential filter, these results would be modified to  $k^{-14/3}$  ( $-14/3 = -5/3 + (-4)$ ) between the cutoff wave number and the microscale. Continuing, it is clear that with the Gaussian filter (which decay exponentially after  $k_C = 1/\delta$ ), exponential decay begins at  $k_C = 1/\delta$ . In other words, with the Gaussian filter,  $k_C = 1/\delta = 1/\eta_{model}^H = 1/\eta_{model}^E$ .

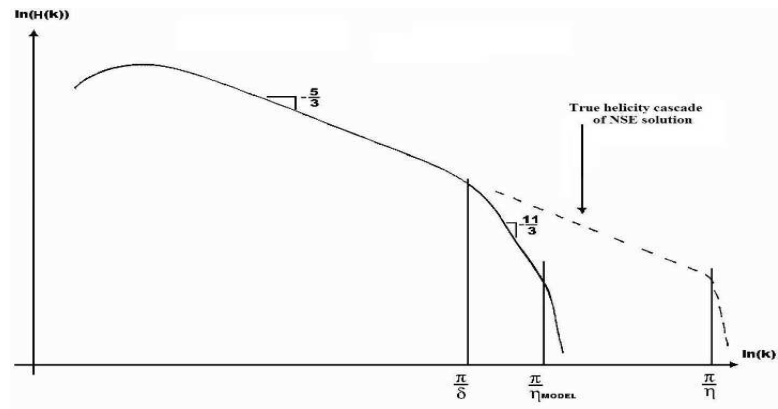


Figure 3: The helicity spectrum of Approximate Deconvolution Models

## 4.0 HELICITY CONSERVATION IN TRAPEZOIDAL GALERKIN DISCRETIZATIONS

This chapter is an investigation of helicity conservation for inviscid periodic flow in energy conserving, three-dimensional, trapezoidal schemes for the ADM and the NSE. In Chapter 2, it was shown that the ADM conserves a model energy and a model helicity. Similarly, the NSE conserves both energy and helicity. However, conservation in a continuous model does not imply conservation in a discretization of the model. It can be shown analytically that trapezoidal Galerkin schemes (which are designed to conserve energy) do not conserve helicity, as the nonlinearity will not vanish when the test function is chosen such that helicity appears in the resulting equation. However, it is not known to what extent these discretizations do not conserve helicity. In other words, we wish to know how significantly the nonlinearity in the NSE can create and dissipate helicity in these discrete schemes. We perform numerical experiments for periodic, inviscid, helical flow to shed light on this matter.

In the numerical experiments presented below, an initial condition of

$$u_0 = \langle \cos(2\pi z), \sin(2\pi z), \sin(2\pi x) \rangle \quad (4.1)$$

was chosen. A uniform mesh with  $h = \frac{1}{16}$  and Taylor-Hood elements  $(X^h, Q^h) = (P_2, P_1)$  (piecewise continuous polynomials of degree 2 and 1 respectively) was used to discretize the periodic box  $(0, 1)^3$ , and solutions were computed at times in  $(0, 1]$  with  $\Delta t = 0.01$  and  $\nu = f = 0$ . All computations were performed on a desktop machine using MATLAB.  $u_h^0$  is chosen to be the interpolant of  $u_0$  in  $X^h$ .

For the NSE, we implemented two schemes: the usual nonlinear trapezoidal Galerkin scheme (note the one-half time step is an average:  $w^{n+1/2} := \frac{w^n + w^{n+1}}{2}$ ,

$$\begin{aligned} \frac{1}{\Delta t}(u_h^{n+1} - u^n, v) + \frac{1}{2}(u_h^{n+1/2} \cdot \nabla u_h^{n+1/2}, v) - \frac{1}{2}(u_h^{n+1/2} \cdot \nabla v, u_h^{n+1/2}) \\ + \nu(\nabla u_h^{n+1/2}, \nabla v) - (p^{n+1/2}, \nabla \cdot v) = (f, v) \quad \forall v \in X^h, \end{aligned} \quad (4.2)$$

$$(\nabla \cdot u_h^{n+1}, q) = 0, \quad \forall q \in Q^h \quad (4.3)$$

and the linear extrapolated trapezoidal Galerkin scheme of Baker (where  $u_h^{-1} := u_h^0$ ) [7]

$$\begin{aligned} \frac{1}{\Delta t}(u_h^{n+1} - u^n, v) + \frac{1}{2}\left(\frac{3}{2}u_h^n - \frac{1}{2}u_h^{n-1}\right) \cdot \nabla u_h^{n+1/2}, v) - \frac{1}{2}\left(\frac{3}{2}u_h^n - \frac{1}{2}u_h^{n-1}\right) \cdot \nabla v, u_h^{n+1/2}) \\ + \nu(\nabla u_h^{n+1/2}, \nabla v) - (p^{n+1/2}, \nabla \cdot v) = (f, v) \quad \forall v \in X^h, \end{aligned} \quad (4.4)$$

$$(\nabla \cdot u_h^{n+1}, q) = 0. \quad \forall q \in Q^h \quad (4.5)$$

Figure 4 shows the results: Helicity is not conserved for either of these NSE energy-conserving schemes. Both schemes seem to approximately conserve helicity on  $(0, .5]$ , but then lose conservation afterward. It is interesting to note how close these two schemes helicities are up until about  $t = .7$ . We also give Figure 5, which shows that energy is conserved in this algorithm, and the solution is at least stable.

For the ADM, we implement the  $0^{th}$  order model in an *ADM-energy* conserving scheme. This model does not conserve energy, but conserves an energy-like quantity  $E_{ADM0} = \frac{1}{2}(\|w\|^2 + \delta^2\|\nabla \times w\|)$  in the periodic, inviscid setting (see Chapter 2). Hence for stability of the discretization, it is  $E_{ADM0}$ , and not the usual energy that should be conserved (see [44]). Thus the scheme we use is

$$\begin{aligned} \frac{1}{\Delta t}(w_h^{n+1} - w_h^n, v) + \overline{(w_h^{n+1/2} \cdot \nabla w_h^{n+1/2} + \frac{1}{2}(\nabla \cdot w_h^{n+1/2})w_h^{n+1/2}, v)} + \overline{(\nabla p_h^{n+1/2}, v)} \\ + \nu(\nabla w_h^{n+1/2}, \nabla v) = (f, v) \quad \forall v \in X^h, \end{aligned} \quad (4.6)$$

$$(\nabla \cdot w_h^{n+1}, q) = 0 \quad \forall q \in Q^h. \quad (4.7)$$

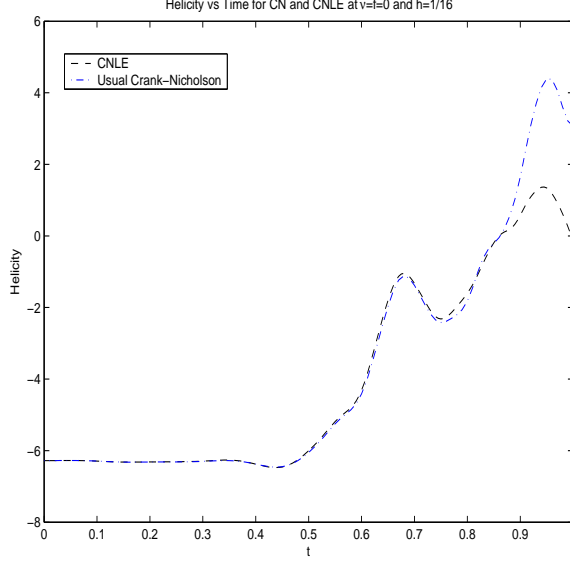


Figure 4: Helicity vs Time for inviscid periodic flow with trapezoidal Galerkin and linearly extrapolated trapezoidal Galerkin schemes for the NSE

Figure 6 shows both helicity and (an approximation of) ADM-helicity,

$$\int_{\Omega} (w \cdot (\nabla \times w) + \delta^2 (\nabla \times w) \cdot (\nabla \times (I^h(\nabla \times w)))) \quad (4.8)$$

(where  $I^h$  is the interpolation operator onto  $X^h$ ), versus time for the given discretization. The figure shows that neither helicity nor the approximation of ADM-helicity of the solution are conserved. From these plots it is clear that the nonlinearity in the schemes adds and dissipates helicity to the discrete solution. This is purely non-physical, as both the NSE and ADM cascade helicity through wave space via the nonlinear term; i.e. the nonlinearity in the continuous case does not add or dissipate helicity. Hence we can conclude that these schemes, designed for energy conservation and stability, in fact do not accurately treat helicity.

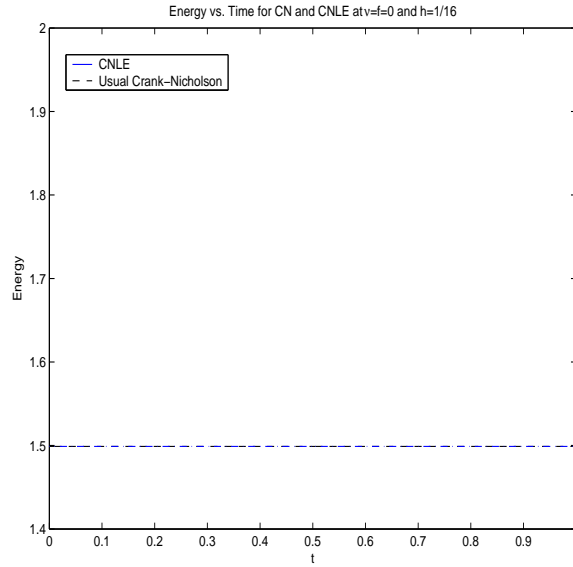


Figure 5: Energy vs Time for inviscid periodic flow with trapezoidal Galerkin and linearly extrapolated trapezoidal Galerkin schemes for the NSE

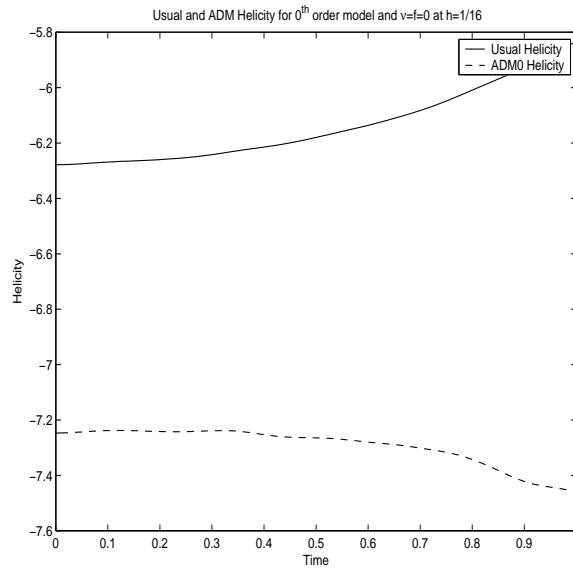


Figure 6: Helicity and ADM-Helicity vs Time for inviscid periodic flow for a trapezoidal Galerkin scheme for the ADM

## 5.0 AN ENERGY AND HELICITY CONSERVING FINITE ELEMENT SCHEME FOR THE NAVIER-STOKES EQUATIONS

### 5.1 INTRODUCTION

For two dimensional flows, schemes such as the classical Arakawa scheme [6] have existed for over forty years which conserve both energy and enstrophy (this and all future references to E/H/Ens conservation implicitly refer to the case of no viscosity or external force). For three dimensional flows, however, it was not until 2004 that Liu and Wang developed the first scheme that conserves both energy and helicity. In [42], they present an energy and helicity preserving scheme for axisymmetric flows, and show this dual conservation eliminates the need for excessive numerical viscosity. It is their work which motivated this chapter.

This chapter presents a new finite element scheme that globally conserves both energy and helicity for general flows. Our development of the scheme herein is for periodic boundaries (and hence we use a box for the domain  $\Omega$ ). The key features that allow the scheme to conserve both energy and helicity is the use of the projection of the vorticity in the scheme, and a new variational formulation of the nonlinearity that vanishes when tested against either the velocity or projected vorticity. For non-periodic boundary conditions, helicity is not necessarily globally conserved. On the other hand, helicity generation and helicity flux are equally important for non-periodic problems, and a numerical method should not generate spurious helicity through its discretization of the nonlinear term.

**Remark 5.1.** *Helicity is not necessarily globally conserved for more general boundary conditions. Consider the Euler equations on  $\Omega = (0, L)^3$ . Multiply by the vorticity  $w := (\nabla \times u)$ ,*

decompose the nonlinearity using (2.6) and integrate over the domain:

$$\int_{\Omega} u_t \cdot w + \int_{\Omega} \left( \frac{1}{2} \nabla u^2 - u \times w \right) \cdot w + \int_{\Omega} \nabla p \cdot w = 0, \quad (5.1)$$

This reduces via integration by parts, and the fact the cross product of two vectors is perpendicular to each of them, to

$$\int_{\Omega} u_t \cdot w + \int_{\partial\Omega} \left( p + \frac{1}{2} \nabla u^2 \right) (w \cdot n) = 0. \quad (5.2)$$

The boundary integral in (5.2) can vanish without periodicity (e.g. if  $w \cdot n = 0$  is imposed), but the resulting equation,  $\int_{\Omega} u_t \cdot w = 0$ , still does not imply the conservation of helicity since integrating by parts with  $u$  decomposed as  $u := \langle u_1, u_2, u_3 \rangle$  shows

$$\begin{aligned} H(T) - H(0) &= \int_0^T \frac{d}{dt} H(t) = \int_0^T \frac{d}{dt} \int_{\Omega} u \cdot w = \int_0^T \int_{\Omega} (u_t \cdot w + u \cdot w_t) = \\ &\left( \int_0^L \int_0^L \left( (u_1 u_3|_{y=0}^{y=L} dz dx) + (u_1 u_2|_{z=0}^{z=L} dy dx) + (u_2 u_3|_{x=0}^{x=L} dz dy) \right) \right) \Big|_{t=0}^{t=T} \quad (5.3) \end{aligned}$$

Thus we see that helicity is conserved for periodic or zero boundary conditions, but not necessarily conserved in general.

This chapter is arranged as follows: We present the energy and helicity conserving scheme in Section 3, after providing the necessary notation in Section 2. Section 4 gives a rigorous numerical analysis for the scheme, Section 5 presents numerical results, and Section 6 presents conclusions.

## 5.2 NOTATION AND PRELIMINARIES

Let  $(\cdot, \cdot)$  and  $\|\cdot\|$  denote the usual  $L^2$  inner product and norm, respectively, and  $\|\cdot\|_k$  the  $H^k(\Omega)$  norm.  $\|\cdot\|_\infty$  will denote the usual  $L^\infty(\Omega)$  norm, and all other norms that appear in this chapter will be clearly labeled with subscripts. The domain  $\Omega$  we use is the box  $(0, L)^3$ .

**Definition 5.1.** *The Hilbert space  $H_{\#}^1(\Omega)$  will be defined as*

$$H_{\#}^1 := \left\{ v \in H^1 : v \text{ periodic on } \Omega, \int_{\Omega} v \, dx = 0 \right\}.$$

This is the natural velocity space for the NSE with periodic boundary conditions, as discussed in [40] and [41]. Note that velocities in this space automatically conserve momentum  $(\int_{\Omega} u)$ , i.e. if  $u \in H_{\#}^1$ ,  $\frac{d}{dt} \int_{\Omega} u = 0$ . This is physically important because the Navier-Stokes equations (with periodic boundary conditions) also conserve momentum [25].

Let  $T^h = T^h(\Omega)$  be a conforming finite element mesh on  $\Omega$ . Define the spaces  $(X^h, Q^h) \subset (H_{\#}^1, L_0^2)$  to be conforming velocity, pressure finite element spaces (see, e.g. [13],[24] or [26] for examples) that satisfy the discrete inf-sup condition (also known as the LBB condition)

$$0 < \beta \leq \inf_{q \in Q^h} \sup_{v \in X^h} \frac{(q, \nabla \cdot v)}{\|v\|_1 \|q\|}. \quad (5.4)$$

Define  $V^h$  to be the space of discretely divergence free, zero-mean, periodic functions.

$$V^h = \{v \in X^h : (\nabla \cdot v, q) = 0 \, \forall q \in Q^h\},$$

$V^{h,*}$  will denote the dual space of  $V^h$ . Since  $V^h$  is a closed subspace of  $H_{\#}^1(\Omega)$ , we have also that  $V^h$  is a Hilbert space, and thus the following result.

**Lemma 5.1.** *Let  $u^h \in V^h$ . Then there exists a unique  $w^h \in V^h$  satisfying*

$$(w^h, v) = (\nabla \times u^h, v) \, \forall v \in V^h \quad (5.5)$$

*Proof.* Since  $u^h \in V^h \subset H^1(\Omega)$ , it follows that  $\nabla \times u^h \in L^2(\Omega)$ . Since  $V^h$  is a closed subset of the Hilbert space  $L^2(\Omega)$ , the Riesz representation theorem implies the existence and uniqueness of a solution  $w^h$  to (5.5). □

The next lemma shows how an elementary property of the cross product can be used for “double” skew symmetry of a trilinear term (i.e. a form of the nonlinearity that will vanish for two different choices of test elements).

**Lemma 5.2.** *Let  $u^h, w^h \in X^h$ . Then*

$$(u^h \times w^h, u^h) = (u^h \times w^h, w^h) = 0.$$

*Proof.* This follows from an elementary property of the cross product; the cross product of two vectors is perpendicular to each of them.  $\square$

The significance of this lemma is that in a finite element scheme, the trilinear form  $(u^h \times w^h, v^h)$  will vanish when  $v^h = u^h$  or  $w^h$ . Such a trilinear form has significance in the NSE if the rotational form of the nonlinearity is used (see, e.g. [25] p.461 or [49]). Our scheme uses this form, and exploits the double skew symmetry to show the scheme conserves both energy and helicity.

The discrete Gronwall lemma will also be an essential tool in the error analysis; we present it now.

**Lemma 5.3.** (*Discrete Gronwall*) *Let  $\Delta t$ ,  $H$ , and  $a_n, b_n, c_n, d_n$  (for integers  $n \geq 0$ ) be nonnegative numbers such that*

$$a_l + \Delta t \sum_{n=0}^l b_n \leq \Delta t \sum_{n=0}^l d_n a_n + \Delta t \sum_{n=0}^l c_n + H \quad \text{for } l \geq 0. \quad (5.6)$$

*Suppose that  $\Delta t d_n < 1 \forall n$ . Then,*

$$a_l + \Delta t \sum_{n=0}^l b_n \leq \exp \left( \Delta t \sum_{n=0}^l \frac{d_n}{1 - \Delta t d_n} \right) \left( \Delta t \sum_{n=0}^l c_n + H \right) \quad \text{for } l \geq 0. \quad (5.7)$$

*Proof.* See [28], for example, for proof of this well known lemma.  $\square$

Another important tool in this analysis is the Poincare-Freidrich’s inequality on the space  $H_{\#}^1$  (and thus  $V^h$ ):

**Lemma 5.4.** *There exists a constant  $C$ , dependent only on  $\Omega$ , such that for  $\phi \in H_{\#}^1$ ,*

$$\|\phi\|_{H^1} \leq \|\nabla \phi\| \quad (5.8)$$

*Proof.* See [13]. □

We end this section with definitions for discrete energy and helicity.

**Definition 5.2.** *We define the discrete energy  $E$  and helicity  $H$  to be, at time  $t^k$ ,*

$$\begin{aligned} E_h(t^k) &= \frac{1}{2} \|u_h^k\|^2, \\ H_h(t^k) &= (u_h^k, \nabla \times u_h^k). \end{aligned}$$

We are now ready to present the scheme.

### 5.3 AN ENERGY AND HELICITY CONSERVING SCHEME FOR PERIODIC FLOWS

The energy and helicity preserving finite element scheme we study is composed of a trapezoidal time discretization with a nonlinearity that is doubly skew-symmetric. The viscous term is split for stability into two pieces: one is the usual form arising from Green's theorem, and the other comes from (2.8) and uses the projected vorticity. Let  $\Delta t$  denote the timestep,  $t^k = k\Delta t$ ,  $t^{k+1/2} = (k + \frac{1}{2})\Delta t$ , and  $u_h^k$  the approximation to  $u(x, t^k)$ .  $u_h^{k+1/2}$  will denote

$$u_h^{k+1/2} := \frac{1}{2}(u_h^{k+1} + u_h^k),$$

and  $f^{n+1/2}(x) := f(t^{n+1/2}, x) \in V^{h,*}$ .  $T = Nk$  denotes the final time. Given  $u_h^0 \in V^h$ , define  $w_h^0$  to be the (unique in  $V^h$  by Lemma 2.2) solution of  $(w_h^0, v) = (\nabla \times u_h^0, v) \forall v \in V^h$ , and find  $(u_h^k; w_h^k; p_h^k) \in X_h \times V_h \times Q_h$  for  $k = 1..N$ , satisfying

$$\begin{aligned} \frac{1}{\Delta t}(u_h^{n+1}, v) + (u_h^{n+1/2} \times w_h^{n+1/2}, v) - (p_h^{n+1/2}, \nabla \cdot v) + \frac{\nu}{2}(\nabla u_h^{n+1/2}, \nabla v) \\ + \frac{\nu}{2}(w_h^{n+1/2}, \nabla \times v) = (f^{n+1/2}, v) + \frac{1}{\Delta t}(u_h^n, v) \quad \forall v \in X^h \end{aligned} \quad (5.9)$$

$$(\nabla \cdot u_h^{n+1}, q) = 0 \quad \forall q \in Q^h \quad (5.10)$$

$$(w_h^{n+1} - \nabla \times u_h^{n+1}, \chi) = 0 \quad \forall \chi \in V^h \quad (5.11)$$

We now prove the conservation properties of the scheme: energy and helicity are exactly conserved in the absence and viscosity and external force.

**Lemma 5.5.** *The scheme (5.9)-(5.11) conserves energy and helicity in the absence of viscosity and body force, that is,  $E_h(t^n) = E_h(t^0)$  and  $H_h(t^n) = H_h(t^0) \forall n \leq N$  provided  $\nu = f = 0$ .*

*Proof.* For the conservation of energy, set  $v = u_h^{n+1/2}$  and  $\nu = f = 0$  in (5.9). This gives

$$(u_h^{n+1}, u_h^{n+1/2}) = (u_h^n, u_h^{n+1/2}). \quad (5.12)$$

By expanding the  $u_h^{n+1/2}$  terms in (5.12), we have

$$\frac{1}{2}\|u_h^{n+1}\|^2 + \frac{1}{2}(u_h^{n+1}, u_h^n) = \frac{1}{2}\|u_h^n\|^2 + \frac{1}{2}(u_h^n, u_h^{n+1}), \quad (5.13)$$

$$E_h(t^{n+1}) = E_h(t^n), \quad (5.14)$$

which implies that  $E_h(t^n) = E_h(t^0)$ .

For helicity conservation, set  $v = w_h^{n+1/2}$  in (5.9). The pressure term vanishes since  $w_h^n, w_h^{n+1} \in V^h$ , and so after setting  $\nu = f = 0$ , we are left with

$$\frac{1}{2}(u_h^{n+1}, w_h^{n+1}) + \frac{1}{2}(u_h^{n+1}, w_h^n) = \frac{1}{2}(u_h^n, w_h^n) + \frac{1}{2}(u_h^n, w_h^{n+1}). \quad (5.15)$$

Using equation (5.11) and integrating by parts, we have the following identities for the terms in (5.15).

$$(u_h^{n+1}, w_h^{n+1}) = (u_h^{n+1}, \nabla \times u_h^{n+1}) = H_h(t^{n+1}) \quad (5.16)$$

$$(u_h^n, w_h^n) = (u_h^n, \nabla \times u_h^n) = H_h(t^n) \quad (5.17)$$

$$(u_h^{n+1}, w_h^n) = (u_h^n, w_h^{n+1}) \quad (5.18)$$

Thus (5.15) can be rewritten as

$$H_h(t^{n+1}) = H_h(t^n), \quad (5.19)$$

which implies that  $H_h(t^n) = H_h(t^0)$ . □

The following lemma shows that the energy and helicity conserving scheme is also stable.

**Lemma 5.6.** *Solutions to the discrete scheme (5.9)-(5.11) satisfy*

$$\|u_h^N\|^2 + \Delta t \sum_{n=0}^{N-1} \left( \frac{\nu}{2} \|\nabla u_h^{n+1/2}\|^2 + \nu \|w_h^{n+1/2}\|^2 \right) \leq \|u_h^0\|^2 + \frac{2\Delta t}{\nu} \sum_{n=0}^{N-1} \|f^{n+1/2}\|_*^2 \quad (5.20)$$

*Proof.* Set  $v = u_h^{n+1/2}$  in (5.9),  $q = p_h^{n+1/2}$  in (5.10) and add the equations. This gives

$$\begin{aligned} \frac{1}{2\Delta t} \|u_h^{n+1}\|^2 + \frac{1}{2\Delta t} (u_h^{n+1}, u_h^n) + \frac{\nu}{2} \|\nabla u_h^{n+1/2}\|^2 + \frac{\nu}{2} (w_h^{n+1/2}, \nabla \times u_h^{n+1/2}) \\ = (f^{n+1/2}, u_h^{n+1/2}) + \frac{1}{2\Delta t} \|u_h^n\|^2 + \frac{1}{2\Delta t} (u_h^n, u_h^{n+1}). \end{aligned} \quad (5.21)$$

Note that  $(w_h^{n+1/2}, \nabla \times u_h^{n+1/2}) = \|w_h^{n+1/2}\|^2$  since (5.11) must hold for  $(n+1)$  replaced by  $(n)$ , and thus also for  $(n+1)$  replaced by  $(n+1/2)$ . By making this substitution, (5.21) reduces to

$$\frac{1}{2\Delta t} \|u_h^{n+1}\|^2 + \frac{\nu}{2} \|\nabla u_h^{n+1/2}\|^2 + \frac{\nu}{2} \|w_h^{n+1/2}\|^2 = (f^{n+1/2}, u_h^{n+1/2}) + \frac{1}{2\Delta t} \|u_h^n\|^2. \quad (5.22)$$

Next we use the bound  $(f^{n+1/2}, u_h^{n+1/2}) \leq \frac{\nu}{4} \|\nabla u_h^{n+1/2}\|^2 + \frac{1}{\nu} \|f^{n+1/2}\|_*^2$ , and sum from  $n = 0..(N-1)$ , yielding

$$\frac{1}{2\Delta t} \|u_h^N\|^2 + \frac{1}{2} \sum_{n=0}^{N-1} \left( \frac{\nu}{2} \|\nabla u_h^{n+1/2}\|^2 + \nu \|w_h^{n+1/2}\|^2 \right) \leq \frac{1}{2\Delta t} \|u_h^0\|^2 + \frac{1}{\nu} \sum_{n=0}^{N-1} \|f^{n+1/2}\|_*^2 \quad (5.23)$$

Now multiplying both sides by  $(2\Delta t)$  proves the lemma.  $\square$

### 5.3.1 Existence of Solutions for the Scheme

Given  $u_h^n, w_h^n \in V^h$ , a nonlinear system must be solved for the approximations at time level  $n + 1$ . The question arises: does that system have a solution? In other words, does imposing two integral invariants overdetermine the system for  $u_h^{n+1}, w_h^{n+1}$ ? The answer is that solutions to (5.9)-(5.11) do exist, as we will show in this section.

For clarity, we show existence for the equivalent nonlinear problem: Given  $\nu, \Delta t > 0$ ,  $f^{n+1/2} \in V^{h,*}$ , and  $u_h^n \in V^h$ , find  $(u_h; w_h) \in V^h \times V^h$  satisfying

$$\begin{aligned} \frac{2}{\Delta t}(u_h, v) + (u_h \times w_h, v) + \frac{\nu}{2}(\nabla u_h, \nabla v) \\ + \frac{\nu}{2}(w_h, \nabla \times v) = (f^{n+1/2}, v) + \frac{2}{\Delta t}(u_h^n, v) \quad \forall v \in V^h, \end{aligned} \quad (5.24)$$

$$(w_h - \nabla \times u_h, \chi) = 0 \quad \forall \chi \in V^h. \quad (5.25)$$

This form of the scheme is derived from (5.9)-(5.11) by defining  $u_h := u_h^{n+1/2}$ ,  $w_h := w_h^{n+1/2}$ , and restricting the test functions to  $V^h$ . The equations (5.24)-(5.25) are equivalent (5.9)-(5.11). To show solutions exist, we formulate (5.24)-(5.25) as a fixed point problem,  $y = F(y)$ , and use the Leray-Schauder fixed point theorem. We will first prove several preliminary lemmas, followed by a theorem which proves a solution to (5.24)-(5.25) exist.

**Lemma 5.7.** *For  $\nu, \Delta t > 0$ , there exists a unique solution  $u_h, w_h \in V^h \times V^h$  to: Given  $g \in V^{h,*}$ , find  $(u_h; w_h) \in V^h \times V^h$  satisfying*

$$\frac{2}{\Delta t}(u_h, v) + \frac{\nu}{2}(\nabla u_h, \nabla v) + \frac{\nu}{2}(w_h, \nabla \times v) = (g, v) \quad \forall v \in V^h, \quad (5.26)$$

$$(w_h - \nabla \times u_h, \chi) = 0 \quad \forall \chi \in V^h. \quad (5.27)$$

*Proof.* We will prove uniqueness of solutions to (5.26)-(5.27) by showing only the trivial solution solves the homogeneous problem, which will also imply the existence of solutions to the finite dimensional problem. Since the space  $V^h$  includes only zero-mean functions, functions and operators are uniquely solvable and thus we need not consider the adjoint problem. However, in  $V^h \subset H_{\#}^1$ , the curl operator is self-adjoint and thus the adjoint

problem is the same (5.26)-(5.27). Choose  $v = u_h$  in (5.26),  $\chi = w_h$  in (5.27) and substitute (5.27) into (5.26). This gives

$$\frac{2}{\Delta t} \|u_h\|^2 + \frac{\nu}{2} \|\nabla u_h\|^2 + \frac{\nu}{2} \|w_h\|^2 = 0, \quad (5.28)$$

which implies  $u_h = w_h = 0$ , i.e. uniqueness.  $\square$

This lemma allows us to define a solution operator to (5.26)-(5.27).

**Definition 5.3.** We define the solution operator  $T : V^{h,*} \rightarrow (V^h \times V^h)$ , to be the solution operator of (5.26)-(5.27): if  $g \in V^{h,*}$ ,  $T(g) = (u_h; w_h)$  solves (5.26)-(5.27).

We have that  $T$  is well defined by the previous lemma, and we now prove it is also bounded and linear.

**Lemma 5.8.** The solution operator  $T$  is linear, bounded, and continuous.

*Proof.* The linearity of  $T$  follows from the fact that  $T$  is a solution operator to a linear problem. To see that  $T$  is bounded (and thus continuous since it is linear), we let  $v = u_h$ ,  $\chi = w_h$  in (5.26)-(5.27), multiply (5.27) by  $\frac{\nu}{2}$ , and add the equations. This gives

$$\frac{2\|u_h\|^2}{\Delta t} + \frac{\nu}{4} \|\nabla u_h\|^2 + \frac{\nu}{2} \|w_h\|^2 \leq \frac{1}{\nu} \|g\|_*^2$$

Then since  $u_h, w_h$  are finite dimensional,  $\|u_h, w_h\|_{V^h \times V^h} \leq C \|g\|_*$ . Hence,

$$\|T\| = \sup_{g \in V^{h,*}} \frac{\|T(g)\|}{\|g\|_*} = \sup_{g \in V^{h,*}} \frac{\|u_h, w_h\|_{V^h \times V^h}}{\|g\|_*} \leq C.$$

$\square$

We next define the operator  $N$ . The function  $F$  that will be used in the formulation of the fixed point problem will be a composition of  $T$  and  $N$ .

**Definition 5.4.** We define the operator  $N$  on  $(V^h \times V^h)$  by

$$N(v, w) := f^{n+1/2} + \frac{2}{\Delta t} u_h^n + v \times w$$

We now prove properties for  $N$  necessary for use in Leray-Schauder.

**Lemma 5.9.** *For the nonlinear operator  $N$ , we have that  $N : V^h \times V^h \rightarrow V^{h,*}$ ,  $N$  is bounded, and  $N$  is continuous.*

*Proof.* To show  $N$  maps as stated, we let  $(u_h, w_h) \in V^h \times V^h$  and write

$$\|N(u_h; w_h)\|_* = \sup_{v \in V^h} \frac{(N(u_h; w_h), v)}{\|v\|_1}.$$

From the definition of  $N$ , we have that  $\frac{(f^{n+1/2}, v) + (2(\Delta t)^{-1} u_h^n, v)}{\|v\|_1} \leq \|f\|_* + C_1 \|u_h^n\| \leq C_2$ , and that

$$\frac{(u_h \times w_h, v)}{\|v\|_1} \leq \|u_h\|_\infty \|w_h\| \leq C_3$$

since  $u_h$  and  $w_h$  are given to be in  $V^h$ , and all norms are equivalent in finite dimension. Hence  $\|N(u_h, w_h)\|_* < C$ , and so  $N$  maps as stated. Note we have also proven that  $N$  is bounded.

The equivalence of norms in finite dimension is also key in showing  $N$  is continuous, as

$$\|N(u; w) - N(u_k; w_k)\|_* \leq C(\|u \times (w - w_k)\|_* + \|(u - u_k) \times w_k\|_*), \quad (5.29)$$

$$\leq C(\|u\|_\infty \|w - w_k\| + \|w_k\|_\infty \|u - u_k\|), \quad (5.30)$$

and thus  $\rightarrow 0$  as  $\|(u; w) - (u_k; w_k)\| \rightarrow 0$ . □

We are now ready to define the operator  $F$ , which will formulate (5.24)-(5.25) as a fixed point problem.

**Definition 5.5.** *Define the operator  $F : (V^h \times V^h) \rightarrow (V^h \times V^h)$  to be composition of  $T$  and  $N$ :  $F(y) = T(N(y))$ .*

**Lemma 5.10.**  *$F$  is well defined and compact, and a solution to  $y = F(y)$  solves (5.24)-(5.25).*

*Proof.*  $F$  is well defined because  $N$  and  $T$  are. The fact that  $F$  is compact follows from the fact that both  $N$  and  $T$  are continuous and bounded operators on a finite dimensional space. It can easily be seen that a fixed point of  $F$  solves (5.24)-(5.25) by expanding  $F$ . □

We are now ready to prove the existence of a solution to (5.24)-(5.25).

**Theorem 5.1.** *Let  $y_\lambda = (u_\lambda; w_\lambda) \in V^h \times V^h$  and consider the family of fixed point problems  $y_\lambda = \lambda F(y_\lambda)$ ,  $0 \leq \lambda \leq 1$ . A solution  $y_\lambda$  to any of these fixed point problems satisfies  $\|y_\lambda\| < K$ , independent of  $\lambda$ . Since  $F$  is compact, and fixed points of  $F$  solve (5.24)-(5.25), by the Leray-Schauder theorem there exist solutions to (5.24)-(5.25).*

*Proof.* All we have to show to prove this theorem is that solutions to  $y_\lambda = \lambda F(y_\lambda)$  are bounded independent of  $\lambda$ . Using the definition of  $F$  and the linearity of  $T$  we have that

$$y_\lambda = \lambda F(y_\lambda) = \lambda T(N(y_\lambda)) = T(\lambda N(y_\lambda)) = T(\lambda(f^{n+1/2} + \frac{2}{\Delta t}u_h^n + u_\lambda \times w_\lambda)),$$

which implies that

$$\begin{aligned} \frac{2}{\Delta t}(u_\lambda, v) - \lambda(u_\lambda \times w_\lambda, v) + \frac{\nu}{2}(\nabla u_\lambda, \nabla v) \\ + \frac{\nu}{2}(w_\lambda, \nabla \times v) = (\lambda f^{n+1/2}, v) + \frac{2\lambda}{\Delta t}(u_h^n, v) \quad \forall v \in V^h, \end{aligned} \quad (5.31)$$

$$(w_\lambda - \nabla \times u_\lambda, \chi) = 0 \quad \forall \chi \in V^h. \quad (5.32)$$

Multiply (5.32) by  $\frac{\nu}{2}$ , let  $\chi = w_\lambda$  in (5.32),  $v = u_\lambda$  in (5.31), and add the equations. Similar to the stability estimate, this gives

$$\begin{aligned} \frac{1}{\Delta t}\|u_\lambda\|^2 + \frac{\nu}{4}\|\nabla u_\lambda\|^2 + \frac{\nu}{2}\|w_\lambda\|^2 \\ \leq \lambda^2 \left( \frac{1}{\nu}\|f^{n+1/2}\|^2 + \frac{1}{\Delta t}\|u_h^n\|^2 \right) \leq \left( \frac{1}{\nu}\|f^{n+1/2}\|^2 + \frac{1}{\Delta t}\|u_h^n\|^2 \right) \leq C \end{aligned} \quad (5.33)$$

which is a bound independent of  $\lambda$ . Thus the theorem is proven.  $\square$

We have now shown that the scheme (5.9)-(5.11) preserves energy and helicity when  $\nu = f = 0$ , is stable, and admits solutions. The final step is an error analysis for the scheme.

## 5.4 ERROR ANALYSIS OF THE SCHEME

This section presents a theorem for the convergence of the scheme, followed by the proof. The restriction that the theorem places on the time step is for the use of the discrete Gronwall lemma. Although we found its use necessary in the proof, it is widely believed that it gives a gross underestimate of the largest timestep one can use and expect the same asymptotic error. Without the projection step, the proof of the theorem is fairly standard; the smoothness assumptions we make are also fairly standard and are similar to those found in, for example, [30],[55].

**Theorem 5.2.** *For  $u \in L^\infty(0, T; W_4^{k+1}) \cap W_2^3(0, T; L^2) \cap W_4^2(0, T, W_2^1)$ ,  $p \in L^4(0, T; W^k)$ ,  $f \in L^2(0, T, V^{h,*})$  satisfying the Navier-Stokes equations on the periodic box  $\Omega = (0, L)^3$ ,  $(u_h^n; w_h^n)$  given by (5.9)-(5.11) with velocity-pressure spaces chosen as  $P_k, P_{k-1}$  ( $k > 1$ ) and time step  $\Delta t$  sufficiently small (for Gronwall's inequality), we have that*

$$\begin{aligned} \|u(T) - u_h^N\|^2 + \frac{3\nu\Delta t}{4} \sum_{n=0}^{N-1} \left( \frac{1}{2} \|\nabla(u^{n+1/2} - u_h^{n+1/2})\|^2 + \|w^{n+1/2} - w_h^{n+1/2}\|^2 \right) \\ \leq C(u, p, \nu, \Omega)(\Delta t^4 + h^{2k}) \end{aligned} \quad (5.34)$$

*Proof.* The proof of the theorem is divided into the following parts. We first develop the error equations by subtracting our scheme from the NSE. The error is then split into parts in and out of the finite element spaces. This is followed by bounding the error in the finite element space by interpolation error, and the proof concludes by bounding the total error. Note we require that the spaces  $X^h, Q^h$  satisfy the discrete inf-sup condition; with such spaces, and since  $(w_h^0 - \nabla \times u_h^0, v) = 0 \forall v \in V^h$ , the energy and helicity conserving scheme is equivalent to finding solutions  $u^n, w^n \in V^h$ ,  $n = 0..N$  satisfying

$$\begin{aligned} \frac{1}{\Delta t}(u_h^{n+1} - u_h^n, v) - (u_h^{n+1/2} \times w_h^{n+1/2}, v) + \frac{\nu}{2}(\nabla u_h^{n+1/2}, \nabla v) + \frac{\nu}{2}(w_h^{n+1/2}, \nabla \times v) \\ = (f^{n+1/2}, v) \quad \forall v \in V^h, \end{aligned} \quad (5.35)$$

$$(w_h^{n+1/2} - \nabla \times u_h^{n+1/2}, \chi) = 0 \quad \forall \chi \in V^h. \quad (5.36)$$

Using a splitting of the viscous term, the identity  $u \cdot \nabla u = \frac{1}{2} \nabla(u^2) - u \times (\nabla \times u)$ , and grouping the usual pressure gradient with the  $\frac{1}{2} \nabla(u^2)$  term to form the Bernoulli pressure, a periodic solution  $(u; p)$  and  $w := \nabla \times u$  of the NSE satisfies

$$\begin{aligned} & \frac{1}{\Delta t}(u^{n+1} - u^n, v) - (u^{n+1/2} \times w^{n+1/2}, v) + \frac{\nu}{2}(\nabla u^{n+1/2}, \nabla v) + \frac{\nu}{2}(w^{n+1/2}, \nabla \times v) \\ & - (p(t^{n+1/2}), \nabla \cdot v) = (f^{n+1/2}, v) + \left(\frac{u^{n+1} - u^n}{\Delta t} - u_t(t^{n+1/2}), v\right) \\ & - (u^{n+1/2} \times w^{n+1/2} - u(t^{n+1/2}) \times w(t^{n+1/2}), v) + \frac{\nu}{2}(\nabla(u^{n+1/2} - u(t^{n+1/2})), \nabla v) \\ & + \frac{\nu}{2}(w^{n+1/2} - w(t^{n+1/2}), \nabla \times v) \quad \forall v \in V^h. \end{aligned} \quad (5.37)$$

Define  $e^i := u^i - u_h^i$  and  $E^i := w^i - w_h^i$  for  $i = n, n+1, n+1/2$ , and form the error equations by subtracting the scheme (5.35), (5.36) from (5.37) and  $w = \nabla \times u$  to get

$$\begin{aligned} & \frac{1}{\Delta t}(e^{n+1} - e^n, v) - (u^{n+1/2} \times E^{n+1/2}, v) - (e^{n+1/2} \times w_h^{n+1/2}, v) + \frac{\nu}{2}(\nabla e^{n+1/2}, \nabla v) \\ & + \frac{\nu}{2}(E^{n+1/2}, \nabla \times v) - (p(t^{n+1/2}), \nabla \cdot v) = IERR(u^n; w^n; v) \quad \forall v \in V^h, \end{aligned} \quad (5.38)$$

$$(E^{n+1/2}, \chi) - (\nabla \times e^{n+1/2}, \chi) = 0 \quad \forall \chi \in V^h, \quad (5.39)$$

where the interpolation error in time,  $IERR$ , is defined by

$$\begin{aligned} IERR(u^n, w^n, v) & := \left(\frac{u^{n+1} - u^n}{\Delta t} - u_t(t^{n+1/2}), v\right) \\ & - (u^{n+1/2} \times w^{n+1/2} - u(t^{n+1/2}) \times w(t^{n+1/2}), v) + \frac{\nu}{2}(\nabla(u^{n+1/2} - u(t^{n+1/2})), \nabla v) \\ & + \frac{\nu}{2}(w^{n+1/2} - w(t^{n+1/2}), \nabla \times v). \end{aligned} \quad (5.40)$$

Next we split the error terms into pieces in and out of  $V^h$ . Let  $U^i$  and  $W^i$  be the projections of  $u^i$  and  $w^i$ , respectively, into  $V^h$ . Then the error terms can be decomposed as

$$e^i = (u^i - U^i) - (u_h^i - U^i) =: \eta^i - \phi_h^i, \quad (5.41)$$

$$E^i = (w^i - W^i) - (w_h^i - W^i) =: r^i - s_h^i. \quad (5.42)$$

Note that  $(\eta^i, v) = 0$  for  $v \in V^h$  by the definition of  $\eta^i$ . Rewriting (5.38),(5.39) with this decomposition gives

$$\begin{aligned}
& \frac{1}{\Delta t}(\phi_h^{n+1} - \phi_h^n, v) - (\phi_h^{n+1/2} \times w_h^{n+1/2}, v) + \frac{\nu}{2}(\nabla \phi_h^{n+1/2}, \nabla v) \\
& \quad + \frac{\nu}{2}(s_h^{n+1/2}, \nabla \times v) = (u^{n+1/2} \times s_h^{n+1/2}, v) - (u^{n+1/2} \times r^{n+1/2}, v) \\
& \quad - (\eta^{n+1/2} \times w_h^{n+1/2}, v) + \frac{\nu}{2}(\nabla \eta^{n+1/2}, \nabla v) + \frac{\nu}{2}(r^{n+1/2}, \nabla \times v) - (p(t^{n+1/2}), \nabla \cdot v) \\
& \quad \quad \quad + IERR(u^n; w^n; v) \quad \forall v \in V^h, \quad (5.43)
\end{aligned}$$

$$(\nabla \times \phi_h^{n+1}, \chi) = (s_h^{n+1/2}, \chi) - (r^{n+1/2}, \chi) + (\nabla \times \eta^{n+1/2}, \chi) = 0 \quad \forall \chi \in V^h. \quad (5.44)$$

Let  $v = \phi_h^{n+1/2}$  and  $\chi = s_h^{n+1/2}$  and combine (5.43) and (5.44) to get

$$\begin{aligned}
& \frac{1}{2\Delta t}(\|\phi_h^{n+1}\|^2 - \|\phi_h^n\|^2) + \frac{\nu}{2}\|\nabla \phi_h^{n+1/2}\|^2 + \frac{\nu}{2}\|s_h^{n+1/2}\|^2 \\
& \quad = (u^{n+1/2} \times s_h^{n+1/2}, \phi_h^{n+1/2}) - (u^{n+1/2} \times r^{n+1/2}, \phi_h^{n+1/2}) \\
& \quad \quad - (\eta^{n+1/2} \times w_h^{n+1/2}, \phi_h^{n+1/2}) + \frac{\nu}{2}(\nabla \eta^{n+1/2}, \nabla \phi_h^{n+1/2}) \\
& \quad \quad + \frac{\nu}{2}(r^{n+1/2}, \nabla \times \phi_h^{n+1/2}) + \frac{\nu}{2}(r^{n+1/2}, s_h^{n+1/2}) + \frac{\nu}{2}(\nabla \times \eta^{n+1/2}, s_h^{n+1/2}) \\
& \quad \quad \quad - (p(t^{n+1/2}), \nabla \cdot \phi_h^{n+1/2}) + IERR(u^n; w^n; \phi_h^{n+1/2}). \quad (5.45)
\end{aligned}$$

The terms on the right hand side of (5.45) are now majorized in the usual way, using Cauchy-Schwarz and Young's inequalities, and the bound  $(u \times w, v) \leq C\|u\|_0\|v\|_1\|w\|_{1/2}$ . Note in this inequality holds no matter the order of  $u, w, v$  (provided the norms exist) due to a well known vector identity from Calculus. We first bound the following right hand side terms:

$$\frac{\nu}{2} \left| (\nabla \eta^{n+1/2}, \nabla \phi_h^{n+1/2}) \right| \leq \frac{\nu}{32} \|\nabla \phi_h^{n+1/2}\|^2 + C\nu \|\nabla \eta^{n+1/2}\|^2, \quad (5.46)$$

$$\frac{\nu}{2} \left| (r^{n+1/2}, \nabla \times \phi_h^{n+1/2}) \right| \leq \frac{\nu}{32} \|\nabla \phi_h^{n+1/2}\|^2 + C\nu \|r^{n+1/2}\|^2, \quad (5.47)$$

$$\frac{\nu}{2} \left| (r^{n+1/2}, s_h^{n+1/2}) \right| \leq \frac{\nu}{32} \|s_h^{n+1/2}\|^2 + C\nu \|r^{n+1/2}\|^2, \quad (5.48)$$

$$\frac{\nu}{2} \left| (\nabla \eta^{n+1/2}, s_h^{n+1/2}) \right| \leq \frac{\nu}{32} \|s_h^{n+1/2}\|^2 + C\nu \|\nabla \eta^{n+1/2}\|^2, \quad (5.49)$$

$$\left| (p(t^{n+1/2}), \nabla \cdot \phi_h^{n+1/2}) \right| \leq \frac{\nu}{32} \|\nabla \phi_h^{n+1/2}\|^2 + C\nu^{-1} \inf_{q \in Q^h} \|p(t^{n+1/2}) - q\|^2. \quad (5.50)$$

The first of the trilinear terms is bounded by

$$\begin{aligned} \left| (u^{n+1/2} \times s_h^{n+1/2}, \phi_h^{n+1/2}) \right| &\leq C \|\nabla u^{n+1/2}\| \|s_h^{n+1/2}\| \|\phi_h^{n+1/2}\|^{1/2} \|\nabla \phi_h^{n+1/2}\|^{1/2} \\ &\leq \frac{\nu}{32} \|s_h^{n+1/2}\|^2 + \frac{\nu}{32} \|\nabla \phi_h^{n+1/2}\|^2 + C\nu^{-3} \|\nabla u^{n+1/2}\|^4 \|\phi_h^{n+1/2}\|^2. \end{aligned} \quad (5.51)$$

Similarly, the second of the trilinear terms is bounded by

$$\begin{aligned} \left| (u^{n+1/2} \times r^{n+1/2}, \phi_h^{n+1/2}) \right| &\leq \frac{\nu}{32} \|r^{n+1/2}\|^2 + \frac{\nu}{32} \|\nabla \phi_h^{n+1/2}\|^2 \\ &\quad + C\nu^{-3} \|\nabla u^{n+1/2}\|^4 \|\phi_h^{n+1/2}\|^2. \end{aligned} \quad (5.52)$$

The third of the trilinear terms is expanded by adding and subtracting  $w^{n+1/2}$  to  $w_h^{n+1/2}$  to form  $w^{n+1/2} - E^{n+1/2}$ , followed by decomposing  $E^{n+1/2}$ , and bounding each of the three resulting trilinear terms to get

$$\begin{aligned} \left| (\eta^{n+1/2} \times w_h^{n+1/2}, \phi_h^{n+1/2}) \right| &\leq \frac{3\nu}{32} \|\nabla \phi_h^{n+1/2}\|^2 + \frac{\nu}{32} \|s_h^{n+1/2}\|^2 \\ &\quad + C\nu^{-1} \|r^{n+1/2}\|^2 \|\nabla \eta^{n+1/2}\|^2 + \frac{1}{2} \|\nabla \eta^{n+1/2}\|^2 \|w^{n+1/2}\|^2 + C\nu^{-1} \|\phi_h^{n+1/2}\|^2 \\ &\quad + C\nu^{-3} \|\nabla \eta^{n+1/2}\|^4 \|\phi_h^{n+1/2}\|^2. \end{aligned} \quad (5.53)$$

Three of the four terms in  $IERR(u^n; w^n; \phi_h^{n+1/2})$  are majorized as

$$\left| \left( \frac{u^{n+1} - u^n}{\Delta t} - u_t(t^{n+1/2}), \phi_h^{n+1/2} \right) \right| \leq \frac{1}{2} \|\phi_h^{n+1/2}\|^2 + \frac{1}{2} \left\| \frac{u^{n+1} - u^n}{\Delta t} - u_t(t^{n+1/2}) \right\|^2, \quad (5.54)$$

$$\left| \frac{\nu}{2} (\nabla(u^{n+1/2} - u(t^{n+1/2})), \nabla \phi_h^{n+1/2}) \right| \leq \frac{\nu}{32} \|\nabla \phi_h^{n+1/2}\|^2 + C\nu \|\nabla(u^{n+1/2} - u(t^{n+1/2}))\|^2, \quad (5.55)$$

$$\left| \frac{\nu}{2} (w^{n+1/2} - w(t^{n+1/2}), \nabla \times \phi_h^{n+1/2}) \right| \leq \frac{\nu}{32} \|\nabla \phi_h^{n+1/2}\|^2 + C\nu \|w^{n+1/2} - w(t^{n+1/2})\|^2, \quad (5.56)$$

with the remaining term bounded by

$$\begin{aligned} (u^{n+1/2} \times w^{n+1/2} - u(t^{n+1/2}) \times w(t^{n+1/2}), \phi_h^{n+1/2}) &\leq \\ &\frac{2\nu}{32} \|\nabla \phi_h^{n+1/2}\|^2 + C\nu^{-1} \|\nabla u^{n+1/2}\|^2 \|w^{n+1/2} - w(t^{n+1/2})\|^2 \\ &\quad + C\nu^{-1} \|w(t^{n+1/2})\|^2 \|\nabla(u^{n+1/2} - u(t^{n+1/2}))\|^2. \end{aligned} \quad (5.57)$$

We may now rewrite (5.45) as

$$\begin{aligned}
& \frac{1}{2\Delta t} (\|\phi_h^{n+1}\|^2 - \|\phi_h^n\|^2) + \frac{3\nu}{32} \|\nabla \phi_h^{n+1/2}\|^2 + \frac{12\nu}{32} \|s_h^{n+1/2}\|^2 \leq \\
& C\nu \|\nabla \eta^{n+1/2}\|^2 + C\nu \|r^{n+1/2}\|^2 + C\nu^{-1} \inf_{q \in Q^h} \|p(t^{n+1/2}) - q\|^2 \\
& + C\nu^{-3} \|\nabla u^{n+1/2}\|^4 \|\phi_h^{n+1/2}\|^2 + C\nu^{-1} \|r^{n+1/2}\|^2 \|\nabla \eta^{n+1/2}\|^2 \\
& + \frac{1}{2} \|\nabla \eta^{n+1/2}\|^2 \|w^{n+1/2}\|^2 + C\nu^{-3} \|\nabla \eta^{n+1/2}\|^4 \|\phi_h^{n+1/2}\|^2 \\
& + C\nu^{-1} \|\phi_h^{n+1/2}\|^2 + \frac{1}{2} \left\| \frac{u^{n+1} - u^n}{\Delta t} - u_t(t^{n+1/2}) \right\|^2 + C\nu \|\nabla(u^{n+1/2} - u(t^{n+1/2}))\|^2 \\
& + C\nu \|w^{n+1/2} - w(t^{n+1/2})\|^2 + C\nu^{-1} \|\nabla u^{n+1/2}\|^2 \|w^{n+1/2} - w(t^{n+1/2})\|^2 \\
& + C\nu^{-1} \|w(t^{n+1/2})\|^2 \|\nabla(u^{n+1/2} - u(t^{n+1/2}))\|^2. \quad (5.58)
\end{aligned}$$

Taylor series can be used to bound the interpolation in time terms, and thus (5.58) can be reduced to

$$\begin{aligned}
& \frac{1}{2\Delta t} (\|\nabla \phi_h^{n+1}\|^2 - \|\nabla \phi_h^n\|^2) + \frac{3\nu}{32} \|\nabla \phi_h^{n+1/2}\|^2 + \frac{12\nu}{32} \|s_h^{n+1/2}\|^2 \leq \\
& C\nu^{-1} \|\nabla \eta^{n+1/2}\|^2 + C(\nu^{-1} + \nu) \|r^{n+1/2}\|^2 + C\nu^{-1} \inf_{q \in Q^h} \|p^{n+1/2} - q\|^2 \\
& + C\nu^{-1} \|r^{n+1/2}\|^2 \|\nabla \eta^{n+1/2}\|^2 + \frac{1}{2} \|\nabla \eta^{n+1/2}\|^2 \|w^{n+1/2}\|^2 \\
& + C(\Delta t)^3 \int_{t^n}^{t^{n+1}} \|u_{ttt}\|^2 dt + C\nu(\Delta t)^3 \int_{t^n}^{t^{n+1}} \|\nabla u_{tt}\|^2 dt \\
& + C\nu(\Delta t)^3 \int_{t^n}^{t^{n+1}} \|w_{tt}\|^2 dt + C\nu^{-1}(\Delta t)^3 \|\nabla u^{n+1/2}\|^2 \int_{t^n}^{t^{n+1}} \|w_{tt}\|^2 dt \\
& + C\nu^{-1}(\Delta t)^3 \|w(t^{n+1/2})\|^2 \int_{t^n}^{t^{n+1}} \|\nabla u_{tt}\|^2 dt \\
& + C(\nu^{-1} + \nu^{-3}) \|\nabla u^{n+1/2}\|^4 + C\nu^{-3} \|\nabla \eta^{n+1/2}\|^4 \|\phi_h^{n+1/2}\|^2. \quad (5.59)
\end{aligned}$$

Next we sum from  $n = 0..N - 1$ , multiply both sides by  $2\Delta t$ , recall  $\phi_h^0 = 0$  and the smoothness assumptions, and simplify. With the choice of  $P_k, P_{k-1}$  velocity-pressure spaces, (5.59)

reduces to

$$\begin{aligned}
\|\phi_h^N\|^2 + \sum_{n=0}^{N-1} \left( \frac{3\nu\Delta t}{16} \|\nabla\phi_h^{n+1/2}\|^2 + \frac{3\nu\Delta t}{4} \|s_h^{n+1/2}\|^2 \right) \leq \\
C((\Delta t)^4 + \nu^{-1}h^{2k} + (\nu^{-1} + \nu)h^{2k+2} + \nu^{-1}h^{2k} + h^{4k+2}) \\
+ \Delta t \sum_{n=0}^{N-1} \|\nabla\eta^{n+1/2}\|^2 \|w^{n+1/2}\|^2 + C\nu^{-1}(\Delta t)^4 \sum_{n=0}^{N-1} \|\nabla u^{n+1/2}\|^2 \int_{t^n}^{t^{n+1}} \|w_{tt}\|^2 dt \\
+ C\nu^{-1}(\Delta t)^4 \sum_{n=0}^{N-1} \|w(t^{n+1/2})\|^2 \int_{t^n}^{t^{n+1}} \|\nabla u_{tt}\|^2 dt \\
+ C\Delta t \sum_{n=0}^{N-1} (\nu^{-1} + \nu^{-3}) \|\nabla u^{n+1/2}\|^4 + \nu^{-3} \|\nabla\eta^{n+1/2}\|^4 \|\phi_h^{n+1/2}\|^2 \quad (5.60)
\end{aligned}$$

Since  $w = \nabla \times u$ , we reduce (5.60) to

$$\begin{aligned}
\|\phi_h^N\|^2 + \sum_{n=0}^{N-1} \left( \frac{3\nu\Delta t}{16} \|\nabla\phi_h^{n+1/2}\|^2 + \frac{3\nu\Delta t}{4} \|s_h^{n+1/2}\|^2 \right) \leq \\
C((\Delta t)^4 + \nu^{-1}h^{2k} + (\nu^{-1} + \nu)h^{2k+2} + \nu^{-1}h^{2k} + h^{4k+2}) \\
+ \Delta t \sum_{n=0}^{N-1} \|\nabla\eta^{n+1/2}\|^2 \|\nabla u^{n+1/2}\|^2 + C\nu^{-1}(\Delta t)^4 \sum_{n=0}^{N-1} \|\nabla u(t^{n+1/2})\|^2 \int_{t^n}^{t^{n+1}} \|\nabla u_{tt}\|^2 dt \\
+ C\Delta t \sum_{n=0}^{N-1} (\nu^{-1} + \nu^{-3}) \|\nabla u^{n+1/2}\|^4 \\
+ \nu^{-3} \|\nabla\eta^{n+1/2}\|^4 \|\phi_h^{n+1/2}\|^2. \quad (5.61)
\end{aligned}$$

We bound the third and second to last terms with Holder's inequality and the smoothness assumptions, then reduce by assuming  $\Delta t, \nu \leq 1$ . This yields

$$\begin{aligned}
\|\phi_h^N\|^2 + \sum_{n=0}^{N-1} \left( \frac{3\nu\Delta t}{16} \|\nabla\phi_h^{n+1/2}\|^2 + \frac{3\nu\Delta t}{4} \|s_h^{n+1/2}\|^2 \right) \leq \\
C((\Delta t)^4 + \nu^{-1}h^{2k}) \\
+ C\Delta t \sum_{n=0}^{N-1} (\nu^{-1} + \nu^{-3}) \|\nabla u^{n+1/2}\|^4 + \nu^{-3} \|\nabla\eta^{n+1/2}\|^4 \|\phi_h^{n+1/2}\|^2. \quad (5.62)
\end{aligned}$$

Now with  $\Delta t$  chosen sufficiently small, we use the discrete Gronwall inequality to get

$$\|\phi_h^N\|^2 + \sum_{n=0}^{N-1} \left( \frac{3\nu\Delta t}{16} \|\nabla\phi_h^{n+1/2}\|^2 + \frac{3\nu\Delta t}{4} \|s_h^{n+1/2}\|^2 \right) \leq C(u, p, \nu, \Omega)(\Delta t)^4 + h^{2k}. \quad (5.63)$$

Using the triangle inequality with equation (5.63) completes the proof.  $\square$

## 5.5 NUMERICAL EXPERIMENTS

We now present numerical experiments for the energy and helicity conserving scheme. This section makes several comparisons between this scheme and the usual convective form of the trapezoidal (Crank-Nicholson) scheme for the NSE

$$\begin{aligned} \frac{1}{\Delta t}(u_h^{n+1} - u_h^n, v) + \frac{1}{2}(u_h^{n+1/2} \cdot \nabla u_h^{n+1/2}, v) - \frac{1}{2}(u_h^{n+1/2} \cdot \nabla v, u_h^{n+1/2}) \\ + \nu(\nabla u_h^{n+1/2}, \nabla v) = (f^{n+1/2}, v) \quad \forall v \in V^h, \end{aligned} \quad (5.64)$$

and the rotational form

$$\begin{aligned} \frac{1}{\Delta t}(u_h^{n+1} - u_h^n, v) - (u_h^{n+1/2} \times (\nabla \times u_h^{n+1/2}), v) + \nu(\nabla u_h^{n+1/2}, \nabla v) \\ = (f^{n+1/2}, v) \quad \forall v \in V^h. \end{aligned} \quad (5.65)$$

All of the schemes were implemented in MATLAB using Taylor Hood elements and periodic boundary conditions and uniform meshes on the unit cube. Simple fixed point iterations were used to solve the nonlinear problem in each time step.

### 5.5.1 Computational Cost

The energy and helicity conserving scheme is more computationally expensive than the usual trapezoidal schemes (5.64) and (5.65). It solves for velocity and a projected vorticity, both in  $V^h$ , and results in linear systems that are double the size of those arising in the usual schemes. Hence, the energy and helicity conserving scheme would be more practical if a linearization or decoupling of the system could be found that would still conserve both energy and helicity. At this point, we do not know if such a linearization can be found. It is possible that an (effective and reliable) iteration between decoupled equations could be discovered. Since the energy and helicity conserving scheme, when decoupled, will take a form much like that of (5.65), one may even be able to take advantage of more efficient solvers designed for rotational form Navier-Stokes schemes such as those described by Benzi and Jia Liu in [9].

### 5.5.2 Experiment 1: Helicity Conservation for $\nu = f = 0$

The first numerical experiment is a comparison of helicity treatment in the three schemes when  $\nu = f = 0$ . This is the case where helicity is exactly conserved in the true physics, and thus for physical fidelity should also be conserved in the numerical schemes. Using

$$u^0 = \langle \cos(2\pi z), \sin(2\pi z), \sin(2\pi x) \rangle \quad (5.66)$$

for the initial condition (since it is simple and has nonzero helicity), we set  $\nu = f = 0$  in each scheme and computed from  $(0, 1]$  on the (periodic) unit cube. The energy and helicity conserving scheme was run on an  $h = 1/8$  uniform mesh, and the other two schemes were run on  $h = 1/8$  and  $h = 1/16$  uniform meshes. Timesteps were chosen to be 0.025 and 0.01 for the two meshes, respectively. Figure 5.5.2 shows a plot of each solution's helicity on  $[0, 1]$ . It is clear that the usual trapezoidal schemes do not conserve helicity and the energy and helicity conserving scheme, as expected, does. All schemes conserved energy.

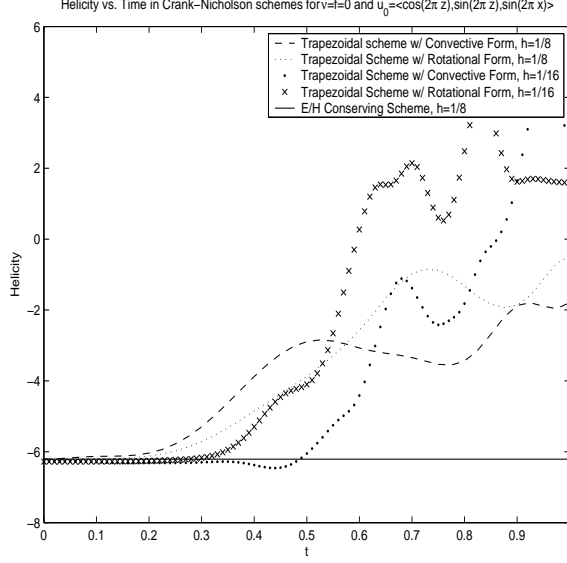


Figure 7: Helicity Conservation in different trapezoid schemes for the NSE with  $\nu = f = 0$  and  $u_0 = (\cos(2\pi z), \sin(2\pi z), \sin(2\pi x))$

### 5.5.3 Experiment 2: Accuracy Comparison for a Known Solution

For the known solution

$$u = ((2 - t) \cos(2\pi z), (1 + t) \sin(2\pi z), (1 - t) \sin(2\pi x)), \quad (5.67)$$

we implemented each of the schemes on a  $h = 1/8$  mesh with  $T = 2$ ,  $\Delta t = 0.025$ , and  $\nu = 1$ . Figures 8,9, and 10 are the plots of helicity error,  $L^2$  error, and  $H^1$  error vs. time for the three schemes. We see from the plots that the usual trapezoidal schemes (5.64) and (5.65) give nearly identical results, and that these schemes have a better  $H^1$  error but worse  $L^2$  error and helicity error than the energy and helicity conserving scheme. We believe that the initial oscillations that appear in the plots of the energy-helicity conserving schemes do not arise from incompatibility of the initial data, but from the use of a vorticity projection on such a coarse mesh coupled with the fact that the scheme is Crank-Nicholson. It is interesting to note that the helicity error in both schemes goes to zero as  $t$  approaches 2. The true helicity goes to zero here also, and it is interesting that both schemes were able to predict

this correctly. We expect that if continued, we would see the absolute helicity error in the energy and helicity conserving scheme again be less than in the other schemes.

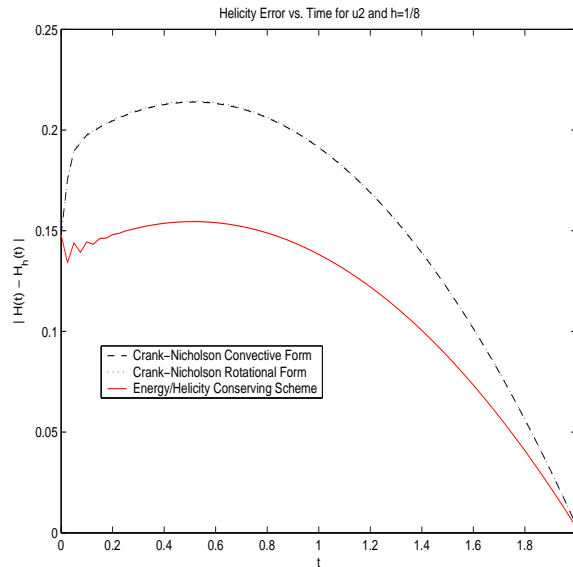


Figure 8: Helicity error in the schemes

## 5.6 CONCLUSIONS

In an effort to find more physically relevant solutions to the Navier-Stokes equations, we have developed an energy and helicity conserving finite element scheme for periodic flows which is second order in time and converges optimally in space. The scheme is able to conserve two inviscid invariants by using the rotational form of the nonlinearity with a projected vorticity. The scheme retains the asymptotic velocity convergence rates of the usual trapezoidal finite element method. Numerical evidence suggests that the scheme can predict helicity more accurately than the usual trapezoidal scheme. However, each linear system that needs to be solved is double the size of those in usual trapezoidal scheme, and thus further work must be done to make this promising scheme more practical.

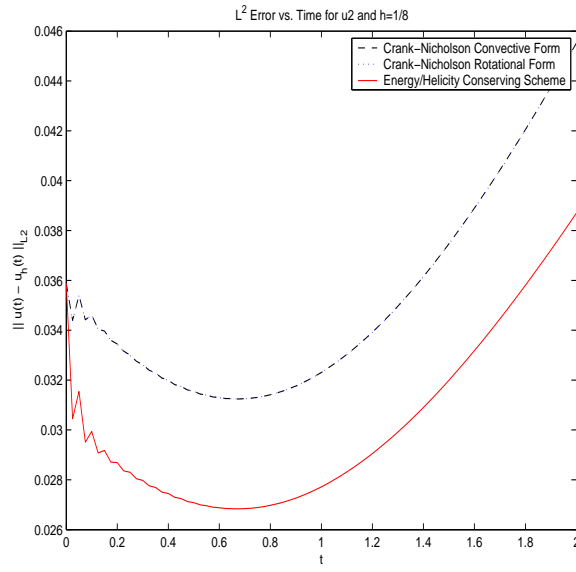


Figure 9:  $L^2$  error in the schemes

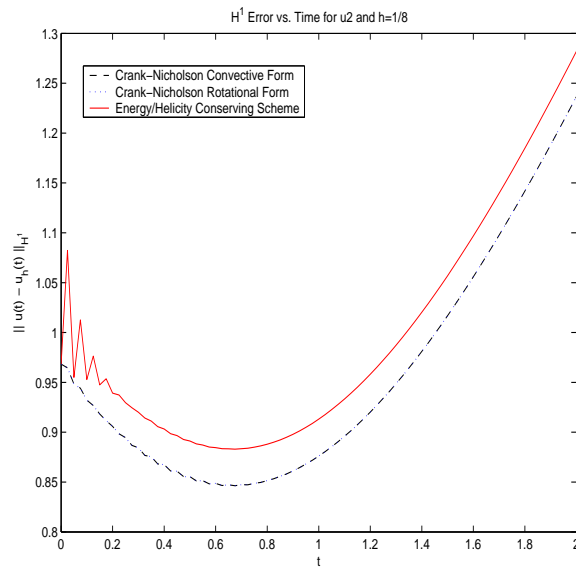


Figure 10:  $H^1$  error in the schemes

## 6.0 A NUMERICAL STUDY OF A HIGHER-ORDER LERAY-DECONVOLUTION TURBULENCE MODEL

### 6.1 INTRODUCTION

The Leray-deconvolution (LerayDC) fluid flow model is a recently developed, high accuracy regularization of the Navier-Stokes equations (NSE). In 1934, J. Leray introduced the following regularization of the NSE (now known as the Leray model) as a theoretical tool:

$$u_t + \bar{u} \cdot \nabla u - \nu \Delta u + \nabla p = f \text{ and } \nabla \cdot u = 0, \quad \text{in } \Omega \times (0, T). \quad (6.1)$$

He chose  $\bar{u} = g_\delta \star u$ , where  $g_\delta$  is a Gaussian associated with a length scale  $\delta$  and proved existence and uniqueness of strong solutions to (6.1) and convergence (modulo a subsequence) to a weak solution of the NSE. If that weak solution is a smooth, strong solution it is not difficult to prove additionally that  $\|u_{NSE} - u_{LerayModel}\|_{L^2} = O(\delta^2)$  using only  $\|u - \bar{u}\|_{L^2} = O(\delta^2)$ .

These and other good theoretical properties have sparked a re-examination of the Leray model (6.1) as a regularized model for simulations of turbulent flows with the modification that the gaussian filter is replaced by a less expensive approximation,  $\bar{u} := (-\delta^2 \Delta + 1)^{-1} u$  [17]. Further mathematical properties of the resulting Leray-alpha model (6.1) are derived by Geurts and Holm [29] test in turbulent flow simulations that reveal

1. the accuracy of the model (6.1) is strictly limited to  $O(\delta^2)$ , and
2. without additional terms added, simulations of the model can result in an accumulation of energy around the cutoff length scale (i.e. wiggles), Guerts and Holm [29]

In this chapter we consider a related, higher order accurate family, the Leray deconvolution models:

$$u_t + D_N(\bar{u}) \cdot \nabla u - \nu \Delta u + \nabla p = f \text{ and } \nabla \cdot u = 0, \quad \text{in } \Omega \times (0, T). \quad (6.2)$$

where  $D_N$  satisfies, for smooth  $u$ ,

$$D_N \bar{u} = u + O(\delta^{2N+2}) \quad N = 0, 1, 2, \dots$$

This family of models is an idea of A. Dunca <sup>1</sup>. It has the following attractive properties:

- for  $N = 0$  they include the Leray-alpha model as the lowest order special case.
- their accuracy is very high,  $O(\delta^{2N+2})$  for arbitrary  $N = 0, 1, 2, \dots$ .
- they share the attractive theoretical properties of the Leray model, e.g., convergence (modulo a subsequence) as  $\delta \rightarrow 0$  to a weak solution of the NSE and  $\|u_{NSE} - u_{LerayDCM}\| = O(\delta^2)$  for a smooth, strong solution  $u_{NSE}$ , [34].
- given  $\bar{u}$  the computation of  $D_N \bar{u}$  is computationally attractive.
- the higher order models (for  $N > 1$ ) give dramatic improvement of accuracy and physical fidelity over the  $N = 0$  case (see section 6.4).
- increasing model accuracy can be done in two ways: (i) cutting  $\delta \rightarrow \delta/2$  increases accuracy by  $\simeq 1/4$  but requires remeshing with  $\simeq 8\times$  as many unknowns, and (ii) increasing  $N \rightarrow N + 1$  increases accuracy from  $O(\delta^{2N+2})$  to  $O(\delta^{2N+4})$  and requires one more Poisson solve  $((-\delta^2 \Delta + 1)^{-1} \phi)$  per time step.
- although our analysis of (6.2) is for differential filters, the model is independent of this filter choice and the analysis is extensible to many other filters with only technical modifications.

---

<sup>1</sup>Private communication.

This chapter has two goals. First, we perform a numerical analysis of a stable algorithm for (6.2). We test this method carefully and delineate some of its advantages and disadvantages beyond the usual error analysis. Second, we test the family of models themselves for accuracy and physical fidelity (Section 6.4) and draw tentative conclusions about the Leray deconvolution family.

The ideas we test are outgrowths of the seminal work of J. Leray [39], the recent work on the Leray-alpha model [17], the early work of G. Baker [7] on extrapolated Crank-Nicolson methods and the development of the deconvolution approach to large eddy simulation. The deconvolution approach to modeling turbulence is an ingenious idea of Stolz and Adams with Kleiser [3], [54] which has interesting and extensive mathematical justification for its accuracy and effectiveness, e.g., [1],[2],[4].

We will formally present the scheme in Section 2 after giving the notation and definitions necessary for the scheme and for the analysis used throughout this chapter. Section 3 develops the theory for the scheme, showing stability, unique existence of solutions, and convergence analysis. Numerical experiments are presented in Section 4, followed by conclusions.

## 6.2 NOTATION AND PRELIMINARIES

This section summarizes the notation, definitions and preliminary lemmas needed. We start by introducing the following notation. The  $L^2(\Omega)$  norm and inner product will be denoted by  $\|\cdot\|$  and  $(\cdot, \cdot)$ . Likewise, the  $L^p(\Omega)$  norms and the Sobolev  $W_p^k(\Omega)$  norms are denoted by  $\|\cdot\|_{L^p}$  and  $\|\cdot\|_{W_p^k}$ , respectively. For the semi-norm in  $W_p^k(\Omega)$  we use  $|\cdot|_{W_p^k}$ .  $H^k$  is used to represent the Sobolev space  $W_2^k$ , and  $\|\cdot\|_k$  denotes the norm in  $H^k$ . For functions  $v(x, t)$  defined on the entire time interval  $(0, T)$ , we define

$$\|v\|_{\infty, k} := \sup_{0 < t < T} \|v(t, \cdot)\|_k, \quad \text{and} \quad \|v\|_{m, k} := \left( \int_0^T \|v(t, \cdot)\|_k^m dt \right)^{1/m}.$$

We consider both the periodic case and the case of internal flow with no slip boundary conditions. (There is mainly only small notational differences between these two cases in the analysis.)

In the periodic case,  $\Omega = (0, L)^d$ ,  $d = 2, 3$  and the velocity pressure spaces are

$$X := H_{\#}^1 := \{v \in H^1(\Omega) \cap L_0^2(\Omega) : v \text{ is } L \text{ periodic}\}, \quad Q := L_0^2(\Omega), \quad (6.3)$$

which in the case of internal flow  $\Omega$  is a regular, bounded domain in  $R^d$  and

$$X := H_0^1(\Omega), \quad Q := L_0^2(\Omega). \quad (6.4)$$

We denote the dual space of  $X$  as  $X^*$ , with the norm  $\|\cdot\|_*$ .

The space of divergence free functions is

$$V := \{v \in X, (\nabla \cdot v, q) = 0 \quad \forall q \in Q\}. \quad (6.5)$$

The velocity-pressure finite element spaces  $X^h \subset X$ ,  $Q^h \subset Q$  are assumed to be conforming and satisfy the LBB<sup>h</sup> condition. The discretely divergence free subspace of  $X^h$  is, as usual

$$V^h = \{v^h \in X^h, (\nabla \cdot v^h, q^h) = 0 \quad \forall q^h \in Q^h\}. \quad (6.6)$$

Taylor-Hood elements (see e.g. [13]) are one common example of such a choice for  $(X^h, Q^h)$ , and are also the elements we use in our numerical experiments.

We employ the usual skew-symmetrization used in many finite element discretizations for fluid flow problems. Using this trilinear form ensures stability of the method.

**Definition 6.1 (Skew Symmetric operator  $b^*$ ).** *Define the skew-symmetric trilinear operator  $b^* : X \times X \times X \rightarrow \mathbf{R}$  as*

$$b^*(u, v, w) := \frac{1}{2}(u \cdot \nabla v, w) - \frac{1}{2}(u \cdot \nabla w, v) \quad (6.7)$$

We now list important estimates for the  $b^*$  operator necessary in Section 3.

**Lemma 6.1.** *For  $u, v, w \in X$ , and also  $v \in L_\infty(\Omega)$  for the first estimate, the trilinear term  $b^*(u, v, w)$  can be bounded in the following ways*

$$b^*(u, v, w) \leq \frac{1}{2} (\|u\| \|\nabla v\|_\infty \|w\| + \|u\| \|v\|_\infty \|\nabla w\|). \quad (6.8)$$

$$b^*(u, v, w) \leq C_0(\Omega) \|\nabla u\| \|\nabla v\| \|\nabla w\|, \quad (6.9)$$

$$b^*(u, v, w) \leq C_0(\Omega) \|u\|^{1/2} \|\nabla u\|^{1/2} \|\nabla v\| \|\nabla w\|. \quad (6.10)$$

*Proof.* The result of the first bound follows immediately from the definition of  $b^*$ . The proof of the other two bounds can be found, for example, in [33].  $\square$

**Definition 6.2 (Continuous differential filter).** *For periodic  $\phi \in L^2(\Omega)$ , denote the filtering operation on  $\phi$  by  $\bar{\phi}$ , where  $\bar{\phi}$  is the unique periodic solution of*

$$-\delta^2 \Delta \bar{\phi} + \bar{\phi} = \phi. \quad (6.11)$$

We denote by  $A := (-\delta^2 \Delta + I)$ , so  $A^{-1}v = \bar{v}$ .

We define next the discrete differential filter following, Manica and Kaya Merdan [43].

**Definition 6.3 (Discrete differential filter).** *Given  $v \in X^h$ , for a given filtering radius  $\delta > 0$ ,  $\bar{v}^h = A_h^{-1}v$  is the unique solution in  $X^h$  of*

$$\delta^2 (\nabla \bar{v}^h, \nabla \chi) + (\bar{v}^h, \chi) = (v, \chi) \quad \forall \chi \in X^h. \quad (6.12)$$

**Definition 6.4.** *Define the  $L^2$  projection  $\Pi^h : X \rightarrow X^h$  and discrete Laplacian operator  $\Delta^h : X \rightarrow X^h$  in the usual way by*

$$(\Pi^h v - v, \chi) = 0, \quad (\Delta^h v, \chi) = -(\nabla v, \nabla \chi) \quad \forall \chi \in X^h. \quad (6.13)$$

With  $\Delta^h$ , we can write  $\bar{v}^h = (-\delta^2 \Delta^h + \Pi^h)^{-1} v^h$  and  $A_h = (-\delta^2 \Delta^h + \Pi^h)$ .

We now define the van Cittert approximate deconvolution operators.

**Definition 6.5.** *The continuous and discrete van Cittert deconvolution operators  $D_N$  and  $D_N^h$  are*

$$D_N v := \sum_{n=0}^N (I - A^{-1})^n v, \quad D_N^h v := \sum_{n=0}^N (I - A_h^{-1})^n v. \quad (6.14)$$

Our numerical experiments use  $N = 0, 1, 2, 3$  for which we have

$$D_0^h v = v, \quad (6.15)$$

$$D_1^h v = 2v - \bar{v}^h, \quad (6.16)$$

$$D_2^h v = 3v - 3\bar{v}^h + \overline{\bar{v}^h}^h, \quad (6.17)$$

$$D_3^h v = 4v - 6\bar{v}^h + 4\overline{\bar{v}^h}^h - \overline{\overline{\bar{v}^h}^h}^h. \quad (6.18)$$

$D_N$  was shown to be an  $O(\delta^{2N+2})$  approximate inverse to the filter operator  $A^{-1}$  in Lemma (2.1) of [20].

**Lemma 6.2.**  *$D_N$  is a bounded, self-adjoint, positive operator that is an  $O(\delta^{2N+2})$  asymptotic inverse to the filter  $A^{-1}$  for very smooth  $\phi$  and as  $\delta \rightarrow 0$ ,*

$$\phi = D_N \bar{\phi} + (-1)^{(N+1)} \delta^{2N+2} \Delta^{N+1} A^{-(N+1)} \phi$$

We begin by recalling from [10], [43] some basic facts about discrete differential filters and deconvolution operators.

**Lemma 6.3.** *For  $v \in X$ , we have the following bounds for the discretely filtered and approximately deconvolved  $v$*

$$\|\bar{v}^h\| \leq \|v\| \quad (6.19)$$

$$\|D_N^h \bar{v}^h\| \leq C(N) \|v\| \quad (6.20)$$

$$\|\nabla \bar{v}^h\| \leq \|\nabla v\| \quad (6.21)$$

$$\|\nabla D_N^h \bar{v}^h\| \leq C(N) \|\nabla v\| \quad (6.22)$$

*Proof.* The proof of (6.19) follows from choosing  $\chi = \bar{v}^h$  in (6.12), and applying Young's inequality. (6.20) follows exactly as in [10].

To prove (6.21), we note that the filter definition can be rewritten using  $\Delta^h$  as

$$-\delta^2(\Delta^h \bar{v}^h, \chi) + (\bar{v}^h, \chi) = (v, \chi) \quad \forall \chi \in X^h.$$

Choosing  $\chi = \Delta^h \bar{v}^h$  and using the definition of  $\Delta^h$  gives

$$\delta^2 \|\Delta^h \bar{v}^h\|^2 + \|\nabla \bar{v}^h\|^2 = (\nabla v, \nabla \bar{v}^h)$$

Now Young's inequality proves (6.21). (6.22) follows immediately from (6.21) and the definition of  $D_N^h$ .  $\square$

**Lemma 6.4.** *For smooth  $\phi$  the discrete approximate deconvolution operator applied using  $P_k$  elements satisfies*

$$\|\phi - D_N^h \bar{\phi}^h\| \leq C \delta^{2N+2} \|\bar{\phi}\|_{H^{2N+2}} + C(\delta h^k + h^{k+1}) \left( \sum_{n=1}^N |(A^{-1})^n \phi|_{k+1} \right). \quad (6.23)$$

and

$$\|\nabla(\phi - D_N^h \bar{\phi}^h)\| \leq C \delta^{2N+2} \|\bar{\phi}\|_{H^{2N+3}} + C(h^k + \delta^{-1} h^{k+1}) \left( \sum_{n=1}^N |(A^{-1})^n \phi|_{k+1} \right). \quad (6.24)$$

*Proof.* We start the proof by splitting the error

$$\|\phi - D_N^h \bar{\phi}^h\| \leq \|\phi - D_N \bar{\phi}\| + \|D_N \bar{\phi} - D_N^h \bar{\phi}\| + \|D_N^h \bar{\phi} - D_N^h \bar{\phi}^h\|. \quad (6.25)$$

Lemma 6.2 gives

$$\|\phi - D_N \bar{\phi}\| \leq C \delta^{2N+2} \|\bar{\phi}\|_{H^{2N+2}}. \quad (6.26)$$

Lemma 6.3 gives for the third term in (6.25) that  $\|D_N^h \bar{\phi} - D_N^h \bar{\phi}^h\| \leq C \|\bar{\phi} - \bar{\phi}^h\|$ . Then, by using standard finite element techniques (i.e. subtracting (6.12) from the continuous scheme of (6.11) and using standard inequalities) we have

$$\|\bar{\phi} - \bar{\phi}^h\| \leq C(\delta h^k + h^{k+1}) |\bar{\phi}|_{k+1}. \quad (6.27)$$

and

$$\|\nabla(\bar{\phi} - \bar{\phi}^h)\| \leq C(h^k + \delta^{-1}h^{k+1})|\bar{\phi}|_{k+1}. \quad (6.28)$$

It is left to bound the second term from (6.25). First, note that for  $N = 0$ ,  $\|D_0\bar{\phi}^h - D_0^h\bar{\phi}\| = 0$ . Based on the Definition 6.5 of continuous and discrete deconvolution operators and their expansion (see (6.15)- (6.18)), the second term in (6.25) is rewritten as

$$\|D_N\bar{\phi} - D_N^h\bar{\phi}\| = \left\| \sum_{n=0}^N \alpha_n ((A^{-1})^n\bar{\phi} - (A_h^{-1})^n\bar{\phi}) \right\| \leq \sum_{n=0}^N \alpha_n \|(A^{-1})^n\bar{\phi} - (A_h^{-1})^n\bar{\phi}\|. \quad (6.29)$$

For  $N = 1$ , the results (6.28) and (6.19) give

$$\begin{aligned} \|(A^{-1})\bar{\phi} - (A_h^{-1})\bar{\phi}\| &= \|\bar{\bar{\phi}} - \bar{\bar{\phi}}^h\| \\ &\leq \|\bar{\bar{\phi}} - \bar{\bar{\phi}}^h\| + \|\bar{\bar{\phi}}^h - \bar{\bar{\phi}}^h\| \\ &\leq \|\bar{\bar{\phi}} - \bar{\bar{\phi}}^h\| + \|\bar{\phi} - \bar{\phi}^h\| \\ &\leq C(\delta h^k + h^{k+1})(|\bar{\bar{\phi}}|_{k+1} + |\bar{\phi}|_{k+1}). \end{aligned} \quad (6.30)$$

Inductively,

$$\|(A^{-1})^N\bar{\phi} - (A_h^{-1})^N\bar{\phi}\| \leq C(\delta h^k + h^{k+1})\left(\sum_{n=1}^N |(A^{-1})^n\bar{\phi}|_{k+1}\right). \quad (6.31)$$

The proof is completed by putting together the derived bounds for the terms in (6.25). The proof for the bound of the gradient follows similarly.  $\square$

Recall that a strong solution of the Navier Stokes equations satisfies  $u \in L^2(0, T; X) \cap L^\infty(0, T; L^2(\Omega)) \cap L^4(0, T; X)$ ,  $p \in L^2(0, T; Q)$  with  $u_t \in L^2(0, T; X')$  such that

$$(u_t, v) + (u \cdot \nabla u, v) - (p, \nabla \cdot v) + \nu(\nabla u, \nabla v) = (f, v), \quad \forall v \in X, \quad (6.32)$$

$$(q, \nabla \cdot u) = 0, \quad \forall q \in Q. \quad (6.33)$$

For the ease of notation in discussion we let  $v(t_{n+1/2}) = v((t_n + t_{n+1})/2)$  for the continuous variable and  $v_{n+1/2} = (v_n + v_{n+1})/2$  for both, continuous and discrete variables.

**Algorithm 6.1.** *[Crank-Nicholson Finite Element Scheme for Leray-deconvolution]* Let  $\Delta t > 0$ ,  $(w_0, q_0) \in (X^h, Q^h)$ ,  $f \in X^*$  and  $M := \frac{T}{\Delta t}$ . For  $n = 0, 1, 2, \dots, M-1$ , find  $(w_{n+1}^h, q_{n+1}^h) \in (X^h, Q^h)$  satisfying

$$\begin{aligned} \frac{1}{\Delta t}(w_{n+1}^h - w_n^h, v^h) + b^*(D_N^h \overline{w_{n+1/2}^h}, w_{n+1/2}^h, v^h) - (q_{n+1/2}^h, \nabla \cdot v^h) \\ + \nu(\nabla w_{n+1/2}^h, \nabla v^h) = (f_{n+1/2}, v^h) \quad \forall v^h \in X^h \end{aligned} \quad (6.34)$$

$$(\nabla \cdot w_{n+1}^h, \chi^h) = 0 \quad \forall \chi^h \in Q^h \quad (6.35)$$

**Remark 6.1.** *Since  $(X^h, Q^h)$  satisfies the  $LBB^h$  condition, (6.34)-(6.35) is equivalent to*

$$\begin{aligned} \frac{1}{\Delta t}(w_{n+1}^h - w_n^h, v^h) + b^*(D_N^h \overline{w_{n+1/2}^h}, w_{n+1/2}^h, v^h) + \nu(\nabla w_{n+1/2}^h, \nabla v^h) \\ = (f_{n+1/2}, v^h) \quad \forall v^h \in V^h. \end{aligned} \quad (6.36)$$

We define the following additional norms:

$$\begin{aligned} \|v\|_{\infty, k} &:= \max_{0 \leq n \leq N_T} \|v^n\|_k, & \|v_{1/2}\|_{\infty, k} &:= \max_{1 \leq n \leq N_T} \|v^{n-1/2}\|_k, \\ \|v\|_{m, k} &:= \left( \sum_{n=0}^{N_T} \|v^n\|_k^m \Delta t \right)^{1/m}, & \|v_{1/2}\|_{m, k} &:= \left( \sum_{n=1}^{N_T} \|v^{n-1/2}\|_k^m \Delta t \right)^{1/m}. \end{aligned}$$

In addition, we make use of the following approximation properties, [13]:

$$\begin{aligned} \inf_{v \in V_h} \|u - v\| &\leq Ch^{k+1} \|u\|_{k+1}, \quad u \in H^{k+1}(\Omega)^d, \\ \inf_{v \in V_h} \|u - v\|_1 &\leq Ch^k \|u\|_{k+1}, \quad u \in H^{k+1}(\Omega)^d, \\ \inf_{r \in P_h} \|p - r\| &\leq Ch^{s+1} \|p\|_{s+1}, \quad p \in H^{s+1}(\Omega). \end{aligned} \quad (6.37)$$

### 6.3 ANALYSIS OF THE SCHEME

In this section, we show that solutions of the scheme (6.36), equivalently (6.34)-(6.35) are unconditionally stable, well defined and optimally convergent to solutions of the NSE.

**Lemma 6.5.** *For the approximation scheme (6.34),(6.35) we have that a solution  $w_l^h$ ,  $l = 1, \dots, M$ , exists at each iteration and satisfies the following a priori bound:*

$$\|w_M^h\|^2 + \nu \Delta t \sum_{n=0}^{M-1} \|\nabla w_{n+1/2}^h\|^2 \leq \|w_0^h\|^2 + \frac{\Delta t}{\nu} \sum_{n=0}^{M-1} \|f_{n+1/2}\|_*^2. \quad (6.38)$$

*Proof.* : The existence of a solution  $w_n^h$  to (6.34),(6.35) follows from the Leray-Schauder Principle [58]. Specifically, with  $A : Z_h \rightarrow Z_h$ , defined by  $y = A(z)$

$$\begin{aligned} (y, v) := & -\Delta t b^*(D_N^h \overline{(z + w_n^h)}/2^h, (z + w_n^h)/2, v) - \Delta t \nu (\nabla(z + w_n^h)/2, \nabla v) \\ & + (w_{n-1}^h, v) + \Delta t (f_{n+1/2}, v). \end{aligned}$$

The operator  $A$  is compact and any solution of  $u = s A(u)$ , for  $0 \leq s < 1$ , satisfied the bound  $\|u\| \leq \gamma$ , where  $\gamma$  is independent of  $s$ .

To obtain the a priori estimate set  $v^h = w_{n+1/2}^h$  in (6.36)

$$\frac{1}{2\Delta t} (\|w_{n+1}^h\|^2 - \|w_n^h\|^2) + \nu \|\nabla w_{n+1/2}^h\|^2 \leq \frac{1}{2\nu} \|f_{n+1/2}\|_*^2 + \frac{\nu}{2} \|\nabla w_{n+1/2}^h\|^2 \quad \text{for every } n,$$

i.e.,

$$\frac{1}{\Delta t} (\|w_{n+1}^h\|^2 - \|w_n^h\|^2) + \nu \|\nabla w_{n+1/2}^h\|^2 \leq \frac{1}{\nu} \|f_{n+1/2}\|_*^2, \quad \text{for every } n.$$

Summing from  $n = 0 \dots M - 1$  gives the desired result. □

**Theorem 6.1.** *Let  $(u(t), p(t))$  be a smooth, zero-mean solution on  $\Omega$  to the NSE. Suppose  $(w_0^h, q_0^h)$  are chosen to be the interpolants of  $(u(0), p(0))$ , respectively. Then there is a constant  $C = C(u, p)$  such that*

$$\begin{aligned} \|u - w^h\|_{\infty,0} & \leq F(\Delta t, h, \delta) + Ch^{k+1} \|u\|_{\infty, k+1}, \quad (6.39) \\ \left( \nu \Delta t \sum_{n=0}^{M-1} \|\nabla(u^{n+1/2} - (w_{n+1}^h + w_n^h)/2)\|^2 \right)^{1/2} & \leq F(\Delta t, h, \delta) + C\nu^{1/2} (\Delta t)^2 \|\nabla u_{tt}\|_{2,0} \\ & \quad + C\nu^{1/2} h^k \|u\|_{2, k+1}. \quad (6.40) \end{aligned}$$

where

$$\begin{aligned}
F(\Delta t, h, \delta) &:= C\nu^{-1/2} h^{k+1/2} (\|u\|_{4,k+1}^2 + \|\nabla u\|_{4,0}^2) + C\nu^{1/2} h^k \|u\|_{2,k+1} \\
&+ C\nu^{-1/2} h^k (\|u\|_{4,k+1}^2 + \nu^{-1/2} (\|w_0^h\| + \nu^{-1/2} \|f\|_{2,*})) + C\nu^{-1/2} h^{s+1} \|p_{1/2}\|_{2,s+1} \\
&+ C\nu^{-1/2} \delta^{2N+2} \|\bar{u}\|_{2,2N+2} + C\nu^{-1/2} (\delta h^k + h^{k+1}) \left( \sum_{n=1}^N \| (A^{-1})^N u \|_{2,k+1} \right) \\
&+ C(\Delta t)^2 (\|u_{ttt}\|_{2,0} + \nu^{-1/2} \|p_{tt}\|_{2,0} + \|f_{tt}\|_{2,0} \\
&\quad + \nu^{1/2} \|\nabla u_{tt}\|_{2,0} + \nu^{-1/2} \|\nabla u_{tt}\|_{4,0}^2 \\
&\quad + \nu^{-1/2} \|\nabla u\|_{4,0}^2 + \nu^{-1/2} \|\nabla u_{1/2}\|_{4,0}^2) . \tag{6.41}
\end{aligned}$$

**Corollary 6.1.** *Suppose that in addition to the assumptions made in Theorem (6.1), the finite element spaces  $X^h$  and  $Q^h$  are composed of Taylor-Hood elements. Then the error in the extrapolated trapezoidal finite element scheme for Leray-deconvolution is of the order*

$$\|u - w^h\|_{\infty,0} + \left( \nu \Delta t \sum_{n=1}^M \|\nabla(u_{n+1/2} - w_{n+1/2}^h)\|^2 \right)^{1/2} = O(h^2 + \Delta t^2 + \delta^{2N+2}). \tag{6.42}$$

*Proof of Theorem 6.1.* Note that for  $u, v, w, \in X$ , with  $\int_{\Omega} q \nabla \cdot u \, dA = 0$ , for all  $q \in Q$ ,

$$b^*(u, v, w) = b(u, v, w) := (u \cdot \nabla v, w) .$$

Then, at time  $t_{n+1/2}$ ,  $u$  given by (6.32)-(6.33) satisfies, for all  $v^h \in V^h$ ,

$$\begin{aligned}
\left( \frac{u_{n+1} - u_n}{\Delta t}, v^h \right) + b^*(D_N^h \overline{u_{n+1/2}}^h, u_{n+1/2}, v^h) + \nu (\nabla u_{n+1/2}, \nabla v^h) - (p_{n+1/2}, \nabla \cdot v^h) \\
= (f_{n+1/2}, v^h) + \text{Intp}(u^n, p^n; v^h), \tag{6.43}
\end{aligned}$$

for all  $v^h \in V^h$ , where  $\text{Intp}(u_n, p_n; v^h)$ , representing the interpolating error, denotes

$$\begin{aligned}
\text{Intp}(u^n, p^n; v^h) &= \left( \frac{u^{n+1} - u^n}{\Delta t} - u_t(t_{n+1/2}), v^h \right) + \nu (\nabla u_{n+1/2} - \nabla u(t_{n+1/2}), \nabla v^h) \\
&+ b^*(u_{n+1/2}, u_{n+1/2}, v^h) - b^*(u(t_{n+1/2}), u(t_{n+1/2}), v^h) \\
&- b^*(u_{n+1/2} - D_N^h \overline{u_{n+1/2}}^h, u_{n+1/2}, v^h) \\
&- (p_{n+1/2} - p(t_{n+1/2}), \nabla \cdot v^h) + (f(t_{n+1/2}) - f_{n+1/2}, v^h) . \tag{6.44}
\end{aligned}$$

Subtracting (6.36) from (6.43) and letting  $e_n = u_n - w_n^h$  we have

$$\begin{aligned} \frac{1}{\Delta t}(e_{n+1} - e_n, v^h) + b^*(D_N^h \overline{u_{n+1/2}}^h, u_{n+1/2}, v^h) - b^*(D_N^h \overline{w_{n+1/2}}^h, w_{n+1/2}, v^h) + \\ \nu(\nabla e_{n+1/2}, \nabla v^h) = (p_{n+1/2}, \nabla \cdot v^h) + \text{Intp}(u^n, p^n; v^h) \quad \forall v^h \in V^h. \end{aligned} \quad (6.45)$$

Decompose the error as  $e_n = (u_n - U_n) - (w_n^h - U_n) := \eta_n - \phi_n^h$  where  $\phi_n^h \in V^h$ . Setting  $v^h = \phi_{n+1/2}^h$  in (6.45) and using  $(q, \nabla \cdot \phi_{n+1/2}) = 0$  for all  $q \in V^h$  we obtain

$$\begin{aligned} (\phi_{n+1}^h - \phi_n^h, \phi_{n+1/2}^h) + \nu \Delta t \|\nabla \phi_{n+1/2}^h\| + \Delta t b^*(D_N^h \overline{w_{n+1/2}}^h, e_{n+1/2}, \phi_{n+1/2}^h) \\ + \Delta t b^*(D_N^h \overline{e_{n+1/2}}^h, u_{n+1/2}, \phi_{n+1/2}^h) = (\eta_{n+1} - \eta_n, \phi_{n+1/2}^h) + \Delta t \nu (\nabla \eta_{n+1/2}, \nabla \phi_{n+1/2}^h) \\ + \Delta t (p_{n+1/2} - q, \nabla \cdot \phi_{n+1/2}^h) + \Delta t \text{Intp}(u^n, p^n; v^h). \end{aligned} \quad (6.46)$$

i.e.,

$$\begin{aligned} \frac{1}{2}(\|\phi_{n+1}^h\| - \|\phi_n^h\|) + \nu \Delta t \|\nabla \phi_{n+1/2}^h\| = (\eta_{n+1} - \eta_n, \phi_{n+1/2}^h) + \Delta t \nu (\nabla \eta_{n+1/2}, \nabla \phi_{n+1/2}^h) \\ - \Delta t b^*(D_N^h \overline{\eta_{n+1/2}}^h, u_{n+1/2}, \phi_{n+1/2}^h) + \Delta t b^*(D_N^h \overline{\phi_{n+1/2}}^h, u_{n+1/2}, \phi_{n+1/2}^h) \\ - \Delta t b^*(D_N^h \overline{w_{n+1/2}}^h, \eta_{n+1/2}, \phi_{n+1/2}^h) + \Delta t (p_{n+1/2} - q, \nabla \cdot \phi_{n+1/2}^h) \\ + \Delta t \text{Intp}(u^n, p^n; v^h). \end{aligned} \quad (6.47)$$

We now bound the terms in the RHS of (6.46) individually.

$(\eta_{n+1} - \eta_n, \phi_{n+1/2}^h) = 0$  since  $U$  is the  $L^2$  projection of  $u$  in  $V^h$ .

Cauchy-Schwarz and Young's inequalities give

$$\begin{aligned} \nu \Delta t (\nabla \eta_{n+1/2}, \nabla \phi_{n+1/2}^h) &\leq \nu \Delta t \|\nabla \eta_{n+1/2}\| \|\nabla \phi_{n+1/2}^h\| \\ &\leq \frac{\nu \Delta t}{12} \|\nabla \phi_{n+1/2}^h\|^2 + C \nu \Delta t \|\nabla \eta_{n+1/2}\|^2. \end{aligned} \quad (6.48)$$

$$\begin{aligned} \Delta t (p_{n+1/2} - q, \nabla \cdot \phi_{n+1/2}^h) &\leq C \Delta t \|p_{n+1/2} - q\| \|\nabla \phi_{n+1/2}^h\| \\ &\leq \frac{\nu \Delta t}{12} \|\nabla \phi_{n+1/2}^h\|^2 + C \Delta t \nu^{-1} \|p_{n+1/2} - \chi^h\|^2. \end{aligned} \quad (6.49)$$

Lemmas 6.1, 6.3 and applying Cauchy-Schwarz and Young give

$$\begin{aligned}
& \Delta t b^*(D_N^h \overline{\eta_{n+1/2}}^h, u_{n+1/2}, \phi_{n+1/2}^h) \\
& \leq C \Delta t \|D_N^h \overline{\eta_{n+1/2}}^h\|^{1/2} \|\nabla D_N^h \overline{\eta_{n+1/2}}^h\|^{1/2} \|\nabla u_{n+1/2}\| \|\nabla \phi_{n+1/2}^h\| \\
& \leq \frac{\nu \Delta t}{12} \|\phi_{n+1/2}^h\|^2 + C \Delta t \nu^{-1} \|\eta_{n+1/2}\| \|\nabla \eta_{n+1/2}\| \|\nabla u_{n+1/2}\|^2. \tag{6.50}
\end{aligned}$$

$$\begin{aligned}
& \Delta t b^*(D_N^h \overline{\phi_{n+1/2}^h}^h, u_{n+1/2}, \phi_{n+1/2}^h) \\
& \leq C \Delta t \|D_N^h \overline{\phi_{n+1/2}^h}^h\|^{1/2} \|\nabla D_N^h \overline{\phi_{n+1/2}^h}^h\|^{1/2} \|\nabla u_{n+1/2}\| \|\nabla \phi_{n+1/2}^h\| \\
& \leq C \Delta t \|\phi_{n+1/2}^h\|^{1/2} \|\nabla \phi_{n+1/2}^h\|^{3/2} \|\nabla u_{n+1/2}\| \\
& \leq \frac{\nu \Delta t}{12} \|\nabla \phi_{n+1/2}^h\|^2 + C \Delta t \nu^{-3} \|\phi_{n+1/2}^h\|^2 \|\nabla u_{n+1/2}\|^4. \tag{6.51}
\end{aligned}$$

$$\begin{aligned}
& \Delta t b^*(D_N^h \overline{w_{n+1/2}^h}^h, \eta_{n+1/2}, \phi_{n+1/2}^h) \\
& \leq C \|D_N^h \overline{w_{n+1/2}^h}^h\|^{1/2} \|\nabla D_N^h \overline{w_{n+1/2}^h}^h\|^{1/2} \|\nabla \eta_{n+1/2}\| \|\nabla \phi_{n+1/2}^h\| \\
& \leq \frac{\nu \Delta t}{12} \|\nabla \phi_{n+1/2}^h\|^2 + C \Delta t \nu^{-1} \|w_{n+1/2}^h\| \|\nabla w_{n+1/2}^h\| \|\nabla \eta_{n+1/2}\|^2. \tag{6.52}
\end{aligned}$$

Combining (6.49), (6.48), (6.50), (6.51), (6.52) and summing from  $n = 0$  to  $M - 1$  (assuming that  $\|\phi_0^h\| = 0$ ) reduces (6.47) to

$$\begin{aligned}
& \|\phi_M^h\|^2 + \nu \Delta t \sum_{n=0}^{M-1} \|\nabla \phi_{n+1/2}^h\|^2 \\
& \leq \Delta t \sum_{n=0}^{M-1} C \nu^{-3} \|\nabla u_{n+1/2}\|^4 \|\phi_{n+1/2}^h\|^2 + \Delta t \sum_{n=0}^{M-1} C \nu \|\nabla \eta_{n+1/2}\|^2 \\
& \quad + \Delta t \sum_{n=0}^{M-1} C \nu^{-1} \|\eta_{n+1/2}\| \|\nabla \eta_{n+1/2}\| \|\nabla u_{n+1/2}\|^2 \\
& \quad + \Delta t \sum_{n=0}^{M-1} C \nu^{-1} \|w_{n+1/2}^h\| \|\nabla w_{n+1/2}^h\| \|\nabla \eta_{n+1/2}\|^2 \\
& \quad + \Delta t \sum_{n=0}^{M-1} C \nu^{-1} \|p_{n+1/2} - q\|^2 + \Delta t \sum_{n=0}^{M-1} C |\text{Intp}(u_n, p_n \phi_{n+1/2}^h)|. \tag{6.53}
\end{aligned}$$

Now, we continue to bound the terms on the RHS of (6.53). We have that

$$\begin{aligned} \Delta t \sum_{n=0}^{M-1} C\nu \|\nabla \eta_{n+1/2}\|^2 &\leq \Delta t C\nu \sum_{n=0}^M \|\nabla \eta_n\|^2 \leq \Delta t C\nu \sum_{n=0}^M h^{2k} |u_n|_{k+1}^2 \\ &\leq C\nu h^{2k} \|u\|_{2,k+1}^2. \end{aligned} \quad (6.54)$$

For the term

$$\begin{aligned} &\Delta t \sum_{n=0}^{M-1} C\nu^{-1} \|\eta_{n+1/2}\| \|\nabla \eta_{n+1/2}\| \|\nabla u_{n+1/2}\|^2 \\ &\leq C\nu^{-1} \Delta t \sum_{n=0}^{M-1} (\|\eta_{n+1}\| \|\nabla \eta_{n+1}\| + \|\eta_n\| \|\nabla \eta_n\| \\ &\quad + \|\eta_n\| \|\nabla \eta_{n+1}\| + \|\eta_{n+1}\| \|\nabla \eta_n\|) \|\nabla u_{n+1/2}\|^2 \\ &\leq C\nu^{-1} h^{2k+1} \left( \Delta t \sum_{n=0}^{M-1} |u_{n+1}|_{k+1}^2 \|\nabla u_{n+1/2}\|^2 + \Delta t \sum_{n=0}^{M-1} |u_{n+1}|_{k+1} |u_n|_{k+1} \|\nabla u_{n+1/2}\|^2 \right. \\ &\quad \left. + \Delta t \sum_{n=0}^{M-1} |u_n|_{k+1}^2 \|\nabla u_{n+1/2}\|^2 \right) \\ &\leq C\nu^{-1} h^{2k+1} \left( \Delta t \sum_{n=0}^M |u_n|_{k+1}^4 + \Delta t \sum_{n=0}^l \|\nabla u_n\|^4 \right) \\ &= C\nu^{-1} h^{2k+1} (\|u\|_{4,k+1}^4 + \|\nabla u\|_{4,0}^4). \end{aligned} \quad (6.55)$$

Using the a priori estimate for  $\|w_n^h\|$ , (6.38),

$$\begin{aligned} &\Delta t \sum_{n=0}^{M-1} C\nu^{-1} (\|w_{n+1/2}^h\| \|\nabla w_{n+1/2}^h\| \|\nabla \eta_{n+1/2}\|^2) \\ &\leq C\nu^{-1} \Delta t \sum_{n=0}^{M-1} \|\nabla w_{n+1/2}^h\| \|\nabla \eta_{n+1/2}\|^2 \\ &\leq C\nu^{-1} \Delta t \sum_{n=0}^{M-1} (\|\nabla \eta_{n+1}\|^2 + \|\nabla \eta_n\|^2) \|\nabla w_{n+1/2}^h\| \\ &\leq C\nu^{-1} h^{2k} \Delta t \sum_{n=0}^{M-1} (|u_{n+1}|_{k+1}^2 + |u_n|_{k+1}^2) \|\nabla w_{n+1/2}^h\| \\ &\leq C\nu^{-1} h^{2k} \left( \Delta t \sum_{n=0}^M |u^n|_{k+1}^4 + \Delta t \sum_{n=0}^M \|\nabla u_{n+1/2}^h\|^2 \right) \\ &\leq C\nu^{-1} h^{2k} (\|u\|_{4,k+1}^4 + \nu^{-1} (\|w_0^h\|^2 + \nu^{-1} \|f\|_{2,*}^2)). \end{aligned} \quad (6.56)$$

Using the triangle inequality and Taylor expansion,

$$\begin{aligned}
& \Delta t \sum_{n=0}^{M-1} C\nu^{-1} \|p_{n+1/2} - q\|^2 \leq C\nu^{-1} \Delta t \sum_{n=0}^{M-1} \|p(t_{n+1/2}) - q\|^2 + \|p_{n+1/2} - p(t_{n+1/2})\|^2 \\
& \leq C\nu^{-1} \left( h^{2s+2} \Delta t \sum_{n=0}^{M-1} \|p(t_{n+1/2})\|_{s+1}^2 + \Delta t \sum_{n=0}^{M-1} \frac{1}{48} (\Delta t)^3 \int_{t_n}^{t_{n+1}} \|p_{tt}\|^2 dt \right) \\
& \leq C\nu^{-1} (h^{2s+2} \|p_{1/2}\|_{2,s+1}^2 + (\Delta t)^4 \|p_{tt}\|_{2,0}^2)
\end{aligned} \tag{6.57}$$

We now bound the terms in  $\text{Intp}(u_n, p_n; \phi_{n+1/2}^h)$ . Using Taylor series expansion and Lemma 6.4,

$$\begin{aligned}
& \left( \frac{u^{n+1} - u_n}{\Delta t} - u_t(t_{n+1/2}), \phi_{n+1/2}^h \right) \\
& \leq \frac{1}{2} \|\phi_{n+1/2}^h\|^2 + \frac{1}{2} \left\| \frac{u^{n+1} - u_n}{\Delta t} - u_t(t_{n+1/2}) \right\|^2 \\
& \leq \frac{1}{2} \|\phi_{n+1}^h\|^2 + \frac{1}{2} \|\phi_n^h\|^2 + \frac{1}{2} \frac{(\Delta t)^3}{1280} \int_{t_n}^{t_{n+1}} \|u_{ttt}\|^2 dt,
\end{aligned} \tag{6.58}$$

$$\begin{aligned}
& (p_{n+1/2} - p(t_{n+1/2}), \nabla \cdot \phi_{n+1/2}^h) \\
& \leq \epsilon_1 \nu \|\nabla \phi_{n+1/2}^h\|^2 + C\nu^{-1} \|p_{n+1/2} - p(t_{n+1/2})\|^2 \\
& \leq \epsilon_1 \nu \|\nabla \phi_{n+1/2}^h\|^2 + C\nu^{-1} \frac{(\Delta t)^3}{48} \int_{t_n}^{t_{n+1}} \|p_{tt}\|^2 dt,
\end{aligned} \tag{6.59}$$

$$\begin{aligned}
& (f(t_{n+1/2}) - f_{n+1/2}, \phi_{n+1/2}^h) \\
& \leq \frac{1}{2} \|\phi_{n+1/2}^h\|^2 + \frac{1}{2} \|f(t_{n+1/2}) - f_{n+1/2}\|^2 \\
& \leq \frac{1}{2} \|\phi_{n+1}^h\|^2 + \frac{1}{2} \|\phi_n^h\|^2 + \frac{(\Delta t)^3}{48} \int_{t_n}^{t_{n+1}} \|f_{tt}\|^2 dt,
\end{aligned} \tag{6.60}$$

$$\begin{aligned}
& (\nabla u_{n+1/2} - \nabla u(t_{n+1/2}), \nabla \phi_{n+1/2}^h) \\
& \leq \epsilon_2 \nu \|\nabla \phi_{n+1/2}^h\|^2 + C\nu \|\nabla u_{n+1/2} - \nabla u(t_{n+1/2})\|^2 \\
& \leq \epsilon_2 \nu \|\nabla \phi_{n+1/2}^h\|^2 + C\nu \frac{(\Delta t)^3}{48} \int_{t_n}^{t_{n+1/2}} \|\nabla u_{tt}\|^2 dt,
\end{aligned} \tag{6.61}$$

$$\begin{aligned}
& b^*(u_{n+1/2}, u_{n+1/2}, \phi_{n+1/2}^h) - b^*(u(t_{n+1/2}), u(t_{n+1/2}), \phi_{n+1/2}^h) \\
= & b^*(u_{n+1/2} - u(t_{n+1/2}), u_{n+1/2}, \phi_{n+1/2}^h) - b^*(u(t_{n+1/2}), u_{n+1/2} - u(t_{n+1/2}), \phi_{n+1/2}^h) \\
\leq & C \|\nabla(u_{n+1/2} - u(t_{n+1/2}))\| \|\nabla\phi_{n+1/2}^h\| (\|\nabla u_{n+1/2}\| + \|\nabla u(t_{n+1/2})\|) \\
\leq & C\nu^{-1} (\|\nabla u_{n+1/2}\|^2 + \|\nabla u(t_{n+1/2})\|^2) \frac{(\Delta t)^3}{48} \int_{t_n}^{t_{n+1}} \|\nabla u_{tt}\|^2 dt + \epsilon_3\nu \|\nabla\phi_{n+1/2}^h\|^2 \\
\leq & C\nu^{-1} \frac{(\Delta t)^3}{48} \left( \int_{t_n}^{t_{n+1}} 2(\|\nabla u_{n+1/2}\|^4 + \|\nabla u(t_{n+1/2})\|^4) dt \right. \\
& \left. + \int_{t_n}^{t_{n+1}} \|\nabla u_{tt}\|^4 dt \right) + \epsilon_3\nu \|\nabla\phi_{n+1/2}^h\|^2 \\
\leq & C\nu^{-1} (\Delta t)^4 (\|\nabla u_{n+1/2}\|^4 + \|\nabla u(t_{n+1/2})\|^4) \\
& + C\nu^{-1} (\Delta t)^3 \int_{t_n}^{t_{n+1}} \|\nabla u_{tt}\|^4 dt + \epsilon_3\nu \|\nabla\phi_{n+1/2}^h\|^2. \tag{6.62}
\end{aligned}$$

$$\begin{aligned}
& b^*(u_{n+1/2} - D_N^h \overline{u_{n+1/2}}^h, u_{n+1/2}, \phi_{n+1/2}^h) \\
\leq & \frac{1}{2} (\|u_{n+1/2} - D_N^h \overline{u_{n+1/2}}^h\| \|\nabla u_{n+1/2}\|_\infty \|\phi_{n+1/2}^h\| \\
& + \|u_{n+1/2} - D_N^h \overline{u_{n+1/2}}^h\| \|u_{n+1/2}\|_\infty \|\nabla\phi_{n+1/2}^h\|) \\
\leq & C \|u_{n+1/2} - D_N^h \overline{u_{n+1/2}}^h\| \|\nabla\phi_{n+1/2}^h\| \\
\leq & \epsilon_4\nu \|\nabla\phi_{n+1/2}^h\| + C\nu^{-1} \|u_{n+1/2} - D_N^h \overline{u_{n+1/2}}^h\|^2 \\
\leq & \epsilon_4\nu \|\nabla\phi_{n+1/2}^h\| + C\nu^{-1} \delta^{4N+4} \|\bar{u}\|_{H^{2N+2}}^2 \\
& + C\nu^{-1} (\delta^2 h^{2k} + h^{2k+2}) \left( \sum_{n=1}^N \|(A^{-1})^N u\|_{k+1}^2 \right). \tag{6.63}
\end{aligned}$$

Combine (6.58)-(6.63) to obtain

$$\begin{aligned}
\Delta t \sum_{n=0}^{M-1} |Intp(u^n, p^n; \phi_{n+1/2}^h)| \leq & \Delta t C \|\phi_{n+1}^h\|^2 + (\epsilon_1 + \epsilon_2 + \epsilon_3 + \epsilon_4) \Delta t \nu \|\nabla\phi_{n+1/2}^h\|^2 \\
& + C\nu^{-1} \delta^{4N+4} \|\bar{u}\|_{2,2N+2}^2 \\
& + C\nu^{-1} (\delta^2 h^{2k} + h^{2k+2}) \left( \sum_{n=1}^N \|(A^{-1})^N u\|_{2,k+1}^2 \right) \\
& + C(\Delta t)^4 (\|u_{ttt}\|_{2,0}^2 + \nu^{-1} \|p_{tt}\|_{2,0}^2 + \|f_{tt}\|_{2,0}^2 \\
& + \nu \|\nabla u_{tt}\|_{2,0}^2 + \nu^{-1} \|\nabla u_{tt}\|_{4,0}^4 \\
& + \nu^{-1} \|\nabla u\|_{4,0}^4 + \nu^{-1} \|\nabla u_{1/2}\|_{4,0}^4). \tag{6.64}
\end{aligned}$$

Let  $\epsilon_1 = \epsilon_2 = \epsilon_3 = \epsilon_4 = 1/12$  and with (6.54)-(6.57), (6.64), from (6.53) we obtain

$$\begin{aligned}
& \|\phi_M^h\|^2 + \nu \Delta t \sum_{n=0}^{M-1} \|\nabla \phi_{n+1/2}^h\|^2 \\
\leq & \Delta t \sum_{n=0}^{M-1} C(\nu^{-3} \|\nabla u_{n+1/2}\|^4 + 1) \|\phi_{n+1/2}^h\|^2 + C\nu h^{2k} \|u\|_{2,k+1}^2 \\
& + C\nu^{-1} h^{2k+1} (\|u\|_{4,k+1}^4 + \|\nabla u\|_{4,0}^4) \\
& + C\nu^{-1} h^{2k} (\|u\|_{4,k+1}^4 + \nu^{-1} (\|w_0^h\|^2 + \nu^{-1} \|f\|_{2,*}^2)) + C\nu^{-1} h^{2s+2} \|p_{1/2}\|_{2,s+1}^2 \\
& + C\nu^{-1} \delta^{4N+4} \|\bar{u}\|_{2,2N+2}^2 + C\nu^{-1} (\delta^2 h^{2k} + h^{2k+2}) \left( \sum_{n=1}^N \|(A^{-1})^N u\|_{2,k+1}^2 \right) \\
& + C(\Delta t)^4 (\|u_{ttt}\|_{2,0}^2 + \nu^{-1} \|p_{tt}\|_{2,0}^2 + \|f_{tt}\|_{2,0}^2 \\
& \quad + \nu \|\nabla u_{tt}\|_{2,0}^2 + \nu^{-1} \|\nabla u_{tt}\|_{4,0}^4 \\
& \quad + \nu^{-1} \|\nabla u\|_{4,0}^4 + \nu^{-1} \|\nabla u_{1/2}\|_{4,0}^4) .
\end{aligned} \tag{6.65}$$

Hence, with  $\Delta t$  sufficiently small, i.e.  $\Delta t < C(\nu^{-3} \|\nabla u\|_{\infty,0}^4 + 1)^{-1}$ , from Gronwall's Lemma (see (5.3), we have

$$\begin{aligned}
& \|\phi_M^h\|^2 + \nu \Delta t \sum_{n=0}^{M-1} \|\nabla \phi_{n+1/2}^h\|^2 \\
\leq & C\nu^{-1} h^{2k+1} (\|u\|_{4,k+1}^4 + \|\nabla u\|_{4,0}^4) + C\nu h^{2k} \|u\|_{2,k+1}^2 \\
& + C\nu^{-1} h^{2k} (\|u\|_{4,k+1}^4 + \nu^{-1} (\|w_0^h\|^2 + \nu^{-1} \|f\|_{2,*}^2)) + C\nu^{-1} h^{2s+2} \|p_{1/2}\|_{2,s+1}^2 \\
& + C\nu^{-1} \delta^{4N+4} \|\bar{u}\|_{2,2N+2}^2 + C\nu^{-1} (\delta^2 h^{2k} + h^{2k+2}) \left( \sum_{n=1}^N \|(A^{-1})^N u\|_{2,k+1}^2 \right) \\
& + C(\Delta t)^4 (\|u_{ttt}\|_{2,0}^2 + \nu^{-1} \|p_{tt}\|_{2,0}^2 + \|f_{tt}\|_{2,0}^2 \\
& \quad + \nu \|\nabla u_{tt}\|_{2,0}^2 + \nu^{-1} \|\nabla u_{tt}\|_{4,0}^4 \\
& \quad + \nu^{-1} \|\nabla u\|_{4,0}^4 + \nu^{-1} \|\nabla u_{1/2}\|_{4,0}^4) .
\end{aligned} \tag{6.66}$$

Estimate (6.39) then follows from the triangle inequality and (6.66).

To obtain (6.40), we use (6.66) and

$$\begin{aligned}
& \|\nabla (u(t_{n+1/2}) - (w_{n+1}^h + w_n^h)/2)\|^2 \\
\leq & \|\nabla(u(t_{n+1/2}) - u_{n+1/2})\|^2 + \|\nabla\eta_{n+1/2}\|^2 + \|\nabla\phi_{n+1/2}^h\|^2 \\
\leq & \frac{(\Delta t)^3}{48} \int_{t_n}^{t_{n+1}} \|\nabla u_{tt}\|^2 dt + Ch^{2k}|u_{n+1}|_{k+1}^2 + Ch^{2k}|u_n|_{k+1}^2 + \|\nabla\phi_{n+1/2}^h\|^2.
\end{aligned}$$

□

## 6.4 NUMERICAL EXPERIMENTS

We now present numerical results for the linear extrapolated Algorithm 6.1, i.e., instead of  $b^*(D_N^h \overline{w_{n+1/2}^h}, w_{n+1/2}^h, v^h)$  we implement  $b^*(D_N^h \overline{\frac{3}{2}w_n^h - \frac{1}{2}w_{n-1}^h}, w_{n+1/2}^h, v^h)$ . The linear extrapolation algorithm for Navier-Stokes equations is investigated in [7] by Baker. It is still second order in time and requires only one solution of a linear system per time, therefore it is useful to connect it with Crank-Nicholson scheme. The code was written in MATLAB and run on desktop machines. The first computations used Taylor-Hood elements on the periodic box  $\Omega = (0, 1)^3$ . The averaging radius  $\delta = O(h)$  in all performed computations. Because of memory limitation, the 3d computations used meshes only as fine as  $h = 1/32$ , i.e. 112,724 degrees of freedom. While this is not sufficient for many applications, it is adequate for verifying convergence rates and comparing errors between models. The 3d code utilized MATLAB's conjugate gradient squared method (CGS) to solve the resulting linear systems from both the filtering and the schemes themselves.

### 6.4.1 3d Convergence Rate Verification

Our first experiment verifies the predicted error rates proven in Section 3 at  $Re = 1$  for the extrapolated trapezoidal Leray-deconvolution schemes  $N = 0, 1, 2, 3$ . For  $(P_2, P_1)$  elements, all four schemes are second order accurate in the  $H^1$  norm. The  $N = 0$  scheme is only second order accurate in the  $L^2$  norm, and the other three higher order (in N) schemes are third

order accurate in the  $L^2$  norm. Thus one conclusion is that higher order ( $N \geq 1$ ) Leray-deconvolution models provide better practical accuracy, even after discretization, than the  $N = 0$  case of the Leray-alpha model.

Table 1 contains errors and convergence rates for the schemes' approximations to the true solution

$$u = \begin{pmatrix} \cos(2\pi(z+t)) \\ \sin(2\pi(z+t)) \\ \sin(2\pi(x+t)) \end{pmatrix}, \quad p = \sin(2\pi(x+t)). \quad (6.67)$$

This particular solution was chosen because it is a simple periodic function with at least a somewhat complex structure: A quick calculation by hand shows that the helicity  $H = -2\pi$  for any  $t$ , and hence we know there is at least some tangledness and knottedness of vortex lines. For these calculations, we set  $\delta = h$  and  $\Delta t < h^{3/2}$  (approximately  $h^{3/2}$ , but a multiple of .005 so that all times coincide). Results are given at  $t = 0.5$ .

Table 1:  $L^2$  and  $H^1$  errors and rates at  $Re = 1$  and  $t=0.5$

h	$\ u - u_{LD0}^h\ _{L^2}$	cvg	$\ u - u_{LD1}^h\ _{L^2}$	cvg	$\ u - u_{LD2}^h\ _{L^2}$	cvg	$\ u - u_{LD3}^h\ _{L^2}$	cvg
1/8	0.0280	-	0.0245	-	0.0240	-	0.239	-
1/16	0.0061	2.19	0.0032	2.91	0.0032	2.91	0.0032	2.91
1/32	0.0015	2.01	0.0004	2.94	0.0004	2.91	0.0004	2.91
h	$\ u - u_{LD0}^h\ _{H^1}$	ratio	$\ u - u_{LD1}^h\ _{H^1}$	ratio	$\ u - u_{LD2}^h\ _{H^1}$	ratio	$\ u - u_{LD3}^h\ _{H^1}$	ratio
1/8	0.6904	-	0.6789	-	0.6772	-	0.6769	-
1/16	0.1809	1.93	0.1750	1.96	0.1749	1.95	0.1748	1.95
1/32	0.0459	1.98	0.0441	1.99	0.0441	1.99	0.0441	1.99

#### 6.4.2 3d Error Comparisons at Re=5000

The goal of the second experiment is to test if the regularizing effect of the Leray-deconvolution model is really advantageous in practical computing. Thus we consider Baker's extrapolated Crank-Nicolson method (called CNLE) for the NSE and the Leray-deconvolution regularization of the NSE.

Figure 11 and 12 presents graphs of the  $L^2$  and  $H^1$  errors for the methods vs. time for  $Re = 5000$  on our finest mesh  $h = 1/32$  and timestep  $\Delta t = 0.005$ . From these graphs it is clear that the extrapolated trapezoidal Leray-deconvolution schemes with  $N = 1, 2, 3$  are all much more accurate than both CNLE and the discrete Leray-alpha model ( $N = 0$  case) in the  $L^2$  and  $H^1$  norms. Furthermore, the graphs indicate that over longer time intervals, the higher order Leray-deconvolution schemes can remain more accurate than CNLE and the Leray-alpha model (LerayDC0).

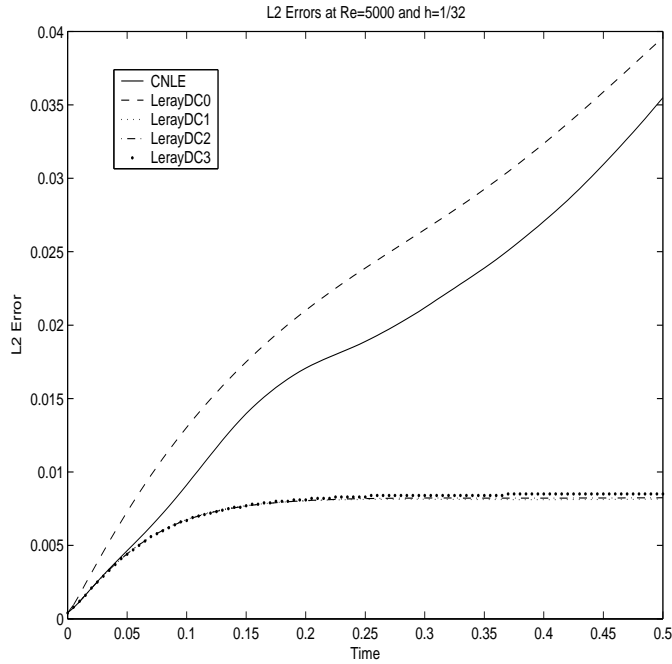


Figure 11:  $L^2$  Error vs. Time for CNLE and LDLE with  $N=0,1,2,3$

### 6.4.3 Underresolved flows in $2d$

Regularization and stabilization can often affect transitional flows negatively. The simplest test of this is to see if the stabilization in the Algorithm 6.1 retards separation of vortices behind a blunt body near the critical Reynolds number. To do so, we study underresolved flow with recirculation, i.e., the flow across a step. The most distinctive feature of this flow is a recirculating vortex behind the step, see Figure 13 for illustration.

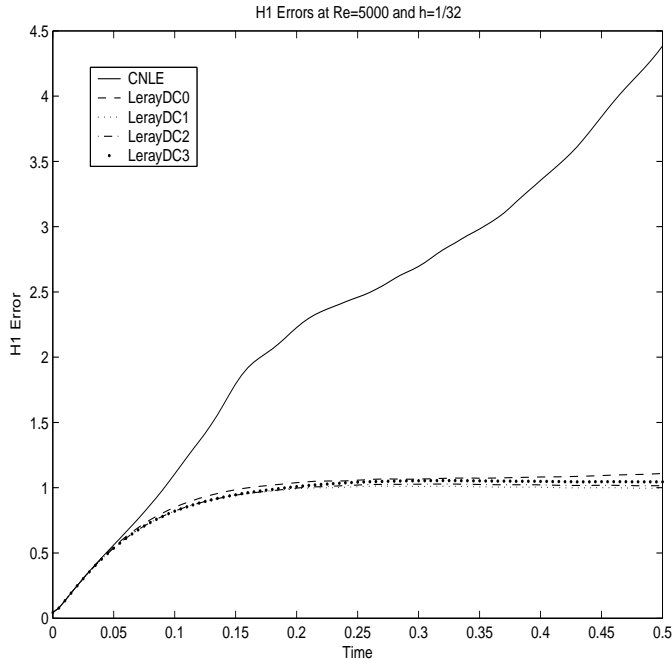


Figure 12:  $H^1$  Error vs. Time for CNLE and LDLE with  $N=0,1,2,3$

We investigate this flow at  $\nu = 1/600$  since about this value of  $\nu$  the flow is in the transition from equilibrium to time dependent, via shedding of eddies behind the step. In our simulations we used Leray Deconvolution Models, i.e. (6.1) with  $N = 0$  (LerayDC0),  $N = 1$  (LerayDC1) and  $N = 2$  (LerayDC2). We will compare these models with often used for underresolved flow simulation - the Smagorinsky model. The only difference between the Navier-Stokes equations (NSE) and the Smagorinsky model (SMA) is in the viscous term, which has the following form:

$$\nabla \cdot ((2\nu + c_s \delta^2 \|\mathbb{D}(u)\|_F) \mathbb{D}(u)).$$

Here,  $c_s$  is a positive constant ( $c_s \sim 0.01$ , see [53]),  $\mathbb{D}(u)$  is the deformation tensor and  $\|\cdot\|_F$  denotes the Frobenius norm. Although the Smagorinsky model is widely used, it has some drawbacks. These are well documented in the literature, e.g. see [57]. For instance, the Smagorinsky model constant  $c_s$  is an á priori input and this single constant is not capable

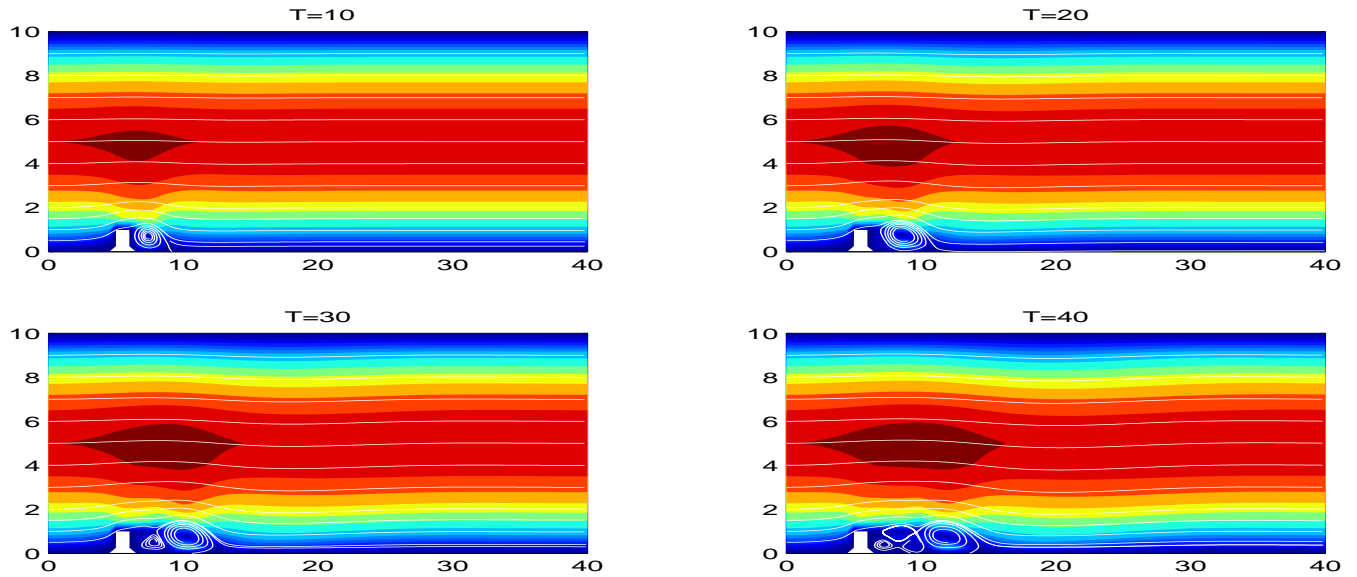


Figure 13: NSE at  $\nu = 1/600$ , 41,538 d.o.f. grid

of representing correctly various turbulent flows. Another drawback of this model is that it introduces too much diffusion into the flow, e.g., see Figure 14.

The domain of the two-dimensional flow across a step is presented in Figure 15. We present results for a parabolic inflow profile, which is given by  $u = (u_1, u_2)^T$ , with  $u_1 = y(10 - y)/25$ ,  $u_2 = 0$ . No-slip boundary condition is prescribed on the top and bottom boundary as well as on the step. At the outflow we also imposed the "do nothing" boundary condition: this is a relatively new outflow boundary condition in CFD that is equivalent to a zero traction (no normal stress) boundary condition except that the Laplacian form of the viscous term is used instead of the stress tensor form.

The computations were performed on various grids. For instance, for the fully resolved NSE simulation, which is our "truth" solution, we used a fine grid (41,538 degrees of freedom) whereas much coarser grids (5,845 d.o.f., and 1,537 d.o.f.) has been used for LerayDC0, LerayDC1, LerayDC2 and SMA. The point is to compare the performance of the various models in underresolved simulations by comparison against a "truth"/fully-resolved solution, Figure 13.

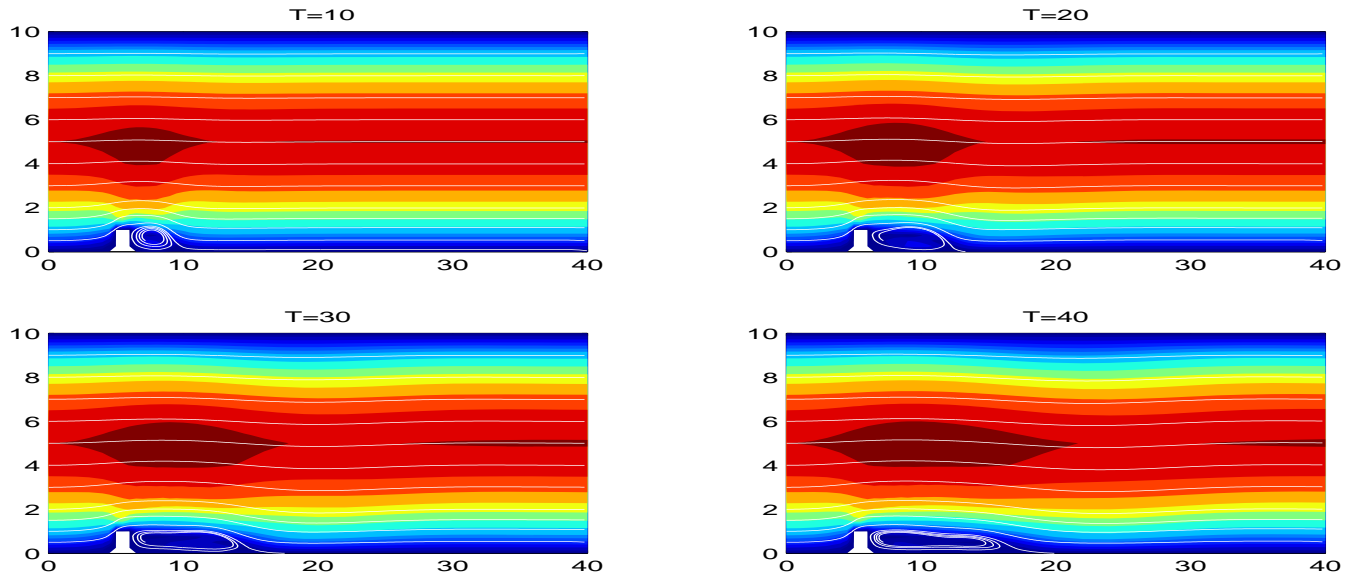


Figure 14: SMA at  $\nu = 1/600$ ,  $\delta = 1.5$  and 5,845 d.o.f. grid

The 2d computations were performed with the software FreeFem++, [27]. The 2d models were discretized using the nonlinear Algorithm 6.1 (i.e. without linear extrapolation) with Taylor Hood finite elements. Computations for this experiment using linear extrapolation failed: eddies would not shed behind the step.

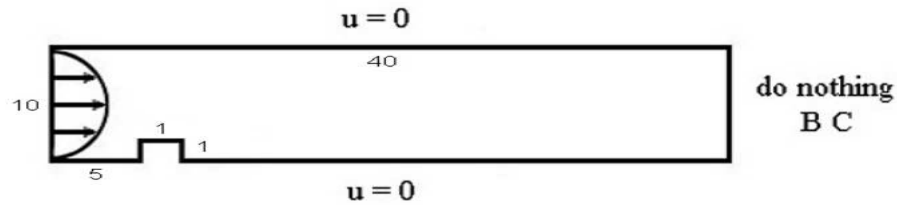


Figure 15: Boundary conditions

Comparing the Figures 14, 17, 18, 19 on the 5845 d.o.f. mesh with 13 we conclude that the LerayDC0, LerayDC1 and LerayDC2 tests replicate the shedding of eddies and the Smagorinsky eddy remains attached. Clearly, the Smagorinsky model is too stabilizing: eddies which should separate and evolve remain attached and attain steady state. On the coarsest mesh, Figure 20 shows none of the models exhibits a shedding behavior.

However, regarding the main point of study, Leray Deconvolution Models improved the simulation results for this transition problem. On the coarsest grid (1,537 d.o.f.), LerayDC0 failed to shed eddies behind the step but LerayDC1 and LerayDC2 (see Figure 20) still give a successful shedding.

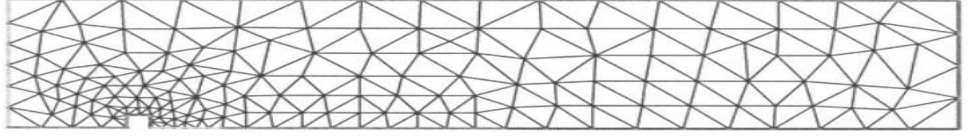


Figure 16: Grid with 1,537 d.o.f.

## 6.5 CONCLUSIONS

The van Cittert deconvolution algorithm requires only a few Poisson solves. The condition number of the linear system associated with each solve of  $(-\delta^2\Delta + 1)$  is  $O(\delta^2/h^2 + 1)$ , i.e.  $O(1)$  if  $\delta = O(h)$ . Thus, the extra complexity of differential filtering and deconvolution is negligible over solving the NSE.

On the other hand, the regularization the higher order Leray-deconvolution models give has remarkable and positive effects on the results of the computations. Errors are observed to be much better over much larger time intervals and the transition from one type of flow to another is not retarded in our experiments as well.

The higher order Leray-deconvolution models had greater accuracy and physical fidelity than the  $N = 0$  case (Leray-alpha model).

The experiments we have given were limited by time and resources but their results have consistently showed that: *higher order is to be strongly preferred to lower order*, i.e. LerayDC

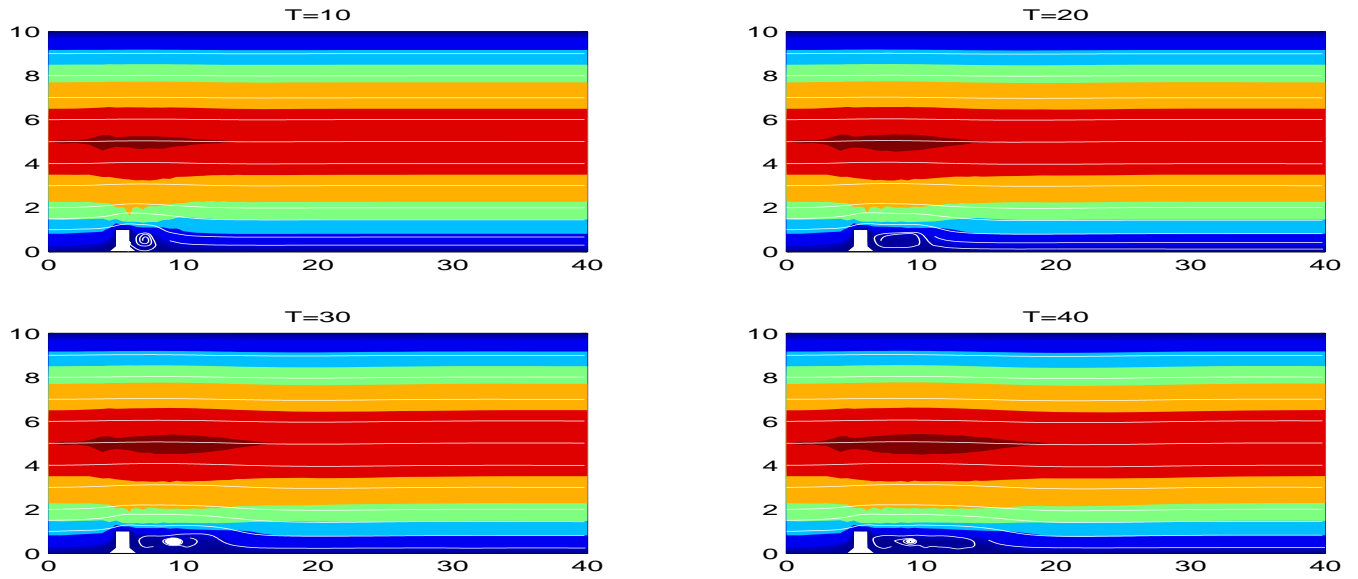


Figure 17: LerayDC0 at  $\nu = 1/600$ ,  $\delta = 1.5$  and 5,845 d.o.f. grid

for higher  $N$  to Leray-alpha (the  $N=0$  case).

The form of the Leray-deconvolution model allows an efficient and unconditionally stable timestepping scheme to be used. We have given a convergence analysis which was also verified in  $3d$  calculations. Naturally, we believe that further explorations would reveal that higher order extrapolation (e.g. quadratic) would perform even better than the linear extrapolation tested herein.

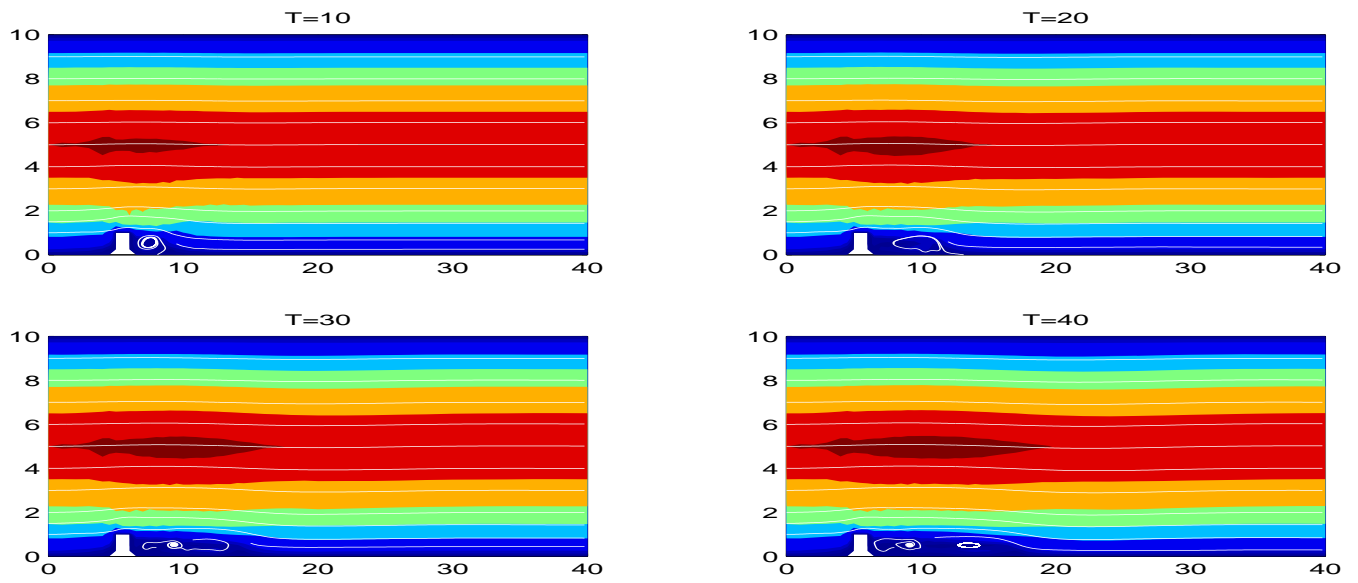


Figure 18: LerayDC1 at  $\nu = 1/600$ ,  $\delta = 1.5$  and 5,845 d.o.f. grid

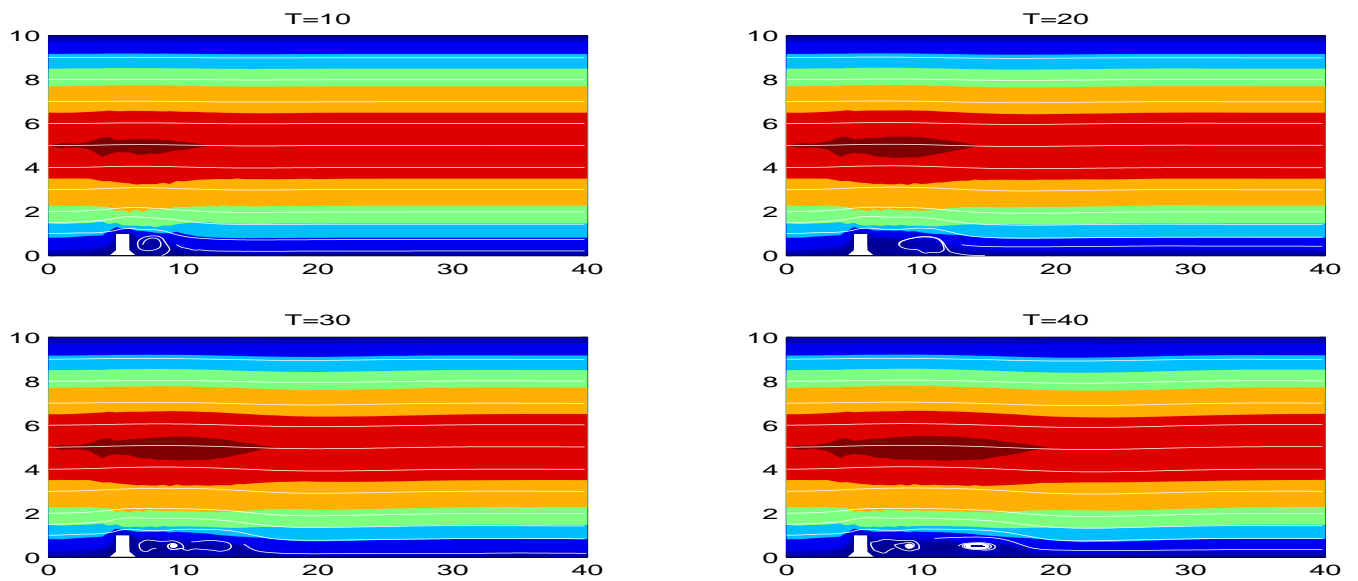


Figure 19: LerayDC2 at  $\nu = 1/600$ ,  $\delta = 1.5$  and 5,845 d.o.f. grid

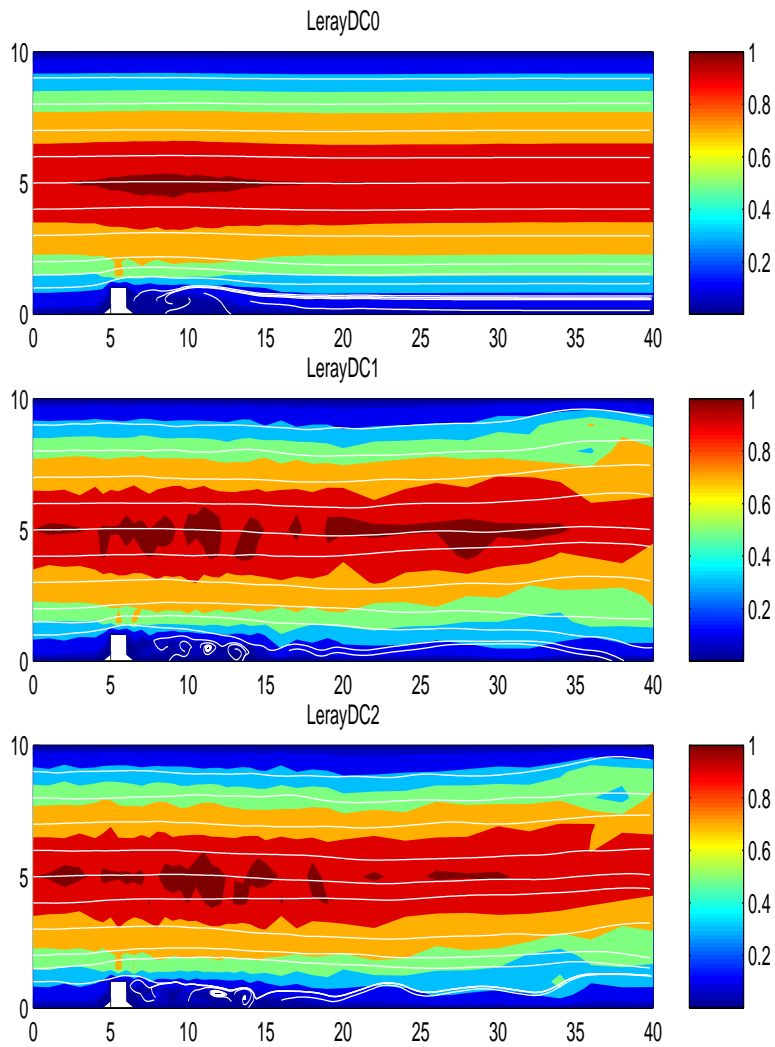


Figure 20: LerayDC0, LerayDC1, LerayDC2, respectively at  $T = 40$ ,  $\nu = 1/600$ ,  $\delta = 3.0$  and 1,537 d.o.f. grid

## 7.0 CONCLUSIONS AND FUTURE WORK

### 7.1 CONCLUSIONS

There are three main conclusions to this thesis: The ADM is a turbulence model with excellent physical fidelity in terms of its helicity treatment, the Leray-deconvolution turbulence model is a higher order and more accurate generalization of the Leray model, and the energy and helicity conserving (trapezoidal Galerkin) scheme for the NSE presented in Chapter 5 more accurately accounts for helicity than the usual trapezoidal Galerkin scheme.

We found in Chapter 2 that the ADM conserves a model helicity, whereas the Leray, Leray-deconvolution and Bardina models do not. Moreover, in Chapter 3, we showed that this ADM-helicity is cascaded through wave space at the same rate as helicity in true fluid flow, up to a length scale dependent on the filtering radius and choice of filter (the ADM truncates scales). Thus not only is the ADM one of just a few models that conserve helicity for inviscid flow (i.e. the *model* itself does not add or dissipate helicity), the ADM is the first turbulence model known to accurately cascade a quantity other than energy (which the ADM also accurately cascades). We believe this sets the ADM apart from other models in terms of the physical fidelity of its solutions.

Discretizations of the NSE and of turbulence models typically do not account for helicity. In Chapter 5, we presented an energy and helicity conserving finite element scheme for the Navier-Stokes equations in an effort to have more physically relevant solutions in simulations. If a scheme for the NSE conserves helicity for inviscid flow, then the nonlinearity in the scheme does not add or dissipate helicity. The presented scheme is a trapezoidal Galerkin scheme that uses a combination of the convective and rotational forms of the nonlinearity, along with a projected vorticity. It is the second energy and helicity conserving approxima-

tion scheme developed; the first scheme was for axisymmetric flow, whereas this scheme is for general flows. We prove stability, conservation, and convergence of the scheme, as well as present numerical experiments that show the schemes's treatment of helicity is better than that of the usual trapezoidal Galerkin method. More efficient implementation of the scheme remains an open problem.

The last conclusion of this thesis is that the higher order Leray-deconvolution model is a more accurate extension of the classical Leray model (which is the  $0^{th}$  order Leray-deconvolution model). We have analyzed a numerical scheme for the Leray-deconvolution model, showing stability and convergence. We also presented numerical experiments which verified convergence rates and showed *higher order is better* for eddy shedding on the step problem using underresolved meshes.

## 7.2 FUTURE WORK

There are several natural extensions of this thesis. I intend to study the following in the near future:

- More efficient solver for Energy and Helicity conserving scheme: Although the scheme presented in Chapter 5 has shown promising results, the linear systems that need to be solved in it are twice the size of the linear systems for usual schemes. The possibility of decoupling the equations and finding a reliable iteration to solve the equations should be investigated.
- Helicity dissipation rates in the NS- $\alpha$  turbulence model: Recent work of Prof. Layton has shown helicity dissipation rates in the ADM are analogous to those predicted by dimensional analysis for homogeneous, isotropic turbulence. At first glance it seems that helicity conservation is the essential ingredient for such a proof. Hence, we can investigate the helicity dissipation rate in the NS- $\alpha$  model, another helicity conserving turbulence model.
- Development of an energy and helicity conserving scheme for the ADM and NS- $\alpha$ : For a scheme such as the one in Chapter 5 to conserve both energy and helicity, the continuous

version of the model must also conserve energy and helicity. Both the ADM and NS- $\alpha$  models conserve model energies and helicities, so an extension of the work in Chapter 5 to these two models may be possible. Also, a study of the joint energy/helicity cascade in the NS-alpha model should be done.

- Development and investigation of the NS- $\alpha$ -deconvolution model.
- Stabilized Linear Extrapolated Trapezoidal Galerkin Scheme for the NSE: Work currently underway with W. Layton, A. Labovsky, C. Manica, M. Neda to study this NSE discretization.

## BIBLIOGRAPHY

- [1] N. Adams and S. Stolz. A subgrid-scale deconvolution approach for shock capturing. *Journal of Computational Physics*, 178, 2002.
- [2] N. A. Adams and S. Stolz. On the Approximate Deconvolution procedure for LES. *Phys. Fluids*, 2:1699–1701, 1999.
- [3] N. A. Adams and S. Stolz. Deconvolution methods for subgrid-scale approximation in large eddy simulation. *Modern Simulation Strategies for Turbulent Flow*, 2001.
- [4] S. Stolz N. Adams and L. Kleiser. The approximate deconvolution model for large-eddy simulations of compressible flows and its application to shock-turbulent-boundary-layer interaction. *Physics of Fluids*, 13, 2001.
- [5] J. C. André and M. Lesieur. Influence of helicity on high Reynolds number isotropic turbulence. *Journal of Fluid Mechanics*, 81:187–207, 1977.
- [6] A. Arakawa. Computational design for long-term numerical integration of the equations of fluid motion: two dimensional incompressible flow, Part I. *J. Comput. Phys.*, 1:119–143, 1966.
- [7] G. Baker. Galerkin approximations for the Navier-Stokes equations. Harvard University, August 1976.
- [8] J.J. Bardina, H. Ferziger, and W.C. Reynolds. Improved subgrid scale models for large eddy simulation. *AIAA Pap.*, 1983.
- [9] M. Benzi and J. Liu. An efficient solver for the Navier-Stokes equations in rotational form. Technical report, Department of Mathematics and Computer Science, Emory University, 2006.
- [10] L.C. Berselli, T. Iliescu, and W. J. Layton. *Mathematics of Large Eddy Simulation of Turbulent Flows*. Scientific Computation. Springer, 2006.
- [11] M. Bertero and B. Boccacci. *Introduction to Inverse Problems in Imaging*. IOP Publishing Ltd., 1998.

- [12] J. Bourne and S. Orszag. Spectra in helical three-dimensional homogeneous isotropic turbulence. *Physics Review Letters E*, 55:7005–7009, 1997.
- [13] S. Brenner and L.R. Scott. *The Mathematical Theory of Finite Element Methods*. Springer-Verlag, 1994.
- [14] A. Brissaud, U. Frisch, J. Leorat, and A. Mazure M. Lesieur. Helicity cascades in fully developed isotropic turbulence. *Physics of Fluids*, 16(8), 1973.
- [15] Q. Chen, S. Chen, and G. Eyink. The joint cascade of energy and helicity in three dimensional turbulence. *Physics of Fluids*, 15(2):361–374, 2003.
- [16] Q. Chen, S. Chen, G. Eyink, and D. Holm. Intermittency in the joint cascade of energy and helicity. *Physical Review Letters*, 90: 214503, 2003.
- [17] A. Cheskidov, D. Holm, E. Olson, and E. Titi. On a Leray-alpha model of turbulence. *Royal Society London, Proceedings, Series A, Mathematical, Physical and Engineering Sciences*, pages 629–649, 2005.
- [18] P. Ditlevsen and P. Giuliani. Dissipation in helical turbulence. *Physics of Fluids*, 13, 2001.
- [19] P. Ditlevson and P. Guiliani. Cascades in helical turbulence. *Physical Review E*, 63, 2001.
- [20] A. Dunca and Y. Epshteyn. On the Stolz-Adams deconvolution model for the large-eddy simulation of turbulent flows. *SIAM J. Math. Anal.*, 37(6):1890–1902, 2005-2006.
- [21] C. Foias, D. Holm, and E. Titi. The Navier-Stokes-alpha model of fluid turbulence. *Physica D*, pages 505–519, May 2001.
- [22] U. Frisch. *Turbulence*. Cambridge University Press, 1995.
- [23] M. Germano. Differential filters for the large eddy numerical simulation of turbulent flows. *Physics of Fluids*, 29:1755–1757, 1986.
- [24] V. Girault and P.-A. Raviart. *Finite element methods for Navier-Stokes equations : theory and algorithms*. Springer-Verlag, 1986.
- [25] P. Gresho and R. Sani. *Incompressible Flow and the Finite Element Method*, volume 2. Wiley, 1998.
- [26] J. Guermond. Finite-element-based faedo-galerkin weak solutions to the Navier-Stokes equations in the three-dimensional torus are suitable. *Journal de Mathematiques Pures et Appliquees*, 2006.
- [27] F. Hecht and O. Pironneau. Freefem++. webpage: <http://www.freefem.org>.

- [28] J. Heywood and R. Rannacher. Finite element approximation of the nonstationary Navier-Stokes problem. Part IV: Error analysis for the second order time discretization. *SIAM J. Numer. Anal.*, 2:353–384, 1990.
- [29] D. Holm and B. Guerts. Leray and LANS- $\alpha$  modeling of turbulent mixing. *J. of Turbulence*, 7(10), 2006.
- [30] S. Kaya and B. Riviere. A discontinuous subgrid eddy viscosity method for the time-dependent Navier-Stokes equations. *SIAM Journal on Numerical Analysis*, 43(4):1572–1595, 2005.
- [31] A. V. Kolmogorov. The local structure of turbulence in incompressible viscous fluids for very large Reynolds number. *Dokl. Akad. Nauk. SSR*, 30:9–13, 1941.
- [32] R. Kraichnan. Inertial-range transfer in two- and three-dimensional turbulence. *Journal of Fluid Mechanics*, 47, 1971.
- [33] W. Layton. Numerical analysis of finite element computational fluid dynamics. Lecture Notes, 2002.
- [34] W. Layton and R. Lewandowski. A high accuracy Leray-deconvolution model of turbulence and its limiting behavior. Technical report, University of Pittsburgh, 2006.
- [35] W. Layton and R. Lewandowski. Residual stress of approximate deconvolution large eddy simulation models of turbulence. *J. of Turbulence*, 2006 - in press.
- [36] W. Layton, C. Manica, M. Neda, and L. Rebholz. The joint helicity-energy cascade for homogeneous isotropic turbulence generated by approximate deconvolution models. Technical report, University of Pittsburgh, 2006.
- [37] W. Layton and M. Neda. The energy cascade for homogeneous, isotropic turbulence generated by approximate deconvolution models. Technical report, University of Pittsburgh, 2006.
- [38] W. Layton and M. Neda. Truncation of scales by time relaxation. *Journal of Mathematical Analysis and Applications*, 2006, in press.
- [39] J. Leray. Sur le mouvement d’un fluide visqueux emplissant l’espace. *Acta. Math.*, 63:193–248, 1934.
- [40] R. Lewandowski. Vorticities in a LES model for 3d periodic turbulent flows,. *Journal Math. Fluid. Dyn.*, 8(3), 2006.
- [41] R. Lewandowski and W. Layton. On a well posed turbulence model. *Discrete and continuous dynamical systems B*, 6(1):111–128, 2006.

- [42] J. Liu and W. Wang. Energy and helicity preserving schemes for hydro and magnetohydro-dynamics flows with symmetry. *Journal of Computational Physics*, 200:8–33, 2004.
- [43] C.C. Manica and S. Kaya Merdan. Convergence analysis of the finite element method for a fundamental model in turbulence. Technical report, University of Pittsburgh, 2006.
- [44] S. Kaya Merdan and C. Manica. New discretizations of turbulent flow problems. Technical report, University of Pittsburgh, 2006.
- [45] H. Moffatt. Simple topological aspects of turbulent vorticity dynamics. In T. Tatsumi, editor, *Proc. IUTAM Symposium on Turbulence and Chaotic Phenomena in Fluids*, pages 223–230. Elsevier, 1984.
- [46] H. Moffatt and A. Tsoniber. Helicity in laminar and turbulent flow. *Annual Review of Fluid Mechanics*, 24:281–312, 1992.
- [47] J.J. Moreau. Constantes d’unilrot tourbillonnaire en fluide parfait barotrope. *C.R. Acad. Sci. Paris*, 252:2810–2812, 1961.
- [48] A. Muschinsky. A similarity theory of locally homogeneous and isotropic turbulence generated by a Smagorinsky-type LES. *Journal of Fluid Mechanics*, 325:239–260, 1996.
- [49] M. Olshanskii and A. Reusken. Navier-Stokes equations in rotation form: A robust multigrid solver for the velocity problem. *SIAM J. Sci. Comput.*, 23:1683–1706, 2002.
- [50] L. Rebholz. An energy and helicity conserving scheme for the Navier-Stokes equations. Technical report, University of Pittsburgh, 2006. Submitted to *SIAM Journal on Numerical Analysis* March 2006, returned for revisions with generally positive comments, resubmitted October 2006.
- [51] L. Rebholz. A multiscale V-P discretization for flow problems. *Applied Mathematics and Computation*, 177(1):24–35, 2006.
- [52] L. Rebholz. Conservation laws of turbulence models. *Journal of Mathematical Analysis and Applications*, 326(1):33–45, 2007.
- [53] P. Saugat. *Large Eddy Simulation for incompressible flows*. Springer-Verlag, Berlin, 2001.
- [54] S. Stolz, N. Adams, and L. Kleiser. On the approximate deconvolution model for large-eddy simulations with application to incompressible wall-bounded flows. *Phys. Fluids*, 13, 2001.
- [55] R. Temam. *Navier-Stokes equations : theory and numerical analysis*. Elsevier North-Holland, 1979.

- [56] F. Waleffe. The nature of triad interactions in homogeneous turbulence. *Phys. Fluids A*, 1992.
- [57] Y. Zang, R. L. Street, and J. R. Koseff. A dynamic mixed subgrid-scale model and its application to turbulent recirculating flows. *Phys. Fluids A*, 5:3186–3196, 1993.
- [58] E. Zeidler. *Applied Functional Analysis: Applications to Mathematical Physics*. Springer-Verlag, New York, 1995.